



MRI 412-1

NON-COOPERATIVE MOVING TARGET RECOGNITION USING ISAR

Navy SBIR Topic No. N99-213 Final Technical Report

A. W. Rihaczek  
R. L. Mitchell  
S. J. Hershkowitz

4 December 2001

Prepared under Contract No. N00014-01-M-0241

Submitted to: Office of Naval Research  
Attn: Mr. G. D. McNeal (ONR 313)  
Program Officer  
Ballston Tower One  
800 North Quincy Street  
Arlington VA 22217-5660

20020312 051

Approved for public release; SBIR report, distribution unlimited.

# REPORT DOCUMENTATION PAGE

Form Approved  
OMB No. 0704-0188

Public reporting burden for this collection of information is estimated to average 1 hour per response, including the time for reviewing instructions, searching existing data sources, gathering and maintaining the data needed, and completing and reviewing the collection of information. Send comments regarding this burden estimate or any other aspect of this collection of information, including suggestions for reducing this burden, to Washington Headquarters Services, Directorate for Information Operations and Reports, 1215 Jefferson Davis Highway, Suite 1204, Arlington, VA 22202-4302, and the Office of Management and Budget, Paperwork Reduction Project (0704-0188), Washington, DC 20503.

1. AGENCY USE ONLY (Leave Blank)

2. REPORT DATE

4 December 2001

3. REPORT TYPE AND DATES COVERED

Final - 5 Jul 2001 - 4 Dec 2001

4. TITLE AND SUBTITLE

Non-Cooperative Moving Target Recognition Using ISAR

5. FUNDING NUMBERS

C: N00014-01-M-0241

6. AUTHOR(S)

A. W. Rihaczek, R. L. Mitchell, S. J. Hershkowitz

7. PERFORMING ORGANIZATION NAME(S) AND ADDRESS(ES)

MARK Resources, Inc.  
3878 Carson Street, Suite 210  
Torrance CA 90503

8. PERFORMING ORGANIZATION  
REPORT NUMBER

MRI 412-1

9. SPONSORING/MONITORING AGENCY NAME(S) AND ADDRESS(ES)

Office of Naval Research  
Attn: G. D. McNeal, Program Officer (Code ONR 313)  
Ballston Tower One  
800 North Quincy Street  
Arlington VA 22217-5660

10. SPONSORING/MONITORING  
AGENCY REPORT NUMBER

11. SUPPLEMENTARY NOTES

12a. DISTRIBUTION/AVAILABILITY STATEMENT (see Section 5.3b of this solicitation)

Approved for public release; SBIR report, distribution unlimited.

12b. DISTRIBUTION CODE

13. ABSTRACT (Maximum 200 words)

Ground vehicles move so irregularly that a radar image formed at an arbitrary time will generally not allow identification. Usable images can be formed only at those times, and with those durations, when the target motion happens to be benign. The key to selecting such intervals is the realization that vehicle motion during an interval is correlated with the quality of individual responses in the corresponding image. We automated an algorithm for selecting intervals of benign motion by measuring distortions of individual responses. Benign motion is necessary but not sufficient for identification; the vehicle's apparent rotation must also provide sufficient crossrange resolution. We automated an algorithm that selects intervals of sufficient rotation by measuring the orientations of the vehicle in a sequence of short-duration images.

14. SUBJECT TERMS

radar, ISAR, identification

15. NUMBER OF PAGES

95

16. PRICE CODE

17. SECURITY CLASSIFICATION OF  
REPORT  
UNCLASSIFIED

18. SECURITY CLASSIFICATION OF  
THIS PAGE  
UNCLASSIFIED

19. SECURITY CLASSIFICATION OF  
ABSTRACT  
UNCLASSIFIED

20. LIMITATION OF ABSTRACT  
SAR

## TABLE OF CONTENTS

<u>Section</u>	<u>Page</u>
Introduction and Summary .....	1
1 Ground Vehicle Imaging .....	4
2 Manual Selection of Imaging Interval .....	5
3 Automated Selection of Imaging Interval .....	9
3.1 Imaging Interval Selection Based on Response Distortions .....	9
3.1.1 Principle of Automated Image Quality Evaluation ...	9
3.1.2 Measurement of Response Distortions .....	11
3.1.3 Illustration of Algorithms Based on Response Distortions .....	14
3.1.3.1 Measurement of Response Distortions .....	14
3.1.3.2 Incorporation of the Measurement of the Rotation Rate .....	16
3.1.3.3 Image Time Selection Under More Demanding Conditions .....	18
3.1.3.4 Imaging Time Selection for a Tractor/Trailer Combination .....	20
3.2 The Actual Procedure for Imaging Interval Selection .....	21
3.2.1 The General Method .....	21
3.2.2 Illustration of the Chosen Procedure .....	22
4 Use of the Images for Vehicle Identification .....	24
5 Summary of the Automated Selection of the Imaging Interval ....	25
6 Status of Automation and Validation .....	27
7 Available Target Data .....	27

# LIST OF ILLUSTRATIONS

<u>Figure</u>		<u>Page</u>
1	Image of Turning Surrogate TEL at Small Aspect Angle .....	30
2	Surrogate TEL Image 0.05 s Later than in Figure 1 .....	31
3	Surrogate TEL Image at a Larger Aspect Angle .....	32
4	Surrogate TEL image 0.1 s Later than in Figure 3 .....	33
5	Surrogate TEL Image 1 s Later than in Figure 3 .....	34
6	Surrogate TEL image 0.3 s Later than in Figure 5 .....	35
7	Image of the Surrogate TEL on a Bumpy Road .....	36
8	Surrogate TEL Image 1.1 s Later than in Figure 7 .....	37
9	Image in Figure 8 after Adjustment of Crossrange Scale Factor .....	38
10	Surrogate TEL Image 0.3 s Later than in Figure 9 .....	39
11	Image Cut and Transform for Range Gate 11.4 in Figure 1 .....	40
12	Image Cut and Transform for Range Gate 11.7 in Figure 2 .....	41
13	Image Cut and Transform for Range Gate 0 in Figure 8 .....	42
14	Image Cut and Transform for Range Gate 0.1 in Figure 7 .....	43
15	Distortions for the Circling Surrogate TEL .....	44
16	0.068 s Image at 68.22 s .....	45
17	Image Cut and Transform Along the Line in Figure 16 .....	46
18	Image with the Same Starting Time as that of Figure 16 but an Interval Duration of 0.094 s .....	47
19	Image with Adjusted Starting Time .....	48
20	0.068 s Image at 71.07 s .....	49
21	Distortion Measurements for Doubled Imaging Duration .....	50
22	0.137 s Image at 68.30 s .....	51
23	0.137 s Image at 68.05 s .....	52
24	Distortion and Slope Measurements for Surrogate TEL on a Smooth Road .....	53
25	Image of Surrogate TEL Moving on Smooth Road at 45.0 s (0.5 s Imaging Interval) .....	54
26	Image of Surrogate TEL Moving on Smooth Road at 42.25 s (0.5 s Imaging Interval) .....	55
27	Image of Surrogate TEL Moving on Smooth Road at 42.15 s (0.5 s Imaging Interval) .....	56
28	Image of Surrogate TEL Moving on Smooth Road at 43.4 s (0.5 s Imaging Interval) .....	57
29	Image of Surrogate TEL Moving on Smooth Road at 44.0 s (0.5 s Imaging Interval) .....	58
30	Image of Surrogate TEL Moving on Smooth Road at 47.3 s (0.5 s Imaging Interval) .....	59
31	Image of Surrogate TEL Moving on Smooth Road at 46.1 s (0.5 s Imaging Interval) .....	60
32	Image of Surrogate TEL Moving on Smooth Road at 46.35 s (0.5 s Imaging Interval) .....	61
33	Image of Surrogate TEL Moving on Smooth Road at 47.8 s (0.5 s Imaging Interval) .....	62

# LIST OF ILLUSTRATIONS (CONCLUDED)

<u>Figure</u>		<u>Page</u>
34	Distortion and Slope Measurements for Imaging Interval of 0.88 s .....	63
35	Image of Surrogate TEL Moving on Smooth Road at 43.9 s (0.88 s Imaging Interval) .....	64
36	Image of Surrogate TEL Moving on Smooth Road at 44.1 s (0.88 s Imaging Interval) .....	65
37	Distortion and Slope Measurements for Imaging Interval of 1.16 s .....	66
38	Image of Surrogate TEL Moving on Smooth Road at 43.1 s (1.16 s Imaging Interval) .....	67
39	Distortion and Slope Measurements for Truck on Bumpy Road .....	68
40	Image of Truck on Bumpy Road at 102.3 s (0.2 s Imaging Interval) .....	69
41	Image of Truck on Bumpy Road at 105.75 s (0.2 s Imaging Interval) .....	70
42	Image of Truck on Bumpy Road at 102.75 s (0.2 s Imaging Interval) .....	71
43	Image of Truck on Bumpy Road at 106.05 s (0.2 s Imaging Interval) .....	72
44	Image of Truck on Bumpy Road at 102.25 s (0.2 s Imaging Interval) .....	73
45	Distortion and Slope Measurements for 0.269 s Imaging Interval) .....	74
46	Image of Truck on Bumpy Road at 102.35 s (0.269 s Imaging Interval) .....	75
47	Distortion and Slope Measurements for Confuser on Bumpy Road ..	76
48	Best Image of Confuser on Bumpy Road .....	77
49	Image of Confuser on Bumpy Road at 73.95 s (0.468 s Imaging Interval).....	78
50	Image of Confuser on Bumpy Road at 73.90 s (0.21 s Imaging Interval).....	79
51	Image of Confuser on Bumpy Road at 71.9 s (0.468 s Imaging Interval).....	80
52	Slope Measurements for the Surrogate TEL on the Smooth Road ...	81
53	Expanded View of the Slope Bars .....	82
54	0.2 s image at 25.85 s .....	83
55	0.25 s Image at 25.40 s .....	84
56	0.55 s Image at 24.3 s .....	85
57	0.45 s Image at 21.5 s .....	86
58	0.1 s Image at 15.95 s .....	87
59	0.5 s Image at 16.1 s .....	88
60	0.40 s Image at 17.3 s .....	89
61	0.9 s Image at 22.4 s .....	90

## INTRODUCTION AND SUMMARY

Radar identification of moving ground vehicles can be approached in two principal ways: Identification via one-dimensional range profiles (usually referred to as the HRR method) and identification via two-dimensional images (ISAR imaging). Based on our extensive experience in this field, it is our conviction that there is no chance the HRR method can deliver the performance required for an operational system. We are equally convinced that identification via two-dimensional imaging can provide the needed performance.

A range profile is an interference pattern from mostly extended scatterers rather than point scatterers, and because of the complicated backscattering behavior of extended scatterers it remains an interference pattern even when range resolution is made very high, even higher than that usually used for HRR. The definition of resolution becomes rather meaningless when some target feature is "resolved" into parts. Spurious responses are generated. The interference pattern, inappropriately called a range profile, changes very rapidly with aspect angle. Thus one would have to provide a database containing the range profiles for all vehicles (in all configurations) over 360° in very small angular increments. This is more difficult than for aircraft, and is impractical even for stationary ground vehicles. If the ground vehicles are individually tracked over a sufficiently long time (but then one can image), their aspect angles can be estimated from the tracks, so that the search during identification can be limited to only part of the database. However, the identification problem still remains worse than for aircraft.

As we have learned from the Dragnet/MTE data collection, when ground vehicles move, their yawing, pitching, rolling, flexing, twisting, and bouncing introduce highly erratic motion components that have surprisingly high frequencies. The consequence is that, in addition to the change with aspect angle, the range profile also changes rapidly with time for a fixed aspect angle. If one uses integration to smooth the range profile, the rapid motion components distort the responses and cause a multitude of spurious responses, even with integration times measured in milliseconds. We believe that this additional problem of profile formation also is unsolvable.

This leaves only the method of identifying moving ground vehicles via ISAR images. Here the problem is that the erratic motion components of the vehicle smear the image in crossrange. It used to be thought that some type of motion compensation could yield an image similar to that of the stationary vehicle. This is impossible, however. Every scatterer on the vehicle may move differently, so no motion compensation will work on the vehicle as a unit. Compensating different scatterers differently is also impossible, because the smeared and unresolved responses of the image do not permit a sufficiently accurate measurement of the scatterers' motions. Perhaps one or the other scatterer could be compensated to the required accuracy, but not enough scatterers to obtain an image usable for identification.

The above discussion might make it appear that identification of moving ground vehicles is impossible. However, our study of real data has shown that when one observes a ground vehicle over some time, as in a SAR system, there will always be short time intervals during which the motion happens to be relatively smooth. If one can find these intervals, then one can generate images of a quality sufficient to permit vehicle identification. Thus, the

critically important step toward the identification of moving ground vehicles is to find imaging intervals that yield usable images. If this can be done, moving ground vehicles can be identified; otherwise they cannot.

In developing the signal processing methods appropriate for such tasks as target identification, we have also developed interactive software with which these optimum imaging intervals can be found in a straightforward way. It does not take any experience in signal processing. Starting at the beginning of the observation time, we form an image with a duration that provides some degree of crossrange resolution. This image is examined to determine whether the short and long illuminated edges of the ground vehicle can be recognized even though the crossrange scale factor typically will be so far from correct that their orientations are far from perpendicular to each other. The edges must be recognized in the presence of spurious responses. If we are unsuccessful, the imaging interval is translated by perhaps 20% of its duration, and again an image is formed and examined. This sliding-window processing is continued over the entire observation time. When we do not find a usable image, the imaging interval is increased by perhaps 20%, and the same search is repeated. The processing is iterated until a good image is found.

Although the described procedure is straightforward, it is very time consuming. This is so because the quality of an image is extremely sensitive to both the center time of the imaging interval and its duration. The search thus is two-dimensional, and must be done in steps of perhaps 0.05 s. Depending on the situation, it might take an hour or more to find the best available image. The method thus is practical only for post-flight identification of a relatively few ground vehicles.

The goal of the work reported here was to automate the selection of the best available imaging interval, both its timing and duration, or the start and stop times. However, automating the process by which an operator can find the optimum imaging interval is impossible because one cannot automate the pattern recognition process by which an operator can detect barely indicated vehicle edges in a highly distorted image containing a multitude of spurious responses. The central issue of the program thus was to find a substitute method that can be automated, and to automate it.

The first idea we pursued was to find good imaging intervals by measuring the distortions of the major responses in the image. As the duration of the imaging interval is increased, responses in the same range gate start to become resolved in crossrange. With a further increase in the duration, these responses become separated in crossrange. However, from some point on (which may come before the responses are separated), the irregular motion of the vehicle distorts the responses, and with still longer imaging intervals the "distortions" become spurious responses in positions where there are no scatterers. Hence, when one performs the two-dimensional search for a good imaging interval, responses for which the distortions are small imply a good image, because it is the progressively more severe response distortions that ruin the image quality. The important point is that the measurement of response distortions can be automated, in contrast to the pattern recognition process discussed above.

The method of measuring the response distortions in order to judge image quality works but is computer intensive. Also, because a two-dimensional search is involved, it is not easy to sort the results in accordance with expected image quality. Lastly, the measurement of response distortions requires that the responses be reasonably well resolved, which is not always

the case. For these reasons, we looked for a simpler method. We found this method, developed it, and achieved even better results than with the distortion measurements. We retain the distortion measurements in our report because they are still used, but for a different purpose as discussed below.

The second method relies on the measurement of the rotation rate of the vehicle. When the vehicle's motion is smooth enough to allow a good image, the rotation rate also must be smooth. Let us for the moment assume that the ground vehicle is a line target. When an image is formed over a very short duration, the responses will lie along a line in the range/crossrange plane. The tilt of the line from vertical will be proportional to the rotation rate of the vehicle. If the rotation rate changes, so will the tilt. Hence, by forming short-term images and measuring the tilt as the imaging interval is shifted in time, we effectively measure the variation in the rotation rate. This is precisely what determines image quality as a function of time. Although a ground vehicle is not a line target and the short term image generally has some spread in crossrange, this does not matter because with a uniform motion the spread will also change at most gradually. Thus, by observing the variations in the measured image tilt, we measure the smoothness of the vehicle's motion. All one need automate is the measurement of the tilt of the image as the imaging window is shifted, and the selection of imaging intervals during which the tilt changes less than some acceptable amount. This is easily automated, as we have done under the program, and the results are easily used.

We want to find one or more imaging intervals that yield images usable for vehicle identification. Our practical definition of a usable image is one image that shows at least one of the short edges of the vehicle, and at least a part of the illuminated long edge adjoining the visible short edge. In some cases we will obtain the complete outline of the vehicle, in others the long illuminated edge and both short edges, in still others the long illuminated edges and one of the short edges, and in the worst class of usable images we have only one short edge and part of the long edge. With this type of "usable" image, we can at least approximately determine the crossrange scale factor and the length of the vehicle. We can also ensure that the responses in the image are genuine responses associated with real scatterers rather than spurious responses that appear anywhere. In better situations the range/crossrange positions of responses will represent actual scatterer positions in the two dimensions. In worse cases only the range positions will be meaningful. This is still much better than a range profile, and is entirely adequate, because crossrange resolution of responses in the same range gate eliminates the interference and the scintillation in a range profile and permits an accurate range measurement on the significant responses.

We also retained the measurement of the response distortions. For good crossrange resolution, we would like to use the longest possible imaging interval. However, the tilt measurement will rarely give a series of constant tilt values. There will be some variation, and the longer the imaging interval is, the more effective these tilt variations will be in generating spurious responses. Thus we need a method of determining the maximum duration of the imaging interval. We use the distortion measurements to limit the duration of the imaging interval, because small distortions imply a good image. The measurements of image tilt and response distortions are

complementary, but by utilizing the tilt measurement before that of the response distortions, we greatly simplify the search for good imaging intervals.

The development of algorithms of the kind described above must be based on real data, because one cannot foresee the possible varieties of vehicle behavior, both in backscattering and motion. We had available data from the Dragnet/MTE data set. Specifically, we had data from the surrogate TEL, the Confuser, an M109 Howitzer, an M60 tank, and an M38 truck, all moving in circles, and data on the TEL, Confuser, and truck moving on a smooth and also on a bumpy straight road. Our algorithms work on all these data, but we would like to obtain more data for vehicles going straight because these are more difficult to identify than turning vehicles. This is not a matter of a training database. A sufficient variety of data is needed to be sure that all kinds of behavior are accommodated by the algorithms. We have no reason to suspect that the data available for this program do not cover all conceivable problems that could appear with ground vehicles, but we still would like to examine a larger variety of data. It would not change our algorithms, but might suggest some fine tuning.

We feel that with this work we have solved the most critical issue in the identification of moving ground vehicles. The remaining processing stages that will lead to ground vehicle identification, and which we have developed in concept, appear to involve much less uncertainty than did automating the selection of good imaging intervals.

## 1. GROUND VEHICLE IMAGING

Reliable radar-based identification of a man-made target requires that a high-quality image be generated, in the sense that image responses represent scatterer returns at the positions of the scatterers. For the major scatterers, this is easy when the target is stationary, but in practice stationary vehicles in the open might be considered special circumstances. During war times, most military vehicles that are not hidden move most of the time, and the conventional thinking is that the target motion can be utilized for generating an image, the so-called ISAR image. In theory, one effectively replaces the motion of a SAR platform and the slow apparent target rotation it causes by the actual rotational motion of the target in order to achieve high crossrange resolution.

The practical implementation of the seemingly simple ISAR principle is rather difficult. Imaging of a moving target requires that it move smoothly on the scale of the radar wavelength, but they hardly ever do so. The smoothest motion is found with aircraft, and a large aircraft may move smoothly enough to make ISAR imaging straightforward. However, problems start to appear with small aircraft, such as fighters, even when they do not intentionally maneuver. Imaging becomes even more difficult for a small ship, which can yaw, pitch, and roll heavily and rapidly. This three-dimensional motion is somewhat counterbalanced by the fact that the angular rotations are relatively large, so that only a short imaging interval is needed to generate an image with adequate crossrange resolution. The most difficult case is that of moving ground vehicles. Their contact with the hard ground causes a rather erratic roll, pitch, yaw, and bounce motion, and for flexible vehicles an additional flexing and twisting motion. These motions usually are not so large that they can be utilized for ISAR imaging as in the case of ships, for which an interval so short that the motion appears smooth may be long enough

to obtain good crossrange resolution. The erratic motions of ground vehicles severely interfere with the process of forming an ISAR image on the basis of the translational motion of the vehicle.

It appears that there used to be a widely spread opinion that the solution to these problems lies in a good motion compensation, but our examination of real data has shown that this is not true. In the case of an aircraft that does not intentionally maneuver, in particular a large aircraft, a good motion compensation typically leads to an image of sufficient quality; but then one must not rely on the absence of even small inadvertent "maneuvers". For ships and ground vehicles, the desired motion compensation does not exist. With ships, the main problem is the three-dimensional motion, which causes a multitude of spurious responses unless the ship happens to rotate about a fixed axis. With ground vehicles, difficulties arise because individual parts of the vehicle move slightly differently. Even if one were willing to perform a motion compensation that varies over the vehicle, the motions of the individual scatterers cannot be measured with the required accuracy. The only solution of these problems comes from our finding that the motion of a target is not always so poor that no useful image can be formed. Within some observation interval, one can find subintervals during which the motion happens to be good enough to obtain an ISAR image good enough for vehicle identification. Thus, if we select the appropriate imaging interval (both timing and duration), we can generate a usable image. There is no other practical approach to ISAR imaging of ground vehicles. The selection of a good imaging interval is the central issue of moving ground vehicle identification.

## 2. MANUAL SELECTION OF IMAGING INTERVAL

We consider the case of a SAR surveillance radar, where the observation time is much longer than needed to form an image of a moving ground vehicle. The question then is, how do we search the available observation interval for a (shorter) imaging interval that will produce a good image? (Consideration of a SAR system does not limit the generality of the discussion, because when a vehicle is individually tracked, one also must track long enough until a good imaging interval is found.)

With use of our interactive imaging software, the selection of a good imaging interval is straightforward but very time consuming: After a simple motion compensation to remove the translational motion of the vehicle, such as range centroid compensation followed by Doppler centroid compensation, we form an ISAR image with an imaging interval so short that crossrange resolution is likely to be inadequate for resolving scatterers in the same range gate. The vehicle appears as a line target in the image. Then we increase the imaging interval in steps until crossrange resolution is barely high enough to obtain a two-dimensional image. We examine the image to determine whether we can recognize the two illuminated edges of the vehicle, despite the image distortions due to a false crossrange scale and the presence of spurious responses. If we cannot find the two edges and recognize the vehicle outline, we shift the imaging interval by a little, perhaps by 20% of its duration, and form another image. This image is again examined as to whether we can recognize the vehicle outline. If unsuccessful, we shift the imaging interval again, iterating the process until the entire dwell has been examined.

As explained above, we must start with a short imaging interval. It is likely that we will not recognize the vehicle outline because crossrange resolution is too poor. Thus we must increase the duration of the imaging interval by, say, 20%, and again form the set of images by sliding-window processing, examining each of the images. If no good image is found, we increase the duration of the imaging interval by another step, and try again. This is continued until the chosen imaging durations evidently are too long, which is recognized from the unacceptable increase in the number and strength of spurious responses. During this iterative processing we will have found some usable images, but we want to find the best image that can be obtained during the dwell.

Such a search for a good image evidently is very time consuming. The quality of the image critically depends on both the position of the imaging window and its duration, and can vary much with only a little change in either of the two parameters. For the Dragnet/MTE data, we have found that a shift of either the start or the end of the imaging interval by as little as 0.05 s can significantly degrade image quality. Thus, even though the search for a good image is so simple that it could be done by someone without experience in signal processing, it takes so long that it is useful only for post-flight processing of vehicles of particular interest. Nevertheless, since the search process reveals the problems of good imaging and its automation, we will illustrate it.

#### Turning Vehicles

It appears that when data collections are carried out, the preferred mode is that of a vehicle moving in a circle. This is an easy way of obtaining data for all aspect angles of the vehicle, but it ignores the fact that it is easier, sometimes much easier, to generate a good image when the vehicle is turning than when it goes straight; yet in practice vehicles go mostly straight. The problem of developing an automated identification system is not only that of obtaining data for different aspect angles. One needs extensive data on vehicles which go straight, because only such data allow one to understand all the possible problems which the identification software must accommodate. The precise nature of these problems cannot be foreseen. This is to say that the purpose of collecting data is not merely to establish a database, but also to obtain insight into the motion behavior of vehicles and the resulting problems that must be solved.

There are two types of Doppler that affect imaging of a ground vehicle. First, there is the rotational Doppler from the aspect angle change caused by the translational motion of the entire vehicle, the same as with SAR imaging. This is the Doppler one would like to utilize for crossrange resolution. Second, the rolling, yawing, pitching, flexing, twisting, and bouncing motion of the vehicle and the vibration of its parts cause an irregularly varying instantaneous Doppler that interferes with imaging. This Doppler is generally different for each part of the vehicle, and it can be very much different. The first type of Doppler usually is stronger in relation to the second when the vehicle turns than when it goes straight. Hence, it is generally easier to form a good image when the vehicle is turning (but they usually are not).

For our illustrations, we selected the surrogate TEL in the Dragnet/MTE data set. When this vehicle goes in a circle, the difficulties of imaging depend on the aspect angle. The important rolling component of the irregular motion, for example, generates only low Dopplers when the aspect angle is

small. With increasing aspect angle, this motion component becomes more effective, so that the image quality degrades even when one selects the best imaging time. Nevertheless, because of the strong turning Doppler it is relatively easy to form a good image at all aspect angles.

Figure 1 shows the image of the turning surrogate TEL at a small aspect angle, with an imaging interval of 0.09 s. Dots are plotted at the stronger of the local maxima in the intensity image, with the size of each dot proportional to the strength of the associated maximum. For our purposes, this presentation of the intensity image is much more convenient than the standard type of image. As long as we can recognize the short and long illuminated edges, we can choose the crossrange scale factor so that the edges appear perpendicular to each other (which may include responses that are too weak to appear in the figure). In this case the scaling in both dimensions in the image will correspond to the range scale. This measurement ordinarily requires the discrimination of spurious responses outside the vehicle, but this is relatively easy to do interactively. For example, it is easy to recognize that the top five dots in Figure 1 do not belong to the vehicle.

As explained above, with a manual search for a good imaging interval, we form a succession of images until one is found in which the two illuminated edges are well enough defined so that they can be oriented perpendicular to each other, as in Figure 1. In Figure 2 we show the equivalent image when the imaging interval is shifted by just 0.05 s. The quality of the image has degraded to such an degree that it is now considerably more difficult to be sure that the crossrange factor was chosen correctly to make the two illuminated edges perpendicular to each other. At such a small aspect angle this adjustment is not critical for the measurement of vehicle length, but when one tries to extract more than vehicle length the image quality becomes much more critical. For example, by comparing some of the responses in Figures 1 and 2, such as those around Range Gate 12, we conclude that the quality of the image in Figure 2 is quite inferior when scatterer positions are to be used for identification. The point we want to make here is that it evidently is easy to decide which image is good and which is poor when we examine a series of images by eye.

In Figure 3 we show an image from the same data file at a larger aspect angle, but again when it is easy to orient the two illuminated edges perpendicular to each other. The image is of high quality in that both the length of the vehicle and the positions of the major scatterers can be determined. The image 0.1 s later is shown in Figure 4. Again, it is obviously easy to decide that this is a poor image, because we are unsure how to choose the crossrange scale factor in order to orient the two illuminated edges perpendicular to each other. At the larger aspect angle, this uncertainty greatly affects the measurement of vehicle length. In addition, Figure 4 has many more responses than Figure 3; that is, many more than the number of wave-trapping features illuminated on such a vehicle for the given aspect angle (compare the number of responses in Figures 3 and 4). Again, it is easy to select the better image by inspection, and even to select an image that is good enough for identification (with some practice).

As the aspect increases, the difference between a well and a poorly selected image becomes even greater. Figure 5 shows a good image about 1 s later, at a larger aspect angle. The line indicates the long illuminated edge. The short illuminated edge is not as well defined as in Figure 3, yet it still is a good image for such a large aspect angle. The image 0.3 s later

is given in Figure 6. The big uncertainty in making the two illuminated edges appear perpendicular to each other translates into a large length error at this aspect angle. We note again our main point here, that is, it is easy to decide by inspection which image is good and which is poor.

#### Vehicle on a Straight Road

We now illustrate that the interactive selection of a good imaging interval is also easy for a vehicle going straight, even though the image quality is generally worse than for a turning vehicle. Since we illustrated imaging of the TEL when it is turning, we choose the case of the TEL on a bumpy straight road. However, we want to point out that the case is not impractically chosen in that such difficulties will occur only rarely. Our experience with the Dragnet/MTE data suggests that the following illustrations might well be representative of what to expect routinely in practice.

For the straight road, we again consider the interactive process of selecting a good imaging interval by forming a succession of images with slightly shifted imaging intervals, and deciding which image is good enough for target identification. More specifically, the more limited objective here is to find an imaging interval that yields an image in which the two illuminated edges can be recognized.

Figure 7 shows one image. The imaging interval now is 0.5 s, about five times longer than for the surrogate TEL traveling in a circle. The reason is the much lower rotational Doppler due to the translational motion. Examination of this image clearly shows that it is impossible to recognize the two illuminated edges. We see at a glance that the image quality is too poor for identification of the vehicle.

Figure 8 shows the analogous image 1.1 s later. The two lowest dots in the image appear to define the direction of the short edge, whereas a series of dots appears to define the lower two thirds of the long edge. When the crossrange scale factor is adjusted in the manner of Figure 9, we conclude that the line does indicate the direction of the long edge. When this line is extended toward the far end of the vehicle (here we do not discuss how to find the far end), we obtain the correct length of the vehicle. The responses of the far half of the vehicle are shifted in crossrange, so that the far half of the long edge cannot be recognized; but extrapolation of the visible part of the long edge allows us to derive the rectangular outline of the vehicle.

Such a partial definition of the long illuminated edge is not rare when ground vehicles go straight. In judging image quality, our objective is to recognize the long illuminated edge well enough for its extrapolation over the length of the vehicle. We can do this in Figure 9. Figure 10 gives the surrogate TEL image only 0.3 s later. Clearly, there is no way in which one can recognize even parts of the two illuminated edges. The rapidity with which the image quality changes with time makes it clear how critical it is to select the proper imaging interval (center time and duration). As demonstrated, with our processing method this is easy (but very tedious) to do interactively.

We have discussed imaging time, but have said little about the duration of the imaging interval. For the circling surrogate TEL the imaging interval had a duration of 0.1 s, and for the same vehicle on the straight road it was 0.5 s. The appropriate duration is also easy to select with manual processing. We start with one that is too short, so that the width of the vehicle in the image is too small for the definition of the short illuminated

edge (or to provide enough resolution on the long illuminated edge when the aspect angle is near broadside). Then we increase the length of the imaging interval in steps, until crossrange resolution becomes high enough to provide a sufficient definition of the two edges. Once a good imaging time is found, we adjust the duration of the imaging interval so that it gives the best image, by the criteria illustrated above. What makes the search so extensive is that the optimum duration of the imaging interval varies throughout the data file, because of changing motion conditions. In summary, finding the best imaging interval (duration and central time) is straightforward when our interactive software is used, but it is too time consuming even if one were willing to use an operator under real conditions.

A comment on our technology is in order at this point. As demonstrated, the methods we use are straightforward with interactive analysis, but they are not straightforward to automate. Recognizing the illuminated edges in an image with the wrong crossrange scale factor and many spurious responses probably cannot be automated. It certainly would be desirable to have some mathematical algorithm that could form a usable image, because the entire process then would already be automated. However, our demonstration of how critical the selection of the correct imaging interval is also shows that a mathematical algorithm that can by itself form usable images cannot possibly exist. For example, how could one develop a motion compensation that correctly compensates the different motions of the various scatterers on the vehicle? This would have to apply when the response smearing is due to the highly complicated erratic motion of a vehicle. It is not possible to measure the different motions of the individual scatterers.

### 3. AUTOMATED SELECTION OF IMAGING INTERVAL

Under this program, we first developed a method of automatically selecting good imaging intervals based on distortions of the image responses. Although the method works, it is cumbersome because of the two-dimensional search for an optimum imaging time and the duration of the imaging interval. We then conceived a simpler method based on the measurement of the smoothness of the target motion. We will explain both methods, because the first approach will be used for determining the maximum allowable duration of the imaging interval to ensure that spurious responses do not present problems. These issues will be discussed in more detail below.

#### 3.1 Imaging Interval Selection Based on Response Distortions

##### 3.1.1 Principle of Automated Image Quality Evaluation

It is clear from the preceding illustrations that the pattern recognition process involved in finding the two illuminated edges in an image, and then deciding that they are sufficiently well defined, cannot be automated. Although this might be possible in some instances when a vehicle is turning sufficiently rapidly and smoothly, for the important practical case of a vehicle that goes straight the problem appears unsolvable. A different approach must be used if the process of imaging interval selection is to be automated.

To find this approach, we must ask why an image is distorted and contains many spurious responses. When the target motion is perfectly smooth, the major scatterers on the vehicle generate relatively sharp responses in the range/crossrange positions of the scatterers. Since the major scatterers are wave-trapping features, one or the other may have a significant phase center

wander with aspect angle to cause some widening or perhaps some small translation of the response, or occasionally even spurious responses far away from the scatterer's position. Such effects also are present with stationary vehicles, for which the apparent smooth motion is supplied by the radar platform. When a vehicle itself moves smoothly, these effects are small enough to allow target identification on the basis of vehicle outline and the positions and characteristics of the major scatterers. This is confirmed by the success of imaging and image exploitation of stationary vehicles. However, as the vehicle's motion becomes more erratic, the phase center wander causes a progressively worse distortion and translation of the individual responses, until the responses may be so heavily smeared that they appear as sets of spurious responses. The important point for the present purpose is that image quality is tied to response quality. If the responses are not distorted, the image quality must be high, as high as obtainable with radar under good conditions.

The conclusion is that in order to select the optimum imaging interval, we need not judge the quality of an image. We need judge only the quality of the image responses. Specifically, if the responses are not distorted, the image quality must be high. If they are somewhat distorted, the image quality must be somewhat worse. If they are highly distorted, the image quality must be poor. Although judging the distortions of responses also involves some form of (response) pattern recognition, the process is much more easily automated than determining whether or not a radar image contains recognizable vehicle edges.

We can use the preceding figures to verify that response distortions and image quality are tied together. Figure 11 shows the image cut and its Fourier transform in Range Gate 11.4 in Figure 1. The top left curve gives the image cut intensity, and the lower left curve the phase of the image cut. The top right plot gives the amplitude of the transform of the image cut, and the lower right the phase. The crosshair lets us recognize that the response is symmetric, and the measured relative half-power width is 1.089, very close to the unity width of a response from an ideal point scatterer. The amplitude of the transform may be considered constant for practical purposes, and the phase is linear (deviations from linearity less than 0.1 cycles). The same measurements are shown in Figure 12 for the same response in Figure 2, the lower-quality image. The response is no longer symmetrical, and there is a sidelobe. The amplitude of the transform is no longer essentially constant, and the phase function has significant curvature. The image in Figure 2 is somewhat worse than that in Figure 1, and the response in Figure 2 is somewhat worse than that in Figure 1. For both the image and response, the degree of distortion is mild in practical terms.

We examine similar image cuts for the surrogate TEL on the straight road, which is a less benign situation than when it travels in a circle. Figure 13 shows the image cut and transform for the range gate of the strongest response in Figure 8. The intensity response, left top curve, is somewhat distorted, which implies that the image does not have the highest quality; but since the distortion is mild, the image is usable for vehicle identification.

Figure 14 shows the analogous image cut for the strongest response in Figure 7, with the same scale of the abscissa as in Figure 13. By comparison with the response in Figure 13, the response now is much wider and more distorted. Although the amplitude of the transform is essentially constant, this is of little help because amplitude modulation does not affect the

response very strongly. The phase function is much more important, and the new phase function is much worse than that in Figure 13. If we consider the phase function curved, the total phase variation due to curvature is about 0.5 cycles, which is inadmissibly large (only a variation below about 0.1 cycles is harmless).

Alternatively, we may interpret the phase function as having different slopes for the first and the second half. Phase slope is equivalent to Doppler, and hence to crossrange position. Our software is normalized so that the phase slope measurement gives the crossrange position. The legend at the upper left of the figure shows the two positions to be Crossrange Gate 1.4 and Gate -0.6. This means that the scatterer essentially has two responses that are separated by two crossrange gates. It is clear that such response distortions are much too high to come from an image that may be used for vehicle identification, a fact that is confirmed by Figure 7. This is the response from an image much too poor to be usable for target identification. The qualities of an image and its responses thus are indeed tied together.

### 3.1.2 Measurement of Response Distortions

Since most ground vehicles are flexible, and rigid ground vehicles often have flexing features, different parts of a ground vehicle generally move in slightly different ways. To obtain an image of the highest quality in benign situations comparable to that of a stationary vehicle, we should select responses distributed over the entire image, measure their distortions, and select an imaging interval during which all of the responses have small distortions. This is impractical for two reasons. First, in order to measure the distortions of a response, the response must be well resolved from others, either because it is much stronger than neighboring responses, or because there is no nearby response. This condition is seldom met, primarily because resolution usually is inadequate and also because the responses may be slightly smeared even in good situations. Thus it will generally be impossible to measure distortions on responses distributed over the entire vehicle. Second, even if these measurements could be performed, it is highly unlikely that one could find an imaging interval during which all these responses have small distortions.

The next best method is to measure the distortions of one response in the near third of the image, of a second response in the middle third, and of a third response in the far third. These three responses permit an estimate of how each of the three parts of the target behaves, and perhaps one can find an imaging interval in which all three parts of the target happen to have a smooth motion. Even if such a coincidence does not occur too often, it is useful to understand how each part of the target behaves during the selected imaging interval. The biggest benefit is that we can give preference to a good behavior of the near part, because that is most critical for orienting the two illuminated edges perpendicular to each other.

The next best method would be to select the three strongest responses in every image, regardless of where they are located, and measure the distortions of these responses. For some images the responses might be distributed over the image, and sometimes they might be clustered. However, the implementation of this approach is simpler than trying to find one response in each of the three parts of the target. The simplest method would be to perform the distortion measurements just on one response, which should be the strongest response in the image. This means that we effectively would measure the

motion behavior of just one part of the target, and this part could change when the strongest response is not associated with a specific scatterer over the entire dwell, as will often be the case.

We decided to employ the best approach that can be practically implemented, which is to measure the distortions on the strongest responses in each third (in range) of the vehicle. At a given imaging time, we select the strongest response in each third of the vehicle, and measure their distortions. As the imaging interval is shifted, we again select the three strongest responses, and measure the distortions. With each shift of the imaging interval, in principle the distortion measurements might be performed on responses from different scatterers, but this does not matter as long as these scatterers are in the three different parts of the vehicle. We obtain estimates of how these parts behave.

With regard to the measurement of the response distortions, there again are various choices. A relatively simple way is to examine a limited region on each side of the amplitude peak in a fixed-range image cut through a response, as shown in Figure 14. The lower boundary of the region is defined by a given percentage of the amplitude of the response peak, such as 10%. The upper boundary also is defined by a percentage of the peak amplitude, such as 50%. The far side of the region is defined by a vertical line determined by how far away in crossrange from the response peak one wants to extend the measurement, such as three gates. The only question on these three boundaries is what peak percentages to use and how far out from the peak to go. The fourth boundary of the search area is more critical.

As one method, for the fourth boundary we can use the response from an ideal point scatterer, with the same peak location and strength as the actual response, based on the argument that we want to consider a widening of the response as a "distortion". This is simple to implement. However, a smooth widening of the response will not cause spurious responses. Also, the response selected for the distortion measurements may come from more than one scatterer, and hence be wider than the ideal point target response even when the vehicle motion is benign. Then we would measure distortions even when the motion is smooth enough to give a good image. This could be avoided by fitting a Gaussian function (separately to each side) to the actual response, and using the fitted function as the fourth boundary. Potential problems could arise because the first consequence of a nonconstant Doppler is the smooth widening of a response, so that our distortion measurement would not indicate that this is occurring.

We discuss these issues in some detail to indicate that extended investigations would be required if we wanted to make sure that the best possible implementation is found. The potential benefits from such an investigation appeared minor, so that we simply chose the response from an ideal point scatterer for the fourth boundary. With this choice, the measurement region appears as indicated for the right side of the response in Figure 14. The distortion parameter is the percentage of the outlined region that is filled by the response.

We defer discussion of the choice of the imaging durations used in the distortion measurements to Section 3.2.2. For a given duration, we form an image, and measure the distortions of the three strongest responses. The imaging interval then is shifted by 20% of its duration, a new image is formed, and the distortions of the three strongest responses are measured. This process is continued until the entire dwell time is covered.

In our first implementation of this type of processing, we selected the strongest responses in the first image of the sliding-window series, with the intent to track the same responses over the entire dwell time. However, we found that a moving ground vehicle typically does not contain three responses that can be tracked over the entire dwell. The motion of a ground vehicle is too erratic for this type of response tracking. Thus we implemented the distortion measurement without tracking of responses: the short-term images are formed in sliding window fashion, and in each third of the image we simply select the strongest responses for the distortion measurements. The scatterers associated with these responses may change from one image to the next, but this really does not matter under the simplifying assumption that the behavior of a scatterer is indicative of the behavior of the entire vehicle.

Because image responses generally are less well resolved than desirable for the distortion measurement, we included a refinement into the measurement. If a response is not well isolated, interference from a neighboring response can fill the search area, and thus falsely indicate high response distortions. For this reason, when distortions are measured, we search for a strong neighboring response in the same range gate. If such a response is found sufficiently close in crossrange that it could interfere with the response under examination, this fact is indicated in the evaluation of the distortion measurement.

The described processing is adequate when the erratic motion component of a vehicle is not too large in relation to the turning motion. However, when a vehicle is going straight, this condition is easily (perhaps usually) invalidated. Since the erratic motion can be rather rapid, one is forced to use very short imaging intervals. The consequence is that the important responses in the image are not well resolved, so that one must operate on response peaks that are barely detectable in the interference from stronger responses. We use a high degree of interpolation (a factor of eight) for these short-term images in order to make these low "peaks" visible.

We would like the motion of the vehicle to be smooth at least over the short selected imaging interval, where smooth means that the instantaneous Doppler should be constant. The reason is that a nonconstant Doppler smears the responses so that the response peaks are easily translated, and also generates spurious responses. Neither effect is detected by the measurement of the response distortions. The fact is that the motion of a ground vehicle typically is so erratic that the imaging interval cannot be made short enough to avoid these effects; crossrange resolution would be insufficient. For this reason, we included a measurement complementary to that of the response distortions. Although it is not needed under benign circumstances, it is always included because it will have no effect when the circumstances are benign.

This complementary algorithm indirectly measures the instantaneous rotation rate of the vehicle, because we cannot obtain a good image when the instantaneous rotation rate varies too much, in particular when the combination of turn rate due to the translational motion and due to the swaying motion changes sign. Among the possible imaging intervals indicated by the response distortions, we select the one for which the rotation rate is most stable.

The rotation rate is estimated by forming an image over such a short duration that the image does not deviate too much from a line, so that it is almost a range profile. The angular deviation of the line from vertical varies in proportion to the instantaneous rotation rate. The imaging interval for the "slope" measurement must be chosen as a compromise between measurement errors when the absolute value of the angle is too small to permit a smooth measurement of the slope variations, and when the resolution of scatterers in the same range gate causes a falsification of the slope measurement (when a reasonably simple measurement method is used). The demands on the accuracy of the slope measurement are low because we are interested more in the variations of the rotation rate than its absolute value.

### 3.1.3 Illustration of Algorithms Based on Response Distortions

#### 3.1.3.1 Measurement of Response Distortions

The selection of the optimum imaging interval consists of two parts, the proper imaging time (start time rather than the center time), and the proper duration of the imaging interval. In this section we address only the problem of automatically selecting the imaging time.

We explained how we measure the distortions of three different responses in an image. There is still the question of how one should evaluate the distortion measurements on the three different responses. This requires formulating some plausible method, testing it on data, and perhaps modifying it until satisfactory results are obtained. Of course, with this type of empirical approach, one never can tell how much more the performance of the algorithms could be improved. One does it only when it is necessary, and this can be determined only by processing a sufficient variety of real data.

Figure 15 shows the distortion measurements performed on a file with the circling surrogate TEL. The top three plots give the distortions measured on the strongest responses in each third of the images generated in sliding window fashion, in this case with an imaging duration of 0.068 s. For each of the three plots, which apply for the three scatterers, the length of the positive bar at a particular starting time gives the magnitude of the distortion (percentage of search area filled by the response) for the right side of the response, and the negative bar for the left side. When a nearby response in the same range gate might be the cause of the "distortion", this is indicated by the symbol I. When the half-power width of a response exceeds two gates, so that no reasonable measurements can be made with our chosen algorithm, this is indicated by the symbol W. Distortions are truncated at 50%.

How do we evaluate the distortions of the three responses in a combined fashion? The fourth plot from the top gives one way, and the fifth plot another. In the fourth plot, at each time the positive bar represents the sum of the absolute lengths of the bars for all three scatterers, so that the response distortions for all three scatterers and both response sides are added. It represents the sum of three positive and three negative bars of the top three plots. This is a measure of the combined distortions for all three responses. We have found that better images can be obtained when the distortions remain low for an entire series of consecutive imaging times, rather than when they decrease to a low value from one imaging time to the next. For this reason, the negative bar gives the sum of the absolute lengths of the positive and negative bars and for all three responses, one imaging

time increment before and one after the one considered. Thus, it is the same kind of bar as depicted positive, except that it applies for the preceding and succeeding imaging times.

The bottom plot presents a variant. Instead of summing the absolute lengths of all bars at a given time, only the shorter bar is selected for each response. In other words, instead of presenting the sum of the distortions on both sides of a response, it takes into account only the side with the smaller distortion. This method largely circumvents the problem of what to decide when interference (I) is identified. We have adopted this second procedure, so that the bottom plot is used for selecting the best imaging interval.

A complication arises because we do not know a priori what imaging duration gives the best compromise between low distortions when the interval is short, and the improved crossrange resolution when the interval is long. Below we discuss the range of possible imaging durations, the shortest as well as the longest interval. For the present explanation of how the information presented in the distortion plots is used, we generate plots of the type in Figure 15 with different durations of the imaging interval.

The conspicuous fact in Figure 15 is that the distortions significantly increase with time. This makes rather obvious the problem of generating good images as the aspect angle increases. The response distortions, and hence the image quality, become worse as the aspect angle increases, as explained earlier. At the beginning of the file of the circling surrogate TEL, the response distortions are very low. However, at this point we do not know whether crossrange resolution is adequate, so that we may have to increase the duration of the imaging interval (a new plot). Toward the end of the plot, the distortions become so large that the image quality might not be adequate, in which case we would have to decrease the duration of the imaging interval. Of course, our intent is to select those imaging times that happen to have low distortions, even when the distortions ordinarily are high for a given aspect angle.

As an illustration, from Figure 15 we select an imaging start time of 68.22 s, at which time the bars of the bottom plot are very short. The resulting image is shown in Figure 16, after adjusting the crossrange scale so that the two edges are perpendicular to each other. The image is good enough to permit an accurate length measurement, even though the long illuminated edge is not well defined. It also appears to be good enough to measure the positions of the weaker scatterers. For example, when we take an image cut as indicated in the image, we obtain Figure 17. The top left plot shows that the responses along the short edge are sufficiently well resolved, so that the scatterer positions are measured accurately. If the resolution of the scatterers were inadequate, we would have to increase the duration of the imaging interval. However, we would then have to measure the response distortions for the new interval, and select a new starting time for the longer interval. It is unlikely that the old starting time would give a good image with the new interval duration. As an illustration, Figure 18 with the same starting time, but an interval duration of 0.094s. Note that the front end of the vehicle image is poorly defined for automated evaluation. When the plot of Figure 15 is rerun for the new interval duration, the corrected starting time is found to be 68.19 s. The corresponding image is shown in Figure 19. By comparison with Figure 18 the front end of the vehicle now is much better defined, despite the fact that the starting time was shifted by only 0.03 s.

At a much larger aspect angle, another good imaging time indicated in Figure 15 is 71.07 s. The corresponding image is shown in Figure 20, which is a relatively good image for such a large aspect angle.

Figure 21 gives the distortion measurements when the duration of the imaging interval is about double that in Figure 15. Examining the bottom plot, we find that the response distortions are higher, at least when they are low enough to be meaningful. This should be expected for the longer imaging interval. We also note that the best imaging times are somewhat changed, again as expected. For example, whereas for the shorter imaging interval one of the best imaging times is 68.30 s, it now is 68.05. The difference of 0.25 s is important for image quality. To demonstrate this, in Figure 22 we show the 0.137 s image of the circling surrogate TEL at 68.30 s, which is a good imaging time for the shorter imaging duration. It is not a good image. The image formed 0.25 s earlier is shown in Figure 23. It is evidently of much higher quality, despite the small timing difference.

We have demonstrated the selection of good imaging intervals based on the response distortions, without paying any attention to the way in which the rotation rate of the vehicle changes, which is the second ingredient to imaging interval selection. The reason is that such a refinement is not needed when the vehicle is turning, as in the above demonstrations, because the imaging intervals are short in relation to the variations in the vehicle motion, at least at the speed at which the surrogate TEL is circling. This refinement is needed when a vehicle goes straight, which should be the more frequent condition in practice. It might perhaps also be needed when a vehicle is turning at a higher speed than the vehicles of our examples.

### 3.1.3.2 Incorporation of the Measurement of the Rotation Rate

For our illustrations of how the combination of distortion and rotation rate (or "slope") measurements can be used to select the best imaging interval, we use the surrogate TEL on the smooth road. Even though the road is supposed to be "smooth", it is not so relative to the wavelength of the radar. The erratic motions of this vehicle greatly affect imaging because of the low turning Doppler, in contrast to when it is circling.

Figure 24 shows the distortion measurements for a 0.5 s imaging duration, together with the slope measurements. The distortions are measured in the manner that yields the bottom plot in Figure 15, that is, the sum of the distortions of the three responses for those sides with smaller distortions. As regards the distortion measurements, we want to select a time when the upper bar has zero or close to zero length, and the lower bar is as short as possible. If there are several such choices, we prefer a time within a longer stretch of good imaging times, rather than a good imaging time appearing between poorer imaging times (short bar between longer bars). For the slope measurement, we prefer a constant slope over a candidate imaging interval to a variable slope, a monotonically increasing or decreasing slope to a slope that reverses direction, and a slope that reverses direction once to one that changes it more than once. The times when the slope changes sign must be ruled out for imaging, because we would superpose an image formed over part of the imaging interval with a horizontally flipped version of an image formed over another part of the imaging interval. Among two times that show equally low distortions and good slope measurements, the choice should be based on a good behavior of the scatterers in the near part rather than the far part of the vehicle.

In Figure 24, we notice that the rotation rate changes its sign once, which means that the swaying Doppler overrides the rotational Doppler due to the motion of the vehicle as a whole for about half the observation interval. This means that the net turning rate must go through zero, which it indeed does around a time of 45 s. We cannot form an image during an interval when the net turn Doppler is zero or close to zero, because crossrange resolution will be insufficient. As an illustration, in Figure 25 we show the image of the surrogate TEL on the smooth road at a time of 45.0 s with an 0.5 s imaging interval. The main responses of the image are vertically arranged, almost like a range profile. There are spurious responses because different parts of the vehicle have individual motions even though the net turn Doppler is zero. The spurious responses can be predicted from the fact that the response distortions at 45.0 s are seen to be considerable in the top plot in Figure 24. The case depicted in Figure 24, where the net instantaneous rotation of the vehicle reverses only once during the dwell, does not present a problem because we have available two long sections when no reversal occurs. It is more detrimental when such a sign reversal occurs repeatedly during the dwell, because the imaging interval must not encompass any sign reversal. The extended imaging interval implies a considerable loss in available imaging times.

Figure 24 indicates that images formed at times of 42.15 s and 42.25 s should have the same quality, because at both times the upper bar of the distortion plot has about zero length, and there is only a minor difference between the slope functions included when the interval is shifted. The actual images are shown in Figures 26 and 27. The quality of the image in Figure 26 appears to be much better than that in Figure 27. However, a closer examination of the two images shows that the main difference is due to some spurious responses near the far end of the vehicle in Figure 27. Most of the stronger responses are the same in both images. Moreover, we "clean" an image of spurious responses by shifting the imaging interval slightly ahead and behind the ideal imaging time, and accepting only those responses that can be readily tracked over the overlapping imaging intervals.

At a time of 43.4 s, the slope measurements give similar results as for the preceding two times, but the distortion measurements indicate higher distortions for the preceding and succeeding intervals. This means that an inferior image should be expected, and this is verified by Figure 28 (compare with Figure 26). Figure 24 shows that a good image should also be expected at a time of 44.0 s, because the distortions are low and the slope does not vary much. However, the slope bars are only about half as long as those for the preceding examples, which means a proportionately reduced rotation rate and crossrange resolution. This expectation is verified by Figure 29, which is a good image but with less than desirable crossrange resolution. This issue is somewhat taken into account in the automated selection of the length of the imaging interval, in which the slope measurement plays a major role. Ultimately, however, the length of the imaging interval is governed by the need for sufficient resolution cells on the two illuminated edges of the vehicle. Both points will be discussed below.

As another illustration of how image quality can be predicted from the curves in Figure 24, we form an image at 47.3 s. Figure 24 shows low distortions at this time. The slope bars are negative rather than positive, are long (high turn rate), and vary monotonically. Thus we would expect an image which is flipped, has better resolution than the earlier images, and has

fairly good quality because the slope varies only monotonically (we would prefer no variation). The image in Figure 30 confirms our expectations. It is a flipped image with relatively high crossrange resolution, and the low density of responses indicates good image quality. The consequences of the slope variation can be illustrated by forming an image at 46.1 s, at which time Figure 24 shows low distortions but a rotation rate that increases and then decreases. This is worse than the monotonic drop over the imaging interval starting at 47.3 s, the earlier example. The corresponding image in Figure 31 shows a much reduced quality when compared with Figure 30.

For the preceding illustrations, we selected mostly good imaging times. To show that the curves in Figure 24 also correctly predict the poor imaging times, in Figure 32 we show the image when Figure 24 gives relatively high distortions and a variable slope. It would be difficult to obtain measurements of much significance from this image. Another example of a poor imaging time indicated by Figure 24 is given in Figure 33. Such images are not good enough for vehicle identification, but at least they indicate an elongated shape of a vehicle. We shall show far worse images below.

For a given rotation rate, if we want higher crossrange resolution for a better definition of the vehicle outline, we must increase the duration of the imaging interval (for the same lengths of the slope bars). A 30% increase changes little, so in Figure 34 we show the distortions and the (same) slope measurements for an imaging interval increased by 76% to 0.88 s. There are few times with small distortions, as would be expected from the fact that it is difficult to find longer intervals during which the motion happens to be benign. A good imaging time is seen to be 43.9 s, both with respect to the level of distortions and the constancy of the rotation rate. The corresponding image is shown in Figure 35. The long illuminated edge now is much better defined than in any of the preceding examples, which fact can be automatically determined from the quality of a fit to a straight line. To show how critical the selection of the imaging interval is, in Figure 36 we show the image only 0.1 s later. This is a poor image if we want to orient the two illuminated edges perpendicular to each other (the direction of the short edge is indicated with a considerable error) and exploit more than the strongest responses.

A still longer imaging interval does not produce good images at any time during the dwell. Figure 37 shows the distortions and the slope for an imaging interval of 1.16 s. There is no time when the distortions are very low (below 10%), and it makes little difference when one chooses the imaging time, the image quality is always poor. As an example, the image for an imaging time of 43.1 s is shown in Figure 38. The long edge is too poorly defined to obtain the correct crossrange scale factor, and many response positions are poorly correlated with those of the good image in Figure 33, even in range. The image in Figure 35 is the image to select from the present data set, and the selection would be based on the distortion/slope measurements rather than on manual inspection.

#### 3.1.3.3 Image Time Selection under More Demanding Conditions

The variety of imaging conditions is almost unlimited. A straight motion on an uneven terrain or road, a large aspect angle, a relatively high speed, and a flexible vehicle pose the greatest challenge. The variety of data we have available is not large enough to determine what the worst-case conditions are, but indicate that the circumstances under which moving ground vehicles

must be imaged will often be quite poor. For a demonstration that our approach to imaging interval selection also works under worse conditions than illustrated so far, we select data on a 5 ton truck, which is flexible and probably empty (more erratic motion than when loaded), on a straight bumpy road.

Figure 39 shows the distortions and slope for the truck on a straight bumpy road. We first select the imaging times with the lowest distortions, and then examine the slope measurements for these times. This results in the Table 1.

Table 1. Evaluation of Distortions and Slope.

<u>Time (s)</u>	<u>Slope</u>
102.30	monotonically decreasing, higher
102.75	inverted U, lower
105.73	U shape, lower
106.05	sign change
106.25	sign change

With the distortion levels about equally low at the listed optimum times for distortion, the evaluation of the imaging time depends on the slope behavior. At the time of 102.3 s, the slope is monotonically decreasing, with a relatively high starting value. At the time of 102.75 s, the slope monotonically decreases to zero, so no sign change occurs; but the values are low for crossrange resolution. At 105.73 s, the slope has U shape and the values also are low. At 106.05 s, the slope is low and changes its sign. At 106.25 s, we have the same conditions as at 106.05 s.

From Table 1, the best quality image should be obtained at 102.3 s, even though the slope changes too much to obtain a good image. The quality of the images at 102.75 s and 105.73 s should be comparable and lower than at 102.3 s, and too low for automated identification. The images at the other times should be too poor to be utilized in any way.

The predicted best image for an imaging interval of 0.2 s is shown in Figure 40. The length of the vehicle, as measured by the line drawn in the figure (offset from the edge for clarity), gives the length of the truck very accurately. Crossrange resolution is lower than desirable, so that one might try longer imaging intervals. The image at 105.75 s is shown in Figure 41. Taking the leftmost response as coming from the leading edge, we still can estimate (at least manually) the length of the vehicle as indicated, but crossrange resolution again is too low. We must test whether an increase in the imaging interval, for better crossrange resolution, leaves the responses sufficiently clean for a usable image. The image at 102.75 s is shown in Figure 42. As expected, it is of comparable (poor) quality with Figure 41.

The expected poor-quality image at 106.05 s is shown in Figure 43. The image might not appear to be inferior to the images in Figures 41 and 42. However, whereas these images allow an accurate length measurement, for the image in Figure 43 there is an error of 16%. At the last time of 106.25 s, the slope plot in Figure 39 indicates (barely discernible on the scale of the plot) that the slope changes its sign twice during the 0.2 s interval, which implies a further degradation of image quality. Figure 44 verifies the expectation. It is a totally useless image.

Note that the reason for these illustrations was not that we are trying to utilize images in which we can at best determine the vehicle length and a few range positions of scatterers. Rather, we merely wanted to demonstrate how well the distortion/slope curves permit one to judge the expected image quality even when the quality is extremely low.

As long as an imaging interval provides a usable image, even though of a lower quality than desirable, we want to determine whether an increase in the duration of the imaging interval might give a better image. This means that we derive the distortion/slope plots for a longer interval, and determine whether the distortions are low enough for some imaging times, and the slope has an acceptable behavior at these times. Since crossrange resolution in our best image, Figure 40, is not high enough for a good definition of the illuminated edges, and for very accurate measurement of the ranges of the scatterers, we must try increasing the duration of the imaging interval. The lack of crossrange resolution also is expressed by the fact that the number of the stronger image responses in Figure 40 is lower than what would be expected for the truck. It should be higher than eight, perhaps double.

The distortions and slope plots for a 30% longer imaging interval are shown in Figure 45. The times with the lowest distortions are 102.35 s, 104.6 s, and 106.03 s. At the second time, the distortions increase rather sharply for the next time increment, and at the third time the slope changes its sign within the imaging interval. The only good imaging time thus is 102.35 s, for which the image is shown in Figure 46. It is not better than the image over 0.2 s, Figure 40, which could be anticipated from the fact that the 30% increase in the length of the imaging interval has led to a significant increase in the distortion level (compare Figures 39 and 45).

Nevertheless, both images would allow vehicle identification. They both give the correct vehicle length. Also important, the ranges of almost all responses in the two images are in good agreement. As a test of the performance of the distortion/slope plot, we shifted the imaging time in steps of 0.1 s over the entire dwell time, examined each image visually, and did not find additional "good" images we might have missed by strictly evaluating the results from the distortion/slope plot. The image quality generally was much worse, again as predictable from the distortions and slope measurements with the rules given earlier. A further increase of the imaging duration by 30% left the time of about 102.3 s as the only choice, but the longer distortion bar correctly predicted a degraded image quality.

#### 3.1.3.4 Imaging Time Selection for a Tractor/Trailer Combination

Perhaps the highest degree of vehicle "flexibility" occurs when a tractor pulls a trailer. We now consider imaging time selection for the Confuser of the Dragnet/MTE data set.

The distortions/slope plot for the Confuser on the bumpy road is shown in Figure 47, for an imaging interval of 0.468 s. Because of the flexible combination of the tractor and trailer, the selection of the correct imaging time now is particularly critical. Although the first consideration is small distortions, the behavior of the rotation rate, or the slope measurement, now is much more important than when the motion is more benign. In Figure 47, among all starting times with very low response distortions, if one asks which of the intervals of 0.468 s duration contain the simplest and smallest slope variations without a change in the sign, the starting time of 70.3 s is the

best, although not good because the slope variation is too complicated. Nevertheless, the interval gives the best obtainable image, shown in Figure 48. Despite the fact that the image of the tractor is offset in crossrange from the image of the trailer, the length of the observable part of the vehicle can be measured as indicated in the figure (the last segment of the flatbed cannot be seen at this aspect because its responses are too weak; it is an unrealistic vehicle). Although the crossrange positions of the responses have relatively little significance, crossrange resolution improves the accuracy with which the ranges of the various scatterers can be measured. This is very important for vehicle identification. The poor quality of the image thus does not imply that the vehicle cannot be identified.

In general, we choose the imaging duration by measuring the response distortions for progressively longer durations, and then determine whether the combination of low distortions and acceptable behavior of the rotation rate (slope) can be found at the longer durations. When the rotation rate varies considerably over the dwell time, we may fine-adjust the length of the imaging interval based on the slopes plot. As an example, in Figure 47 we note that low image distortions occur at a starting time of 73.95 s, but that the slope increases drastically at this time. Consequently, one would expect a low-quality image, as verified by Figure 49. This image is of little use for automated identification, although it does provide the range positions of the major scatterers. However, the long bar of the slopes plot in that interval implies a high instantaneous rotation rate, so that the imaging interval can be shortened. The complicated variation of the slope over the 0.46 s imaging interval then is avoided, so that the image quality should improve. This is verified by Figure 50, which is the image for a starting time of 73.90 s and an imaging interval of 0.21 s. The image is not only much better than that in Figure 49, but is almost as good as the image in Figure 48. It allows a length measurement, aside from the range positions of the stronger scatterers.

As can be deduced from the distortions plot in Figure 45, there are few usable images that can be formed of the Confuser on the bumpy road. Even the manual selection of a usable image would be very time consuming, because one cannot recognize at a glance whether the image contains features that would permit the adjustment of the crossrange scale and identification of the vehicle. In Figure 51 we show a typical image of the Confuser. Such an image cannot be interpreted even manually.

### 3.2 The Actual Procedure for Imaging Interval Selection

#### 3.2.1 The General Method

The preceding lengthy discussions and illustrations have shown the importance of selecting the correct imaging interval, and that one can replace the pattern recognition process used by an operator to find a usable image by measurements that can be automated. However, relying on response distortion measurements has several implementation problems. Perhaps the worst is that the duration of the imaging interval is unknown before the measurements, so that the distortions must be measured for an entire set of imaging durations. This is computer intensive. Furthermore, the quality of distortion measurements is degraded by the general lack of resolution in the images. When this is to be combined with the slope measurements, developing a good procedure for imaging interval selection is difficult. For this reason, we have modified our actual approach, making it simpler and improving performance. We have retained the detailed discussions of imaging interval selection based on

response distortions, because it illustrates the difficulties that must be overcome when usable images of moving ground vehicles are to be generated automatically. The modified approach will be the better appreciated.

The primary advance lies in the better design and utilization of the slope measurement, so that it can do essentially the entire job of interval selection. The distortion measurement is relegated to determining the maximum duration of the imaging interval, so as to ensure that the image responses represent scatterer responses rather than spurious responses.

The biggest improvement of the slope measurement algorithm comes from the realization that the imaging durations used for measuring the image slope must be so short that no significant averaging of the erratic motion of a vehicle takes place. It came as a surprise to learn from the data that perhaps the maximum duration for the type of data represented by the Dragnet/MTE set is about 0.05 s. This is clear from the fact that changes of that order in the timing or the duration of the imaging interval used to form the image for target ID already significantly affect the image quality. Basically, it may be argued that even for the short imaging duration used for the slope measurement, a change in the motion of the target not only affects the slope of the responses of the "image" but also its width. However, if the motion is smooth, the change in the width will also be smooth; and all we want to measure is the smoothness of the motion.

### 3.2.2 Illustration of the Chosen Procedure

Figure 52 shows an example of the refined slope measurements, with an imaging duration of 0.041 s. The vertical bars of the top plot give the image slopes measured as a function of time. For better visibility of these bars, Figure 53 gives an expanded view of the top plot of Figure 52. Before we discuss the significance of these measurements, we want to point out that the appearance of Figure 53 is in no way representative of a particular vehicle or conditions of motion. In this instance we find limited intervals of a relatively high turn rate of the vehicle, with many intervals during which the motion is far too slow for imaging. Even the same vehicle under different conditions might generate slope bars that are as frequently negative as positive, or slope bars whose amplitudes gradually increase or decrease rather than alternate between high and low. This is so because of the huge variations of motion conditions of ground vehicles. The example chosen here merely serves to explain our method.

We would like to image over an interval during which the motion is perfectly smooth, which implies a series of slope bars with equal height, or at least a height that varies minimally (perhaps 5 or 10%, at most). Usually one will find that such a set of slope bars can be found only over intervals too short for obtaining useful crossrange resolution. (This must be tested by forming an image and determining whether crossrange resolution is sufficient to have the short illuminated edge well defined.) If the interval over which we consider the slope measurement is long enough for the desired crossrange resolution, the quality of the image will degrade with deviations from constant-height slope bars. When the deviations are random, they will generate spurious responses, with the strength and number of spurious responses increasing with the deviation from constant height. If the slope bars have essentially constant height but some deviate significantly, the severity of the spurious responses will depend on the percentage of slope bars that fall outside the pattern. If the height of the slope bars changes

smoothly, the consequence will be a distortion of the image, with the distortion increasing as the variation in the length of the bars increases. This behavior allows us to select the best imaging intervals, both start and end times, from measurements such as shown in Figure 53.

As a first example, consider the three bars (the fourth shown in Figure 52 is separated by a gap) starting at 25.85 s in Figure 53. Their heights vary little enough to give a good image, provided crossrange resolution is sufficient to define the short illuminated edge. The corresponding image is shown in Figure 54. The short illuminated edge is well defined, and so is the larger part of the long illuminated edge. This is a good image for a vehicle going straight.

Next, consider the three bars starting at 25.5 s. Their heights again vary little, but crossrange resolution might be too low if the phasing of the scatterers differs from that of the preceding example. The associated image is shown in Figure 55. The short illuminated edge is not as well defined as in Figure 54, but well enough for our purposes.

The group of 12 bars starting at 24.3 s is well behaved, but 4 bars have substantially different amplitudes. This should give an acceptable image with somewhat more spurious responses than in the previous two images. The corresponding image is shown in Figure 56. Whereas the images of Figures 54 and 55 each have 17 responses, Figure 56 has 19 responses.

The group of responses starting at 21.5 s has an acceptable height variation, but it is smooth rather than random. Thus we would expect a somewhat distorted image with relatively few spurious responses. The image of Figure 57 shows that the visible part of the long edge is bent. The total number of responses is 16, lower than in any of the preceding images.

We can easily demonstrate that the above are the only usable imaging intervals. For example, if we image over the two bars starting at 15.95 s, we combine the problem of low crossrange resolution with that of a flipped image. Figure 58 gives the corresponding image. The image is much worse than any of the images shown above.

Imaging in the regions where the bars are low is totally impossible, because we need a long interval to obtain sufficient crossrange resolution, but the bars vary too much, often changing their signs. As an example, Figure 59 shows the image when the interval starts at 16.1 s and has a duration of 0.5 s. The image is evidently useless for automated target identification.

The interval starting at 17.3 s and extending over the three bars shown in Figure 53 is poor because only three bars out of six that would fill the interval have significant strength. The corresponding image is shown in Figure 60. It is not suitable for target identification, at least not as suitable as the good images shown earlier.

As a last example, consider the set of bars starting at 22.5 s. The heights of the strong bars are quite constant, but too many bars are weak. This interval is unsuitable for imaging, as verified by Figure 61.

These examples demonstrate that the slope measurement is a reliable indicator of image quality. Moreover, the criteria by which we select the imaging intervals are easily automated. The automated selection of the imaging intervals is shown by the horizontal bars of the lower plot of Figure 52. The lower the bar in the plot, the higher the expected image quality. A comparison of the images shown above verifies that the lowest horizontal bars in Figure 52 do indeed give the best imaging times.

We can now explain the main reason why we switched from the primary use of the distortion measurements to the utilization of the slope bars, even though the distortion measurements give good results. The plot of slope bars immediately shows the maximum extent of a potential imaging interval, by simply observing the variation of the heights. With the distortion measurements, we must determine the usable duration of the imaging interval as a function of time, and this requires computationally intensive rerunning of the measurements for an entire set of imaging durations, starting with the shortest possible duration and ending with the longest possible duration. This is not only computationally intensive, but the measurements are not easily evaluated automatically. The approach via the slope measurements is much simpler.

Despite this emphasis on the slope measurements, the distortion measurements have not become irrelevant. Even though we have included many examples in this report, there still are many conditions that we have not illustrated. The slope measurements shown in Figure 52 illustrate a case where the possible imaging intervals are all relatively short. There are situations in which a good sequence of slope bars may extend over a much longer interval, but the slope measurement is not sensitive enough to let one recognize when the spurious responses become a problem in these cases. Hence, whatever imaging interval one may select on the basis of the slope measurements, one must verify that spurious responses will not interfere with target identification. This is done by measuring the response distortions. Since the measurement is performed only on a small part of the data, it is not computationally intensive.

#### 4. USE OF THE IMAGES FOR VEHICLE IDENTIFICATION

Although the objective of the work reported here is to automatically find optimum imaging intervals, one cannot ignore the ultimate goal of vehicle identification. We will summarize our plan, based on our experience under this program.

Under the best circumstances, we obtain an image in which the vehicle outline is well defined and undistorted (after adjusting the crossrange scale factor). We can measure the length and width of the vehicle, the positions of the stronger scatterers in the range/crossrange plane, and the characteristics of the strongest scatterers (primarily the dimensions).

Images of the next level of quality still let us recognize the vehicle outline, so that length and width of the vehicle can be determined. The difference relative to the best class of images is that the crossrange positions of the stronger scatterers are too uncertain to utilize for vehicle identification. Only the range positions will be accurately measurable. Thus we can use length and width of the vehicle for identification (primarily length), and the range positions of the stronger scatterers. Even aside from the length and width measurement, this will give much improved performance over that obtainable from range profiles only. First, because scatterers in the same range cell are resolved in crossrange, the measured range positions are more reliable and more accurate. Second, delayed and other spurious responses often make it impossible to determine the "end" of the target in a range profile. This problem is solved with two-dimensional imaging, because we will discriminate the spurious from the genuine responses, using sliding-window imaging and response tracking around the optimum imaging time. Third, we will know the aspect angle of the vehicle relatively well from the image,

so that the search during the identification is restricted to a small aspect angle sector. We have not studied the question whether for this kind of image quality one can determine the characteristics of the strongest scatterers.

The third level of image quality comprises those images for which, because of the bending of the vehicle, the long illuminated edge will not be straight. It might be curved, have S form, or be broken when one part of the vehicle is offset in crossrange from another (the example of the Confuser). Such an image still allows the measurement of vehicle length and of the ranges of the stronger scatterers; this is sufficient for vehicle identification.

A similar level of image quality is obtained if the vehicle twists so that the crossrange scale derived from the front end of the vehicle does not apply to the rear end. When both near and far short edges are visible in the image, as is sometimes the case, the fact that they appear parallel to each other is a good indication that the outline is undistorted. When they do not appear parallel to each other, one knows that the two ends of the vehicle move differently. We have found the best approach to be the averaging of the crossrange scale factor obtained from the two vehicle ends.

The next level of image quality is defined by images which do not permit the recognition of either of the two illuminated edges, so that dimensional measurements cannot be performed. In our examination of all data files we have on the Dragnet/MTE data, we have always been able to find imaging intervals that permitted dimensional measurements (the objective of automated imaging interval selection); thus we do not know whether this situation is of practical interest. If this should be the case, however, the ranges of the scatterers are still meaningful and can be used for vehicle identification. It is similar to identification on the basis of range profiles, but will give improved performance because crossrange resolution improves the measurement of scatterer ranges.

The lowest level of image quality arises when the erratic motion of a vehicle creates a great number of spurious responses, so that not even the ranges of the scatterers can be utilized for identification. We have no reason to think that this situation might occur when the imaging interval is properly selected.

## 5. SUMMARY OF THE AUTOMATED SELECTION OF THE IMAGING INTERVAL

### Step 1: Slope Measurements and Evaluation

If target ID is to be performed after all the data were collected, as in a conventional SAR system, the slope measurements are run on the entire data file. If the system is to operate such that data collection stops when the target can be identified, consecutive data segments of about 1 s duration are analyzed in the same manner, with overlap between consecutive segments in case the best imaging time is at the boundary of a segment. The software finds the best imaging intervals by evaluating the sequences of slope bars, ordering the intervals in accordance with the expected image quality.

### Step 2: Evaluating Crossrange Resolution

The software determines whether the selected imaging intervals provide sufficient crossrange resolution, starting with the best interval selected from the slope measurement. An image is formed over that interval. A second image is formed with the imaging interval advanced by 20% of its duration, and

a third image with the interval delayed by 20%. The range/crossrange positions of the 20 strongest responses of the central image are found, and it is determined whether the same responses also exist in the two other images, and are close to the positions in the central image. Those responses whose positions closely agree in all three images are retained. The others are eliminated from the (central) image.

A straight line is fitted to the long illuminated edge, and it is noted whether the line is at one side of the vehicle image (responses away from the line mostly on one side), or whether the fit goes more or less through the center of the image (responses away from the line on both sides of the line). A search for the near short (illuminated) edge as well as one for the far short edge are attempted, by rotating lines through the last scatterers on the fitted line. It is determined whether or not at least one other point lies on either of the two rotated lines, so as to define either the near short edge, the far short edge, or both.

The entire process is repeated for the imaging intervals with lower qualities, until at least several intervals that give images with sufficient crossrange resolution have been found, or all candidate imaging intervals as obtained from the slope measurements have been tested.

### Step 3: Selection of the Final Image

If only a single image that meets the selection criteria has been found, this becomes the image used for identification.

If several candidate images have been found, their qualities are evaluated by noting (1) whether the straight-line fit to the long edge gave a one-sided fit (long edge well defined), or a two-sided fit (long edge not well defined). In the first case, it is determined over what part of the range extent of the image the fit to the long edge is good (response on the line or away from the line). It is also noted whether only one of the two short edges was found, and by how many responses a short edge is defined. When both edges were found, it is also noted to what degree they are parallel to each other.

The image qualities are ordered as follows, should multiple candidate images be available:

- (1) Well-defined long edge, both short edges visible, and parallel to each other.
- (2) Well-defined long edge, both short edges visible, not parallel to each other.
- (3) Well-defined long edge, one short edge defined by more than two responses.
- (4) Well-defined long edge, one short edge defined by two responses.
- (5) Long edge defined only for the front part of the vehicle.
- (6) Long edge defined only for the rear part of the vehicle.
- (7) Long edge not defined, both short edges defined.
- (8) Long edge not defined, only one short edge defined.

In case multiple possible choices are available, the best image in accordance with the above ordering becomes the image for vehicle identification. If more than one image are available, and none is much superior to the others, identification is based on several images of comparable quality.

The image or images selected in accordance with the above procedure are used to measure the aspect angle of the image and the dimensions of the target. For the use of scatterer positions (and characteristics) in the identification process, each image is tested via the distortion measurements. If the response distortions are too large to be sure that spurious responses are not a problem, the duration of the imaging interval is reduced until the response distortions are low enough. It does not matter if in this process the responses defining the short edges disappear.

#### 6. STATUS OF AUTOMATION AND VALIDATION

We have completed the automation of the distortion and slope measurements, and will soon complete the automation of the specification of imaging intervals from the combination of these measurements. We have validated the automated measurements by comparing them to interactive analysis of several complete Dragnet/MTE data files, representative of the motion conditions in the data set. Once we have automated the specification of imaging intervals, we will validate this and the measurements by applying the automated code to all the Dragnet/MTE data files we have available, and verifying that the selected intervals do yield images of good quality. We will determine, as a function of motion conditions, the fraction of examined cases that are problematic.

#### 7. AVAILABLE TARGET DATA

We are aware of only two available large scale collections of high-resolution SAR data on moving ground vehicles, the Dragnet/MTE and AMSTE collections. Unfortunately, most of the former data and all of the latter were collected for vehicles moving in circles, which is not representative of the motions likely to be encountered in practice. We have examined a large quantity of Dragnet/MTE data as well as AMSTE data of one target moving through one circle. The data quality of both sets is acceptable. We will divide the available AMSTE data into three nonoverlapping sets: an initial training set, a set for verification and validation, and a sequestered set for demonstrating performance. Our current plan for the three sets is given in Tables 2 through 4.

Table 2. Initial Training Set.

Target	Speed	Pol	Dep Ang
T-72 w/o Skirts	12	HH	8
T-72 w/Skirts	12	HH	8
T-72 w/Reactive Armor	12	HH	8
ZSU D13	12	HH	8
ZSU w/Antenna Rotating	12	HH	8
Zil Flatbed E10	12	HH	8
2S1	12	HH	8
Scud	12	HH	8
M2	12	HH	17
BTR-80 Antenna Down	12	HH	17
BTR-80 Antenna Up	12	HH	17

Table 3. Verification and Validation Set.

Target	Speed	Pol	Dep Ang
T-72 w/o Skirts	20	HH	8
T-72 w/Skirts	20	HH	8
T-72 w/Reactive Armor	20	HH	8
ZSU D13	20	HH	8
ZSU w/Antenna Rotating	20	HH	8
Zil Flatbed E10	20	HH	8
2S1	20	HH	8
Scud	20	HH	8
M2	20	HH	17
BTR-80 Antenna Down	20	HH	17
BTR-80 Antenna Up	20	HH	17

Table 4. Test Set.

Target	Speed	Pol	Dep Ang
T-72 w/Reactive Armor	12	VV	8
T-72 w/Reactive Armor	20	VV	8
T-72 w/Skirts	12	HH	10
T-72 w/Skirts	20	HH	10
T-72 w/o Skirts	12	HH	10
T-72 w/o Skirts	20	HH	10
ZSU (Antenna On)	20	HH	10
ZSU (Antenna Off)	12	HH	10
ZSU (Antenna Off)	20	HH	10
Zil Flatbed (Loaded)	20	HH	10
Zil Flatbed	12	HH	17
Zil Flatbed	20	HH	17
Zil Flatbed	12	VV	17
Zil Flatbed	20	VV	17
2S1	12	HH	10
2S1	20	HH	10
Scud	12	HH	10
Scud	20	HH	10
M2	12	VV	17
M2	20	VV	17
BTR-80 (Antenna Down)	12	VV	17
BTR-80 (Antenna Up)	12	VV	17
BTR-80 (Antenna Down)	20	VV	17
BTR-80 (Antenna Up)	20	VV	17

01.03 last action: Edit

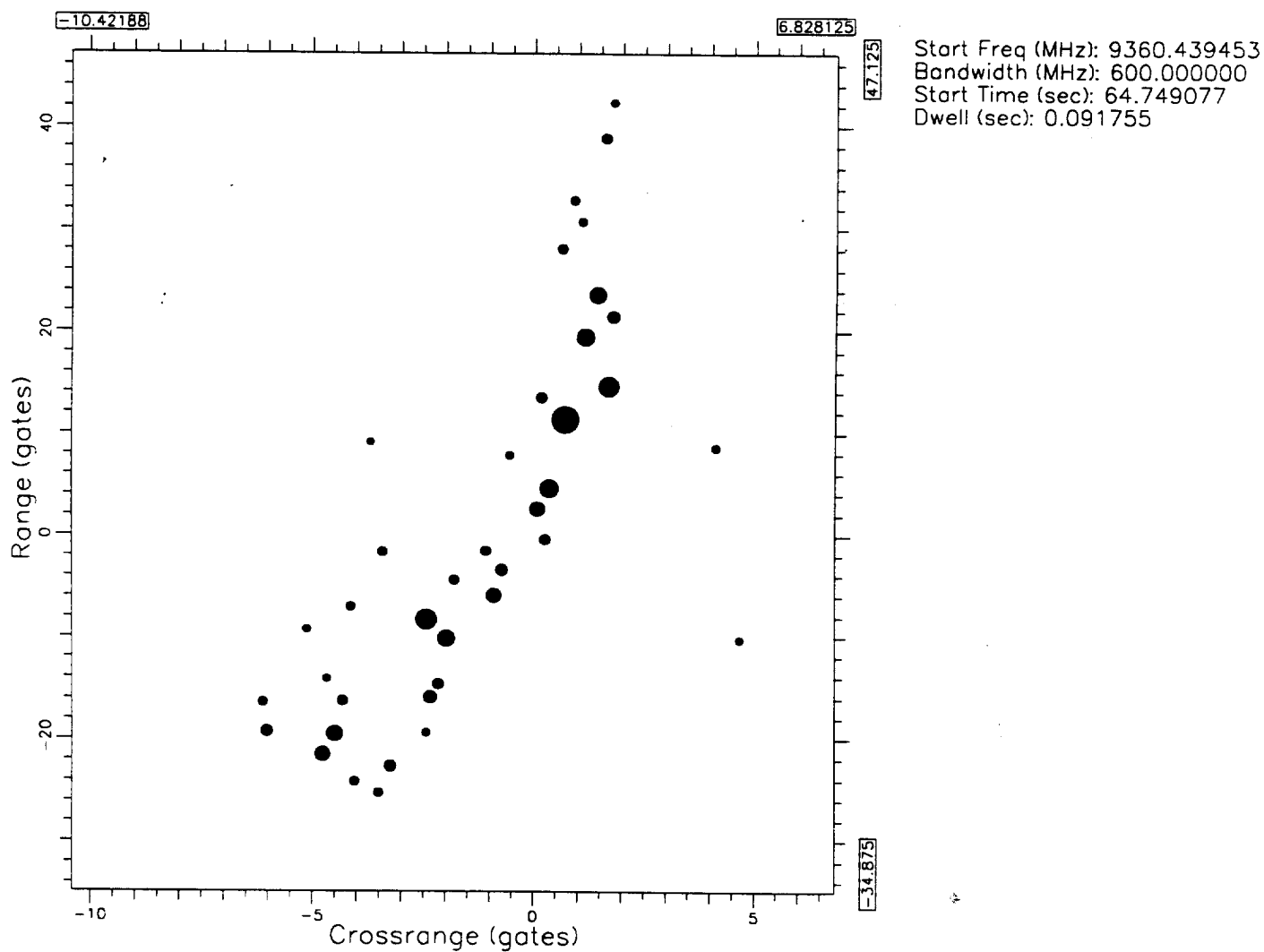
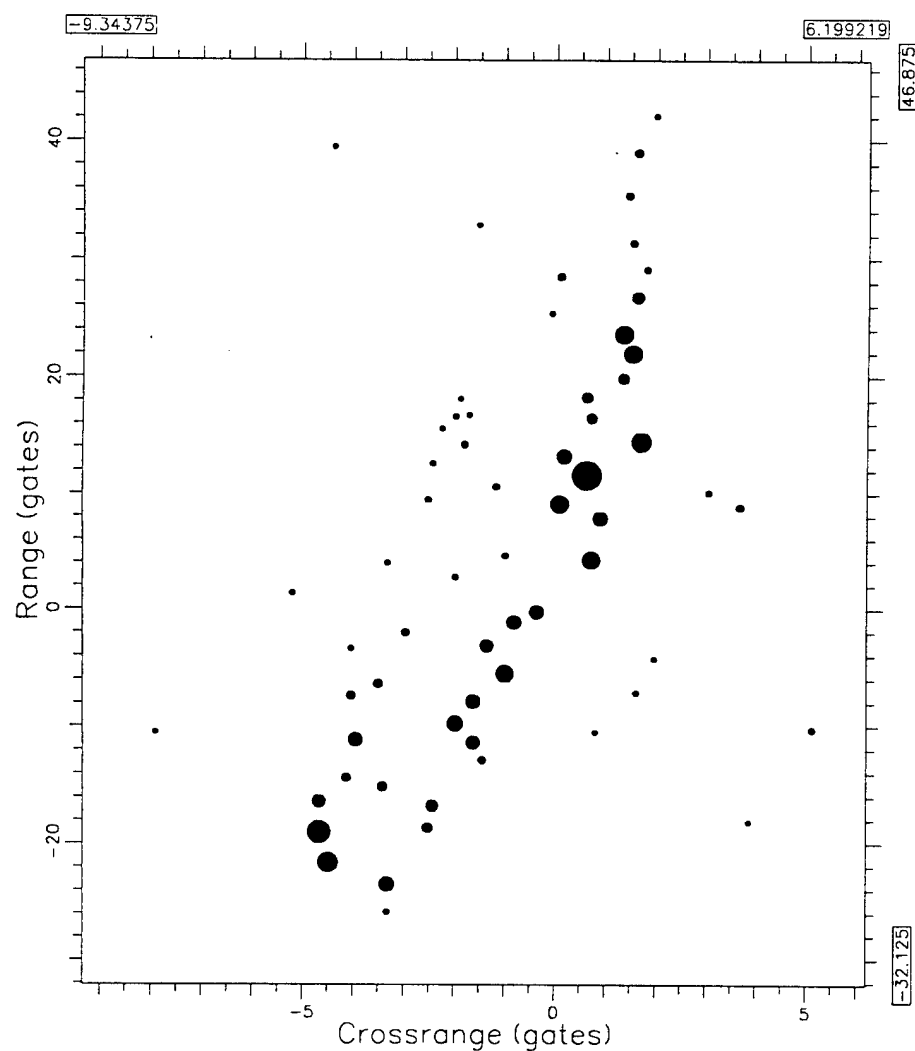


Figure 1. Image of Turning Surrogate TEL at Small Aspect Angle.

0302

last action: Edit

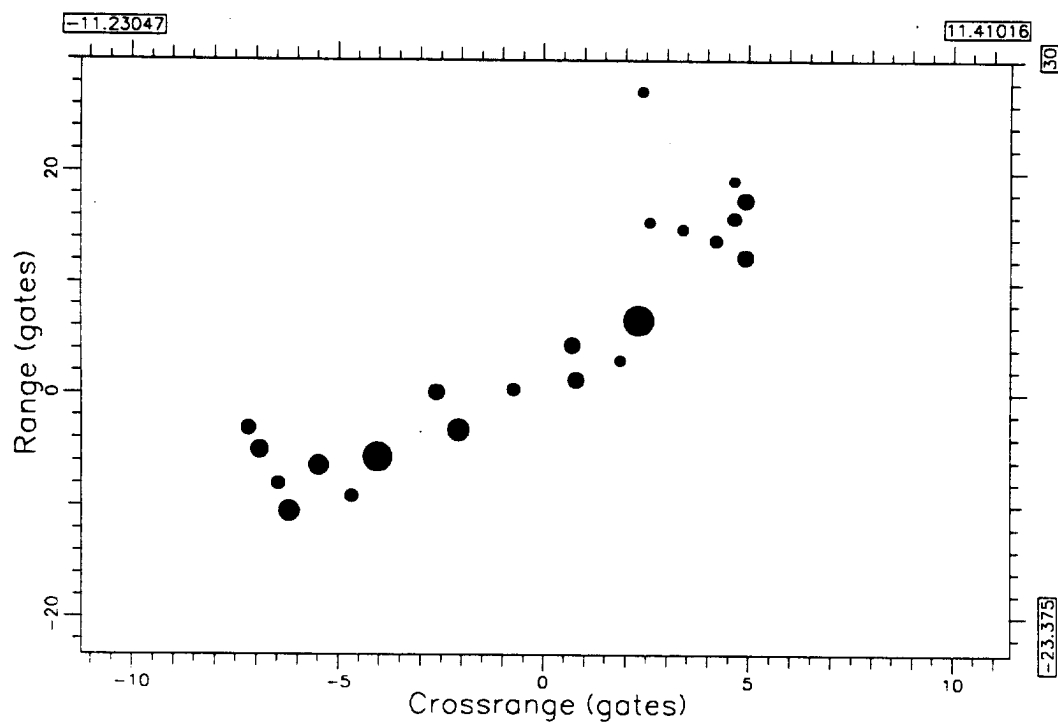


Start Freq (MHz): 9360.439453  
Bandwidth (MHz): 600.000000  
Start Time (sec): 64.800941  
Dwell (sec): 0.091755

Figure 2. Surrogate TEL Image 0.05 s Later than in Figure 1.

0103

last action: Change Peak Scaling

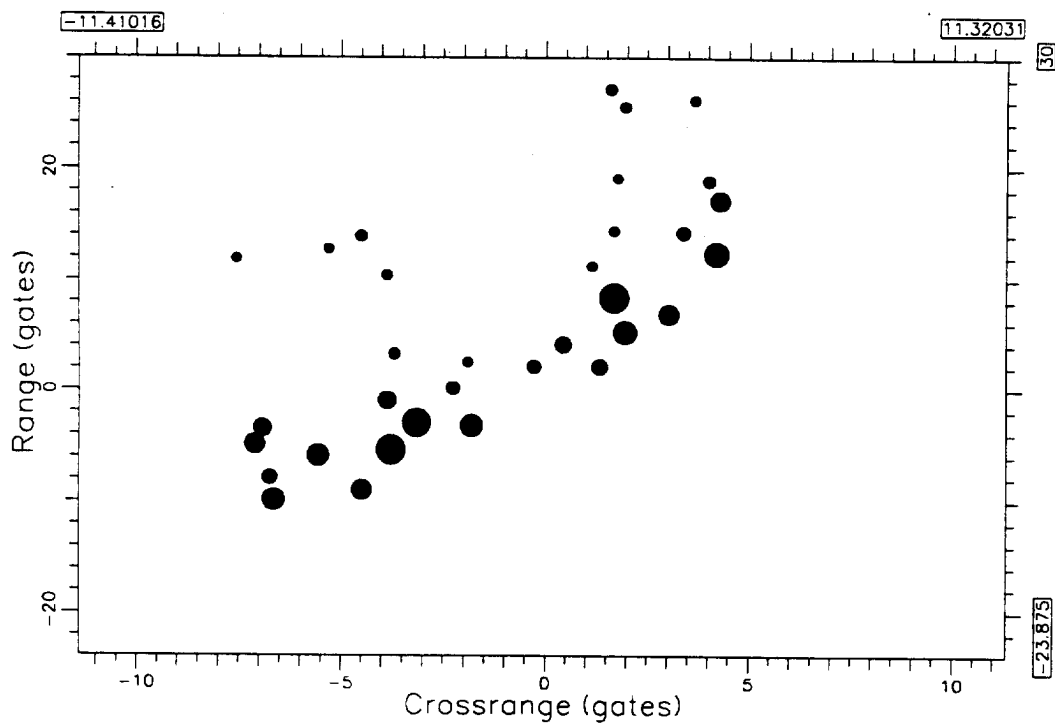


Start Freq (MHz): 9360.439453  
Bandwidth (MHz): 600.000000  
Start Time (sec): 68.199852  
Dwell (sec): 0.091755

Figure 3. Surrogate TEL Image at a Larger Aspect Angle.

0102

last action: Edit

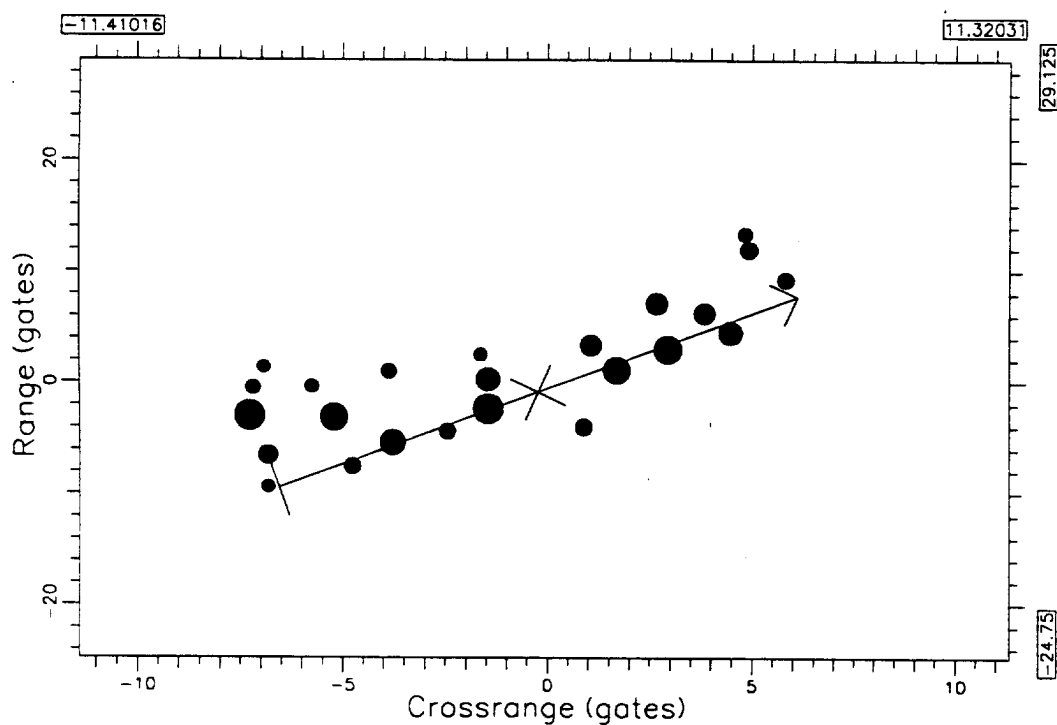


Start Freq (MHz): 9360.439453  
Bandwidth (MHz): 600.000000  
Start Time (sec): 68.299583  
Dwell (sec): 0.091755

Figure 4. Surrogate TEL image 0.1 s Later than in Figure 3.

0105

last action: Change Peak Scaling



Start Freq (MHz): 9360.439453  
Bandwidth (MHz): 600.000000  
Start Time (sec): 69.201172  
Dwell (sec): 0.091755

Figure 5. Surrogate TEL Image 1 s Later than in Figure 3.

0117 lost action: Change Peak Scaling

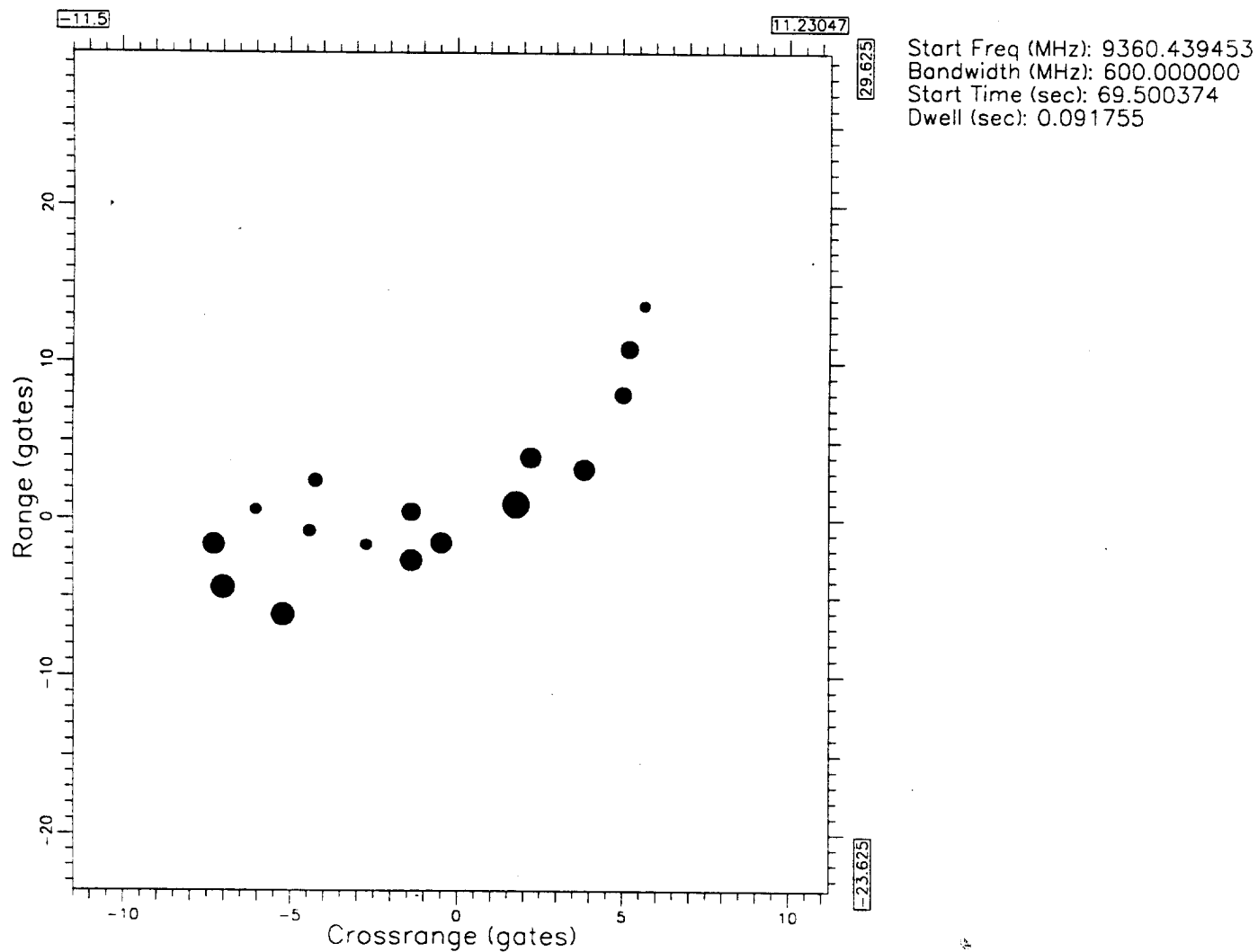


Figure 6. Surrogate TEL image 0.3 s Later than in Figure 5.

0301

last action: Edit

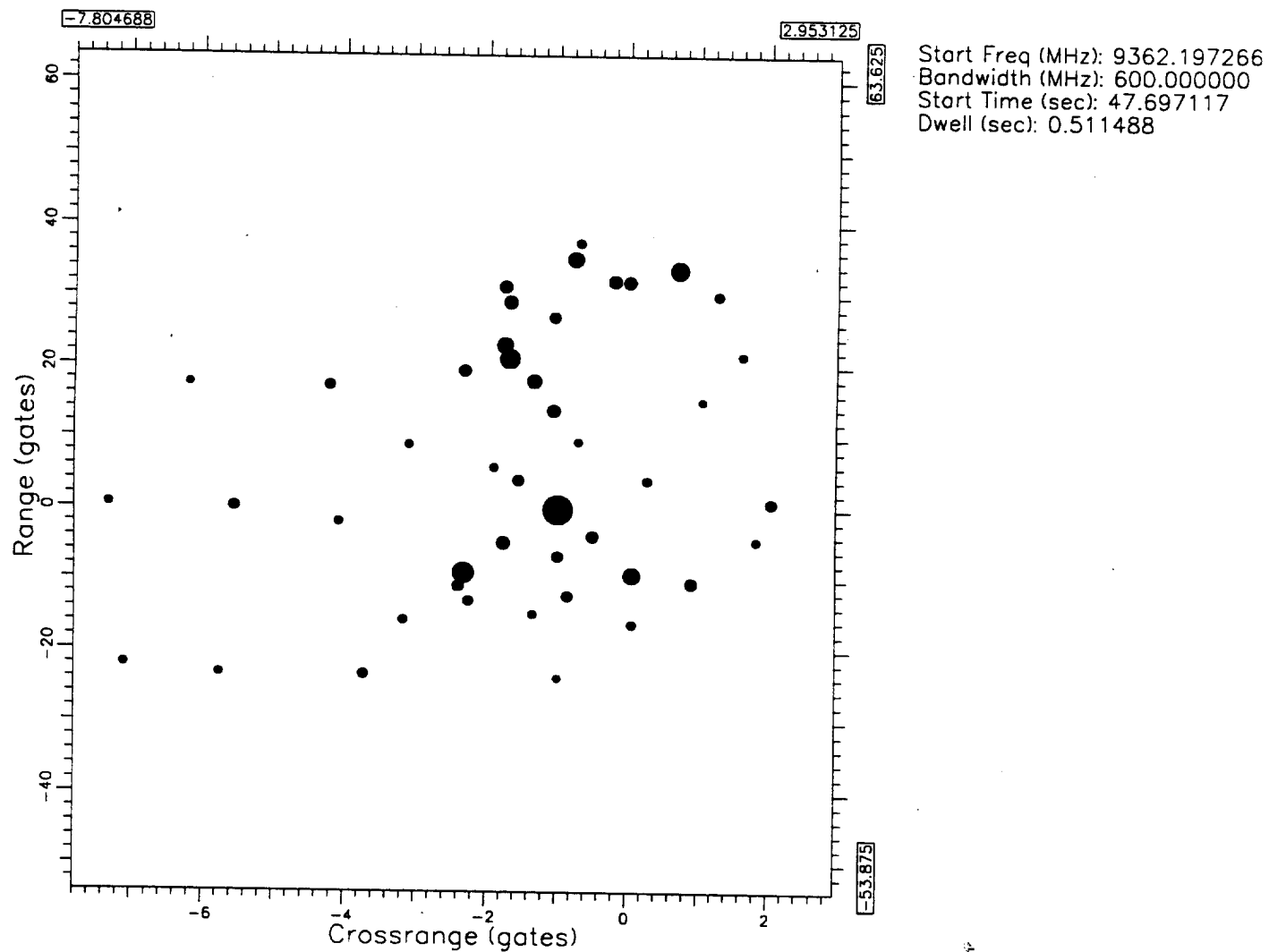
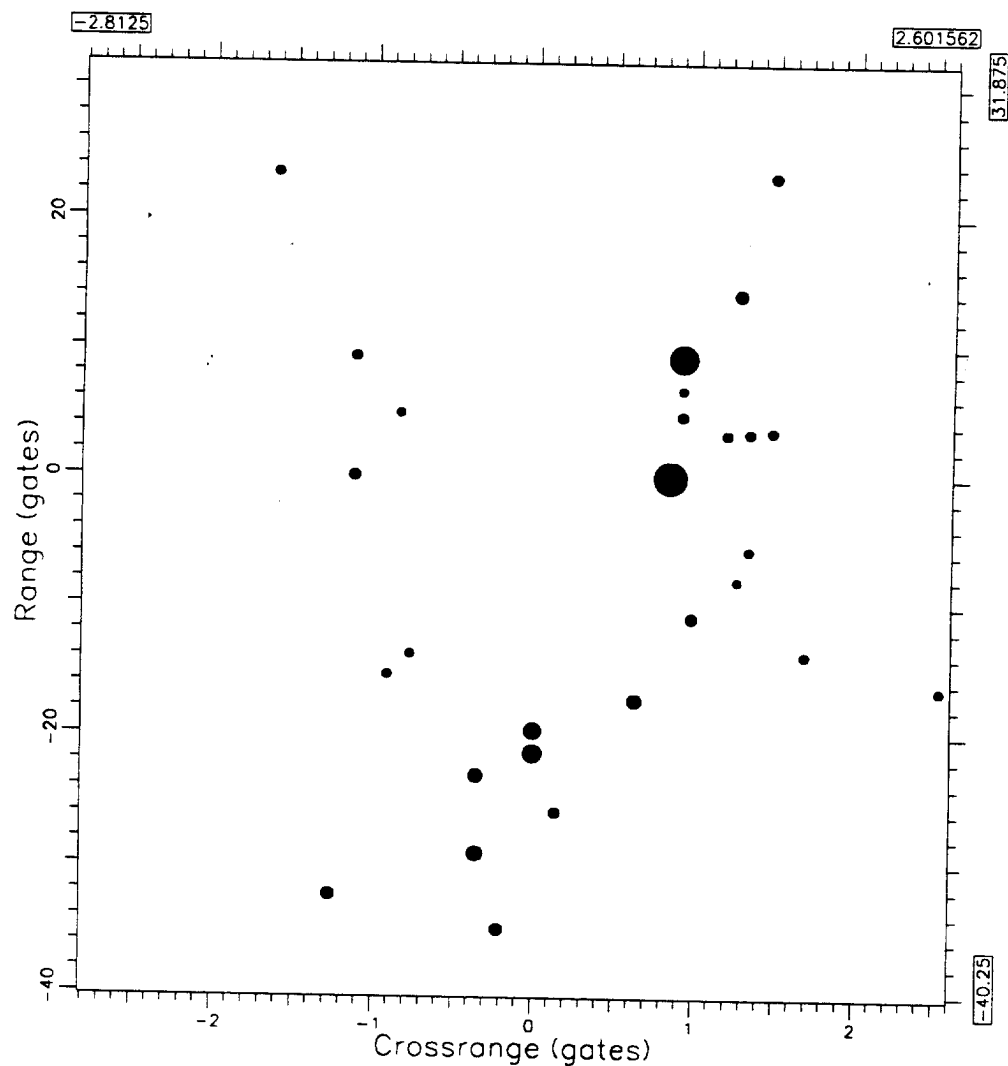


Figure 7. Image of the Surrogate TEL on a Bumpy Road.

0103

last action: Edit



Start Freq (MHz): 9362.197266  
Bandwidth (MHz): 600.000000  
Start Time (sec): 48.805340  
Dwell (sec): 0.511488

Figure 8. Surrogate TEL Image 1.1 s Later than in Figure 7.

0103

last action: Edit

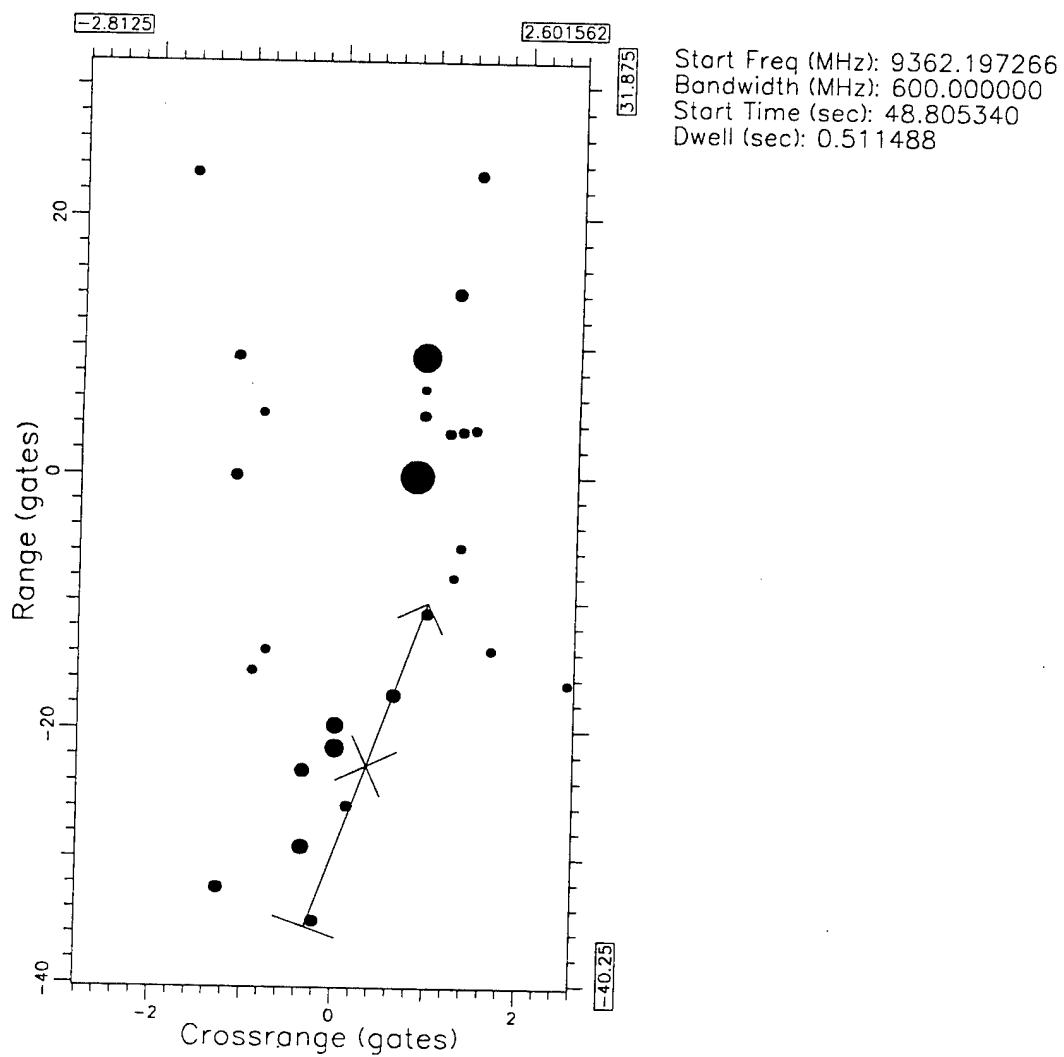
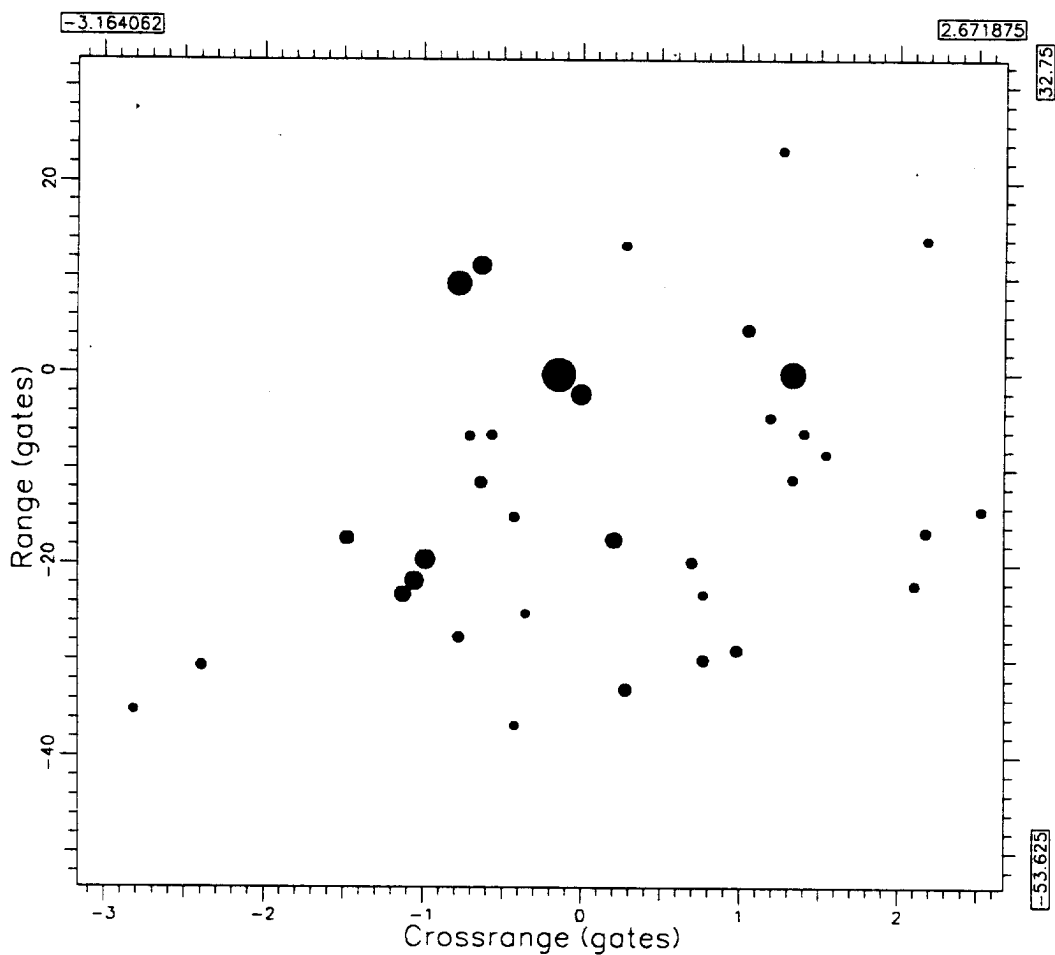


Figure 9. Image in Figure 8 after Adjustment of Crossrange Scale Factor.

0304

last action: Edit



Start Freq (MHz): 9362.197266  
Bandwidth (MHz): 600.000000  
Start Time (sec): 49.089500  
Dwell (sec): 0.511488

Figure 10. Surrogate TEL Image 0.3 s Later than in Figure 9.

010501 last action: pk params/n xhrs

Position	Width	Skewness
0.731	1.089	1.017

#### Image Cut Information

Length of cut (gates)	11
Sample spacing (gates)	0.250
Crossrange pivot point (gates)	0.730
Range pivot point (gates)	11.430
Angle (deg)	0.000
Bias	0.000

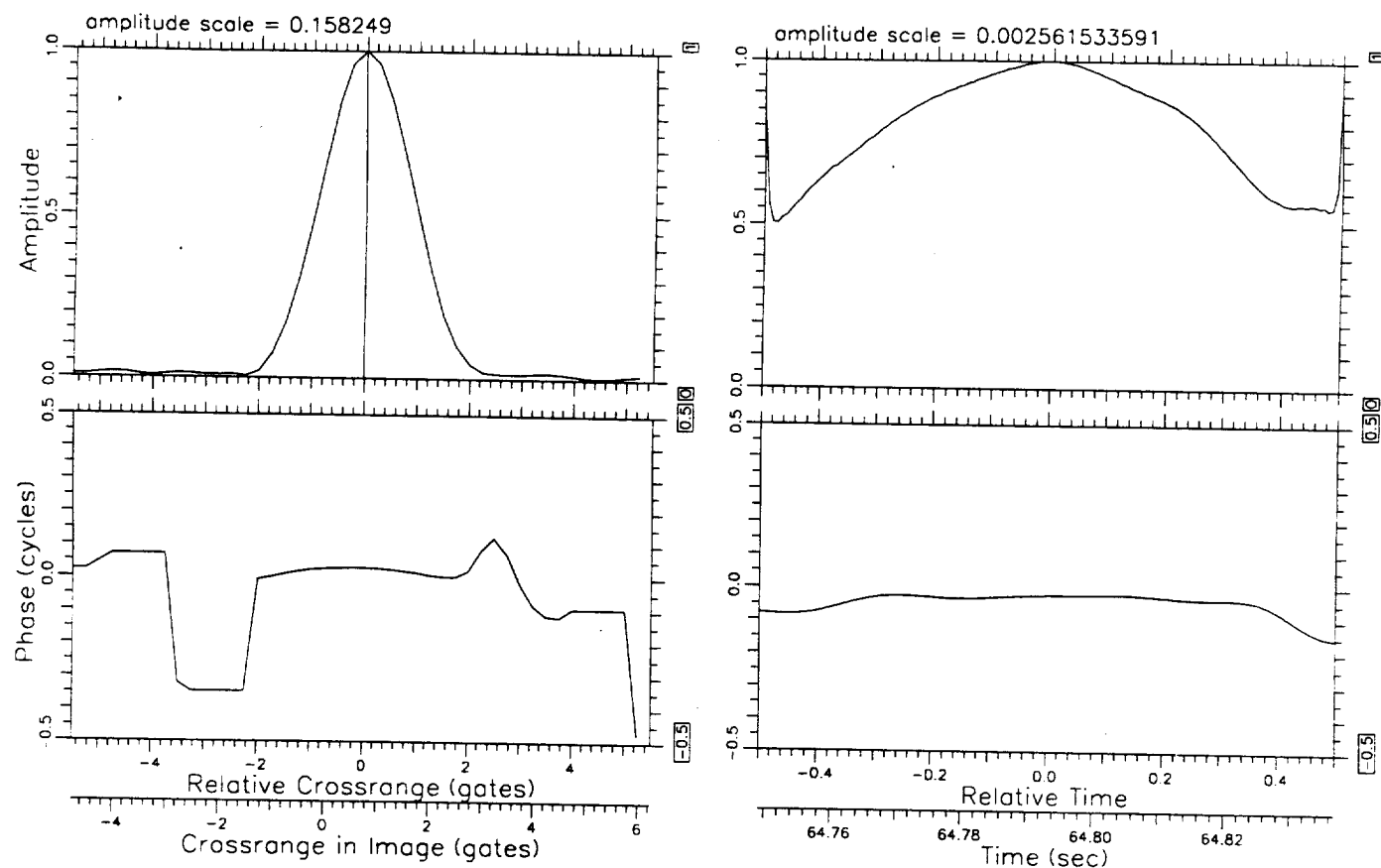


Figure 11. Image Cut and Transform for Range Gate 11.4 in Figure 1.

010301 last action: pk params/n xhrs

Position	Width	Skewness
0.658	1.123	1.126

Image Cut Information	
Length of cut (gates)	12
Sample spacing (gates)	0.250
Crossrange pivot point (gates)	0.630
Range pivot point (gates)	11.710
Angle (deg)	0.000
Bias	0.000

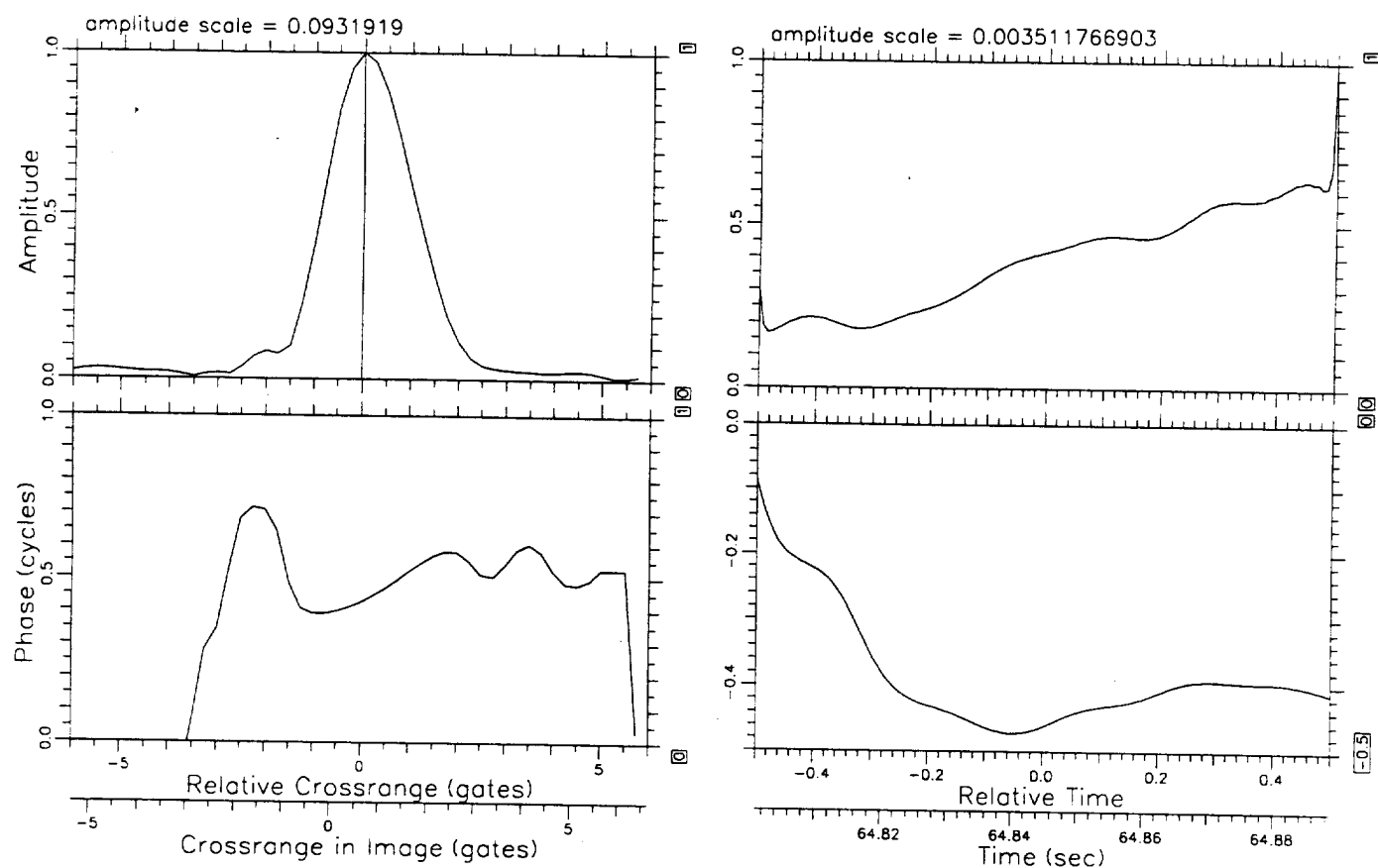


Figure 12. Image Cut and Transform for Range Gate 11.7 in Figure 2.

010400

last action: Initialization

# Image Cut information

Length of cut (gates)	10
Sample spacing (gates)	0.250
Crossrange pivot point (gates)	0.850
Range pivot point (gates)	0.040
Angle (deg)	0.000
Bias	0.000

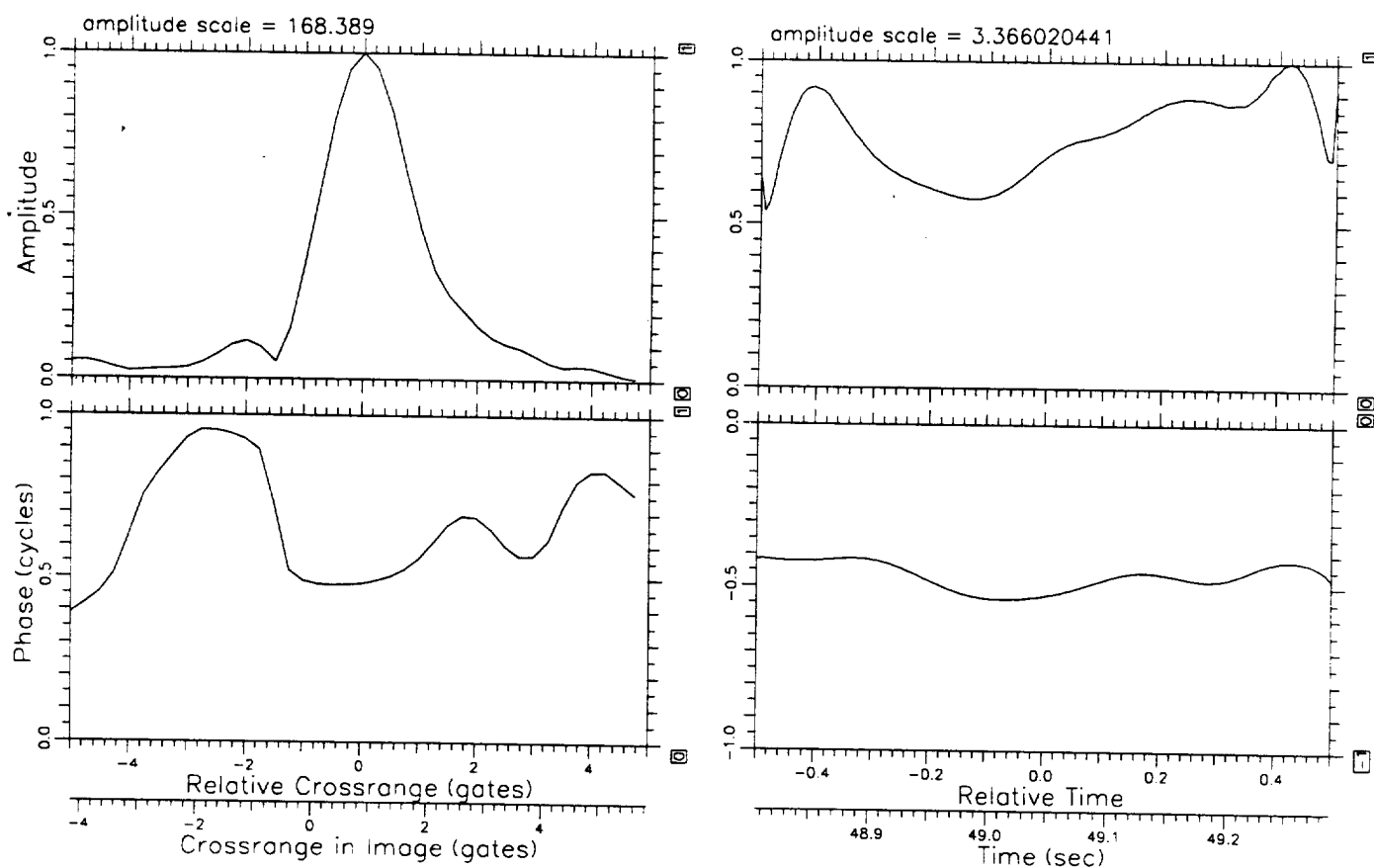


Figure 13. Image Cut and Transform for Range Gate 0 in Figure 8.

010302 last action: measure phase slope

xhr0	xhr1	slope	rms	pk dev	bias
-0.414	-0.156	1.398	0.015	0.024	0.000
0.008	0.453	-0.583	0.018	-0.033	0.000

Image Cut Information	
Length of cut (gates)	10
Sample spacing (gates)	0.250
Crossrange pivot point (gates)	-0.980
Range pivot point (gates)	0.060
Angle (deg)	0.000
Bias	0.000

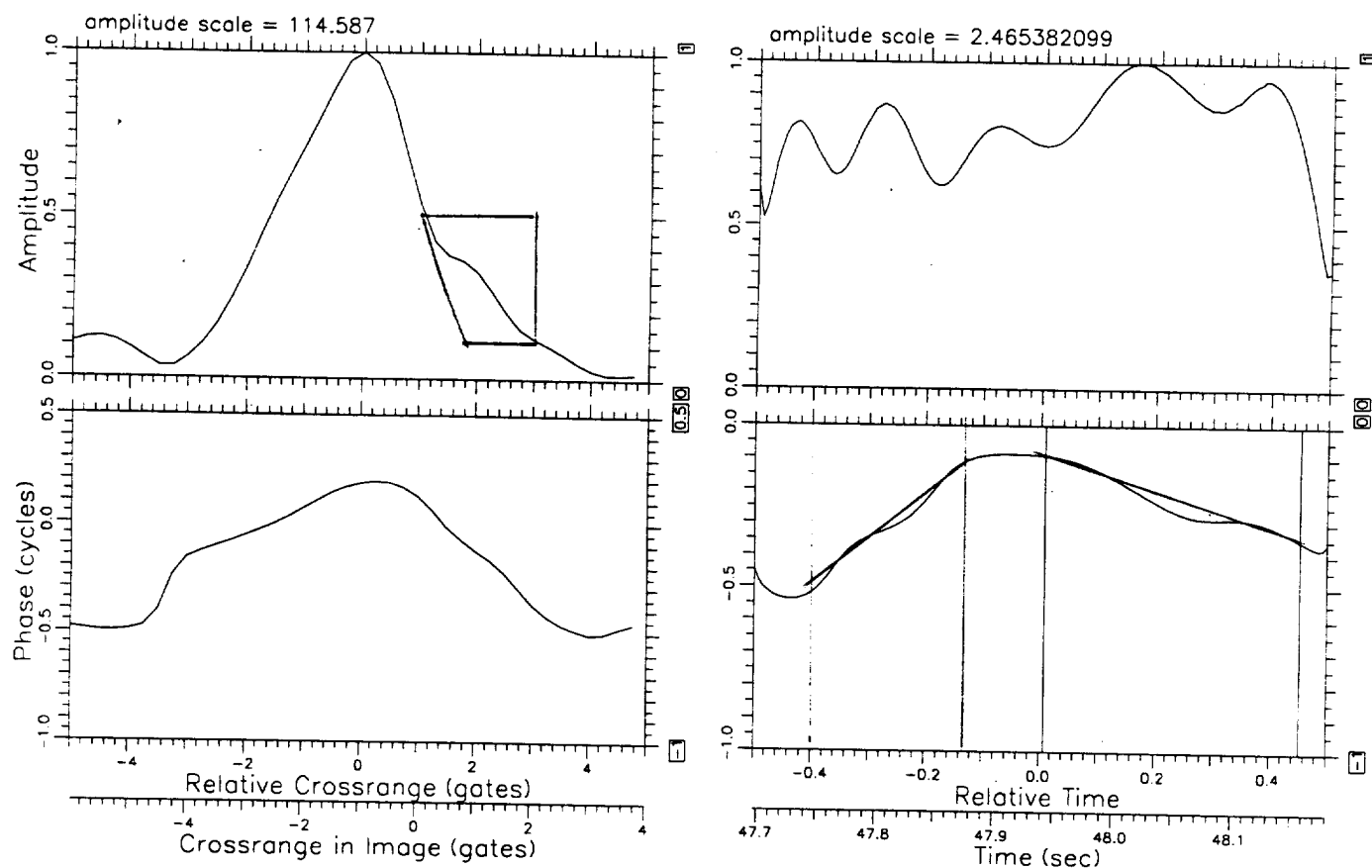


Figure 14. Image Cut and Transform for Range Gate 0.1 in Figure 7.

Continue

Switch XY

Zoom x2

IngDur 0.068

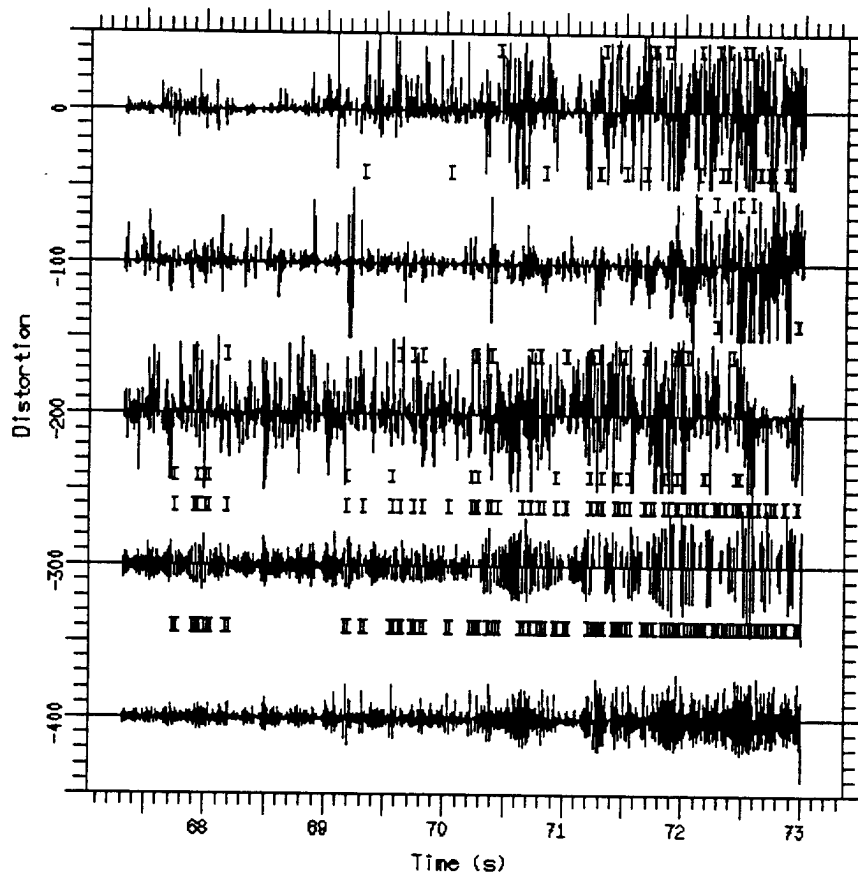
/bos/usr3/awr/dra/dra106a90rcv1rdd.pfx

14:52:14

Scott 1.

Scott 2.

Scott 3.

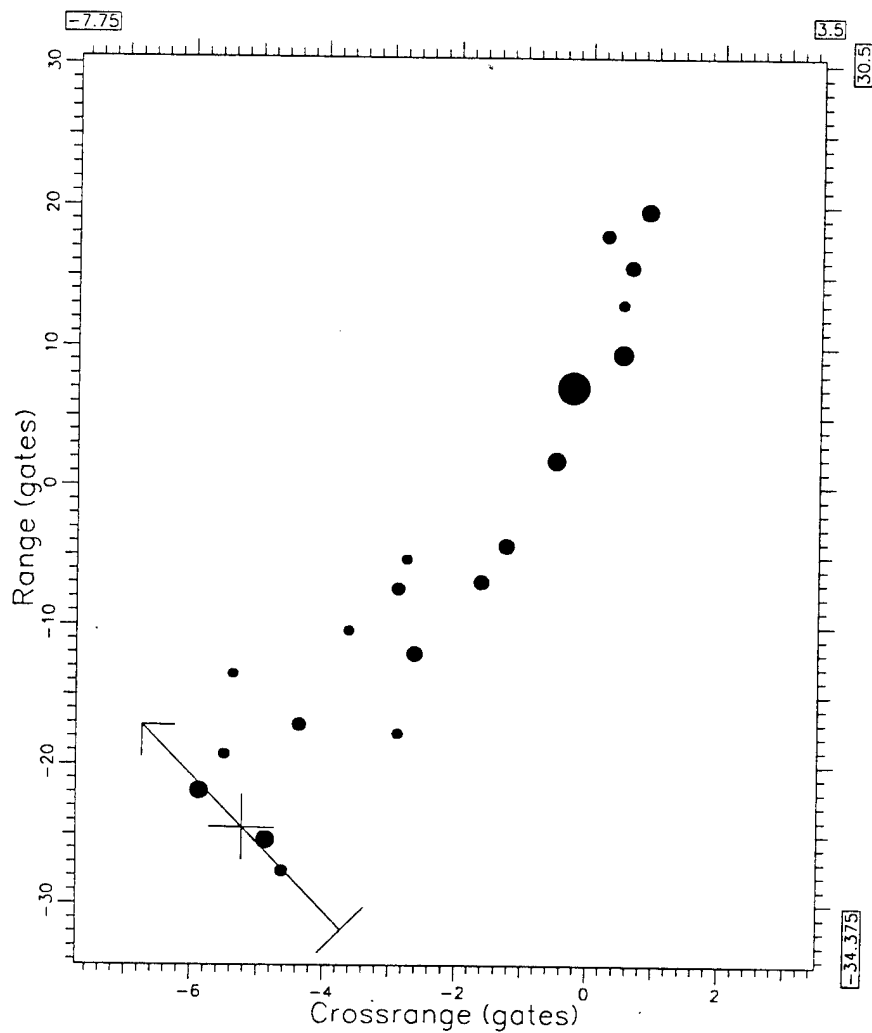


25-Feb-02 14:52:10

Figure 15. Distortions for the Circling Surrogate TEL.

0103

last action: Compute Cut



Start Freq (MHz): 9360.439453  
Bandwidth (MHz): 600.000000  
Start Time (sec): 68.217941  
Dwell (sec): 0.068267

Figure 16. 0.068 s Image at 68.22 s.

010300

last action: Initialization

Image Cut Information	
Length of cut (gates)	15
Sample spacing (gates)	0.250
Crossrange pivot point (gates)	-5.230
Range pivot point (gates)	-24.530
Angle (deg)	101.600
Bias	0.000

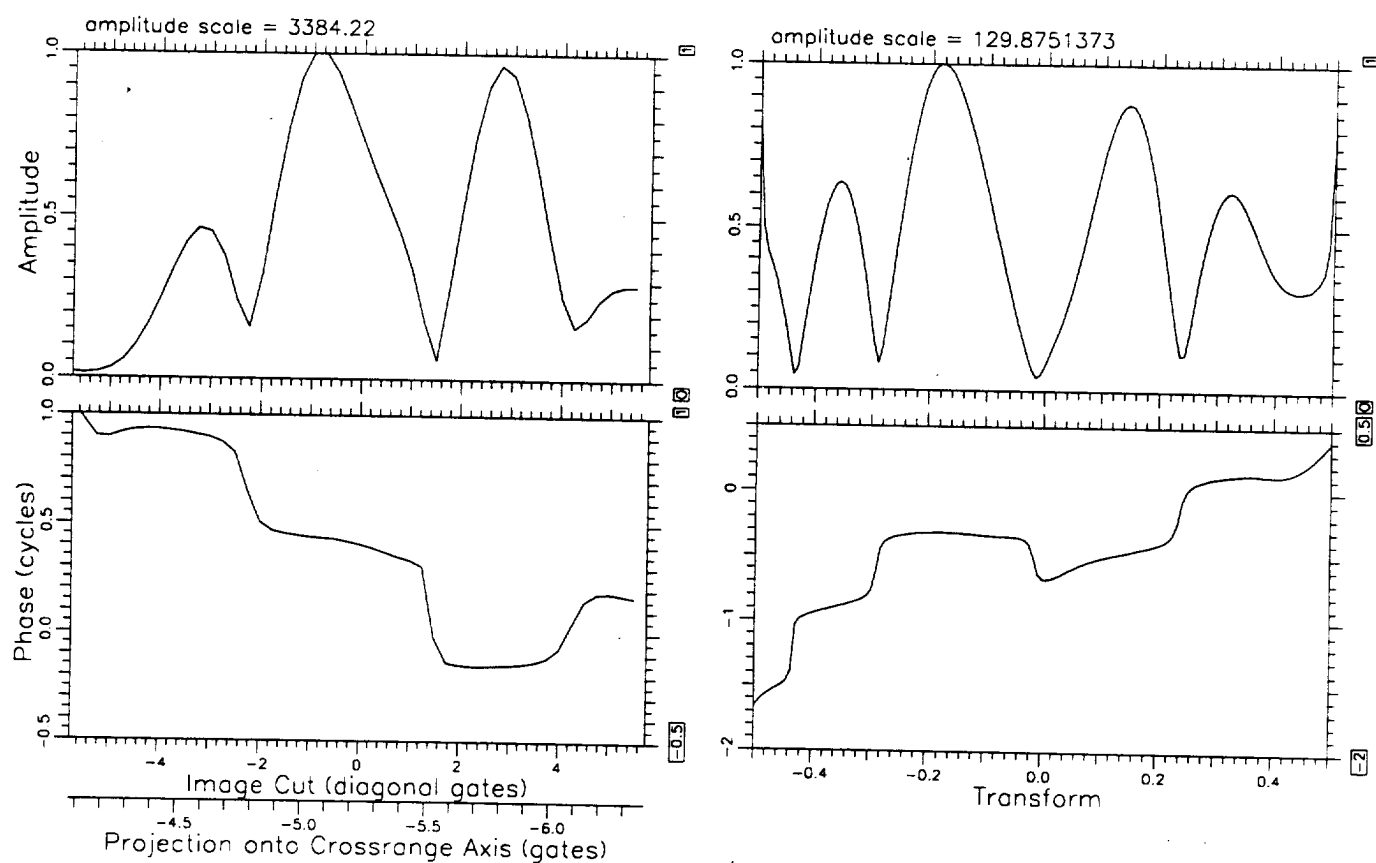


Figure 17. Image Cut and Transform Along the Line in Figure 16.

0102 last action: Edit

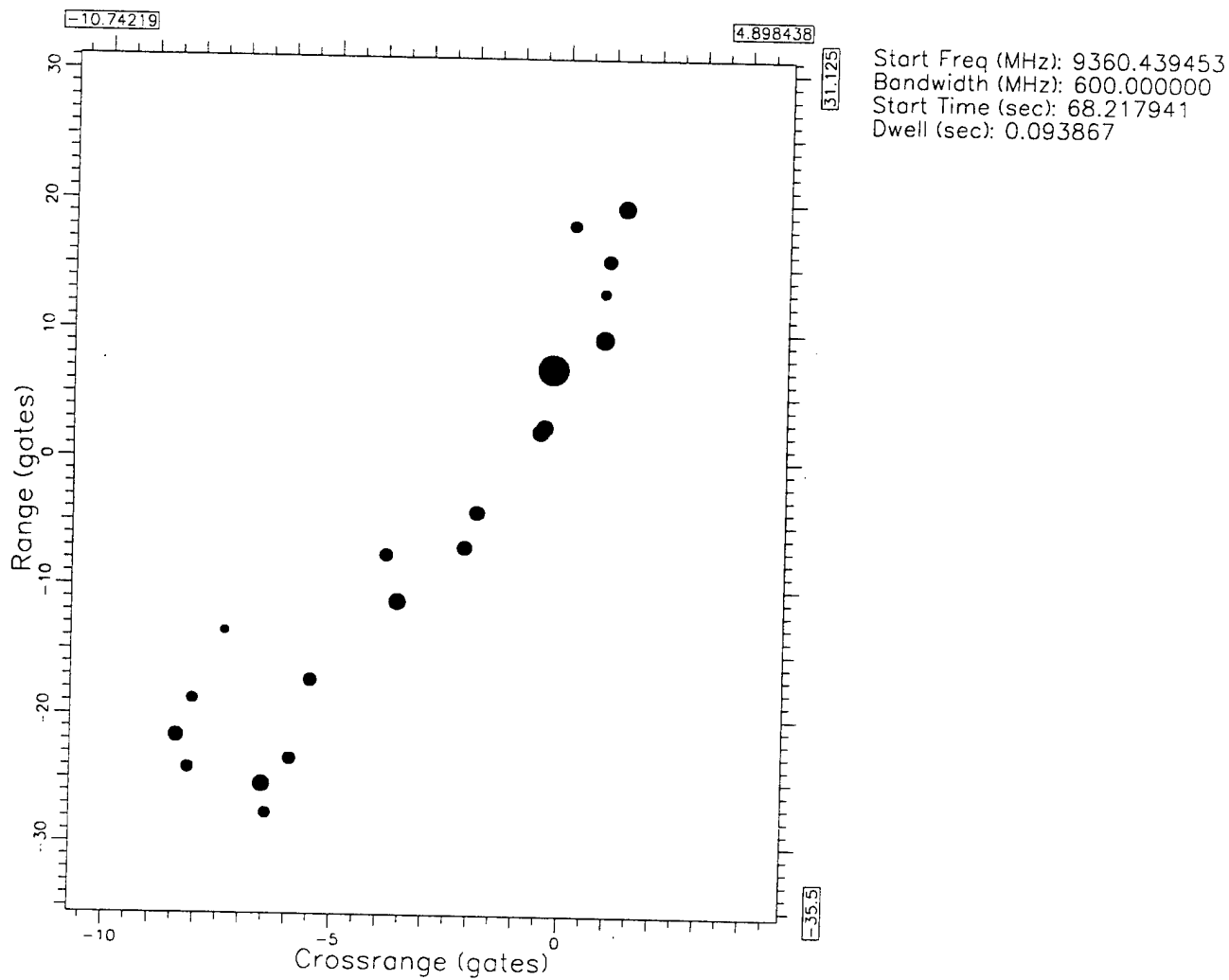
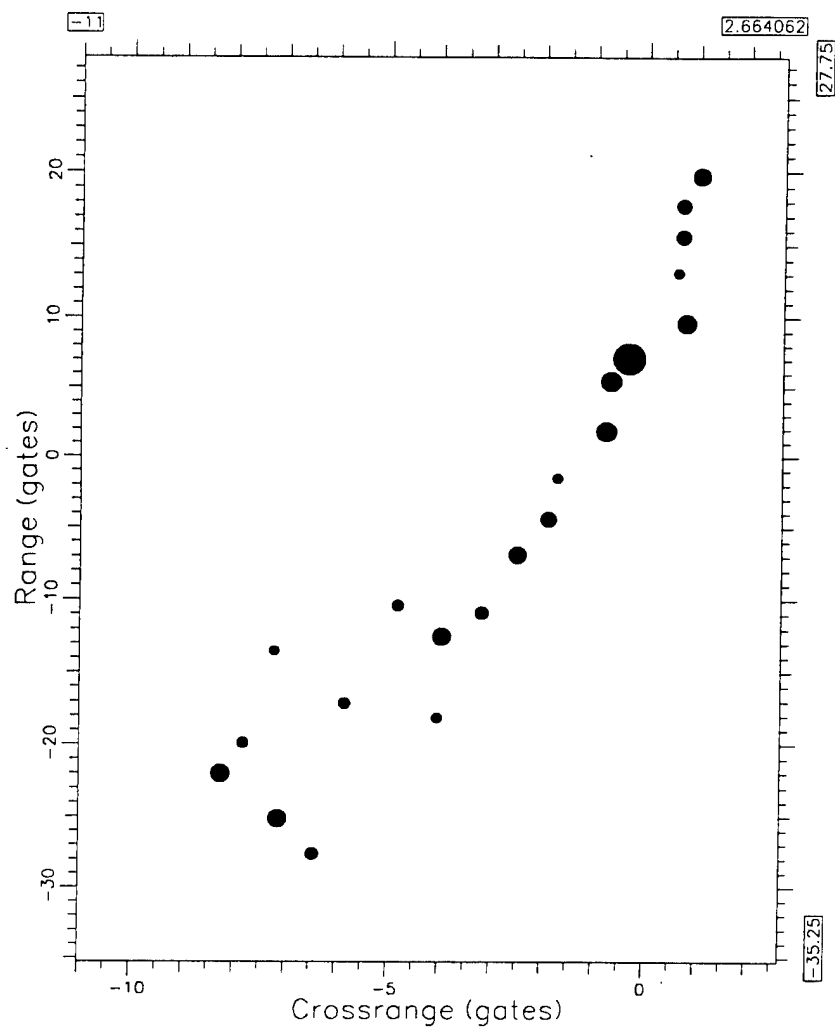


Figure 18. Image with the Same Starting Time as that of Figure 16 but an Interval Duration of 0.094 s.

0302

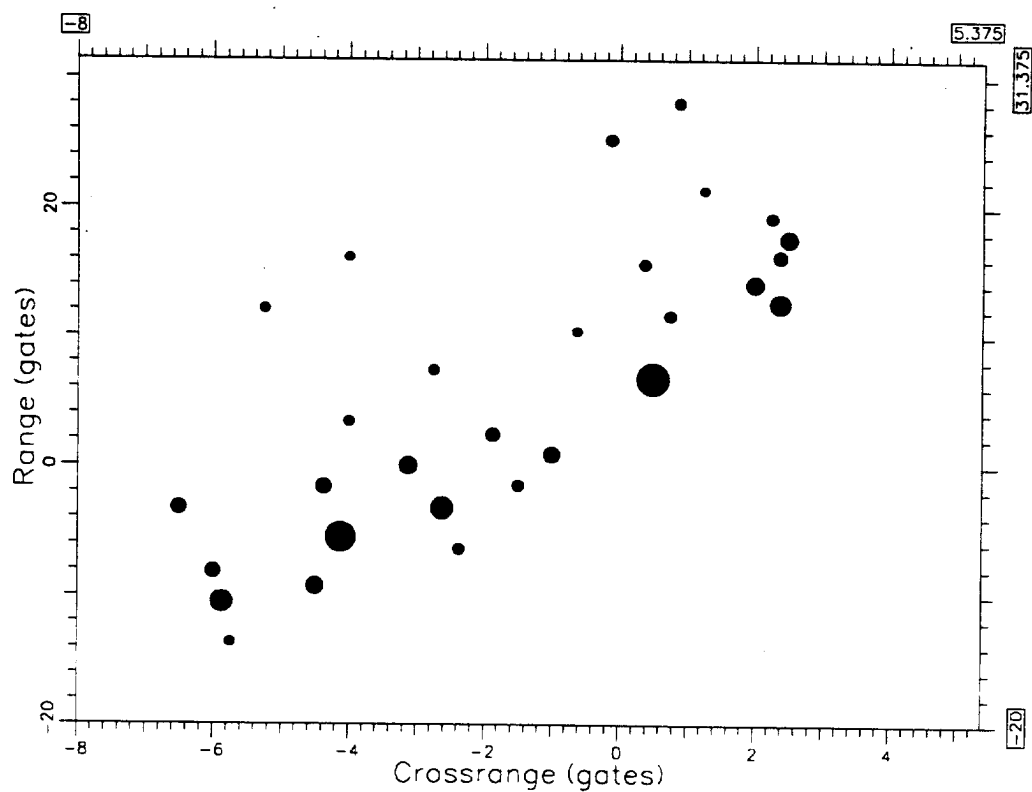
last action: Edit



Start Freq (MHz): 9360.439453  
Bandwidth (MHz): 600.000000  
Start Time (sec): 68.188072  
Dwell (sec): 0.093867

Figure 19. Image with Adjusted Starting Time.

0102 last action: Edit



Start Freq (MHz): 9360.439453  
Bandwidth (MHz): 600.000000  
Start Time (sec): 71.068077  
Dwell (sec): 0.068267

Figure 20. 0.068 s Image at 71.07 s.

Continue	Hard Copy	Switch XY	Zoom x2
----------	-----------	-----------	---------

IngDur 0.137

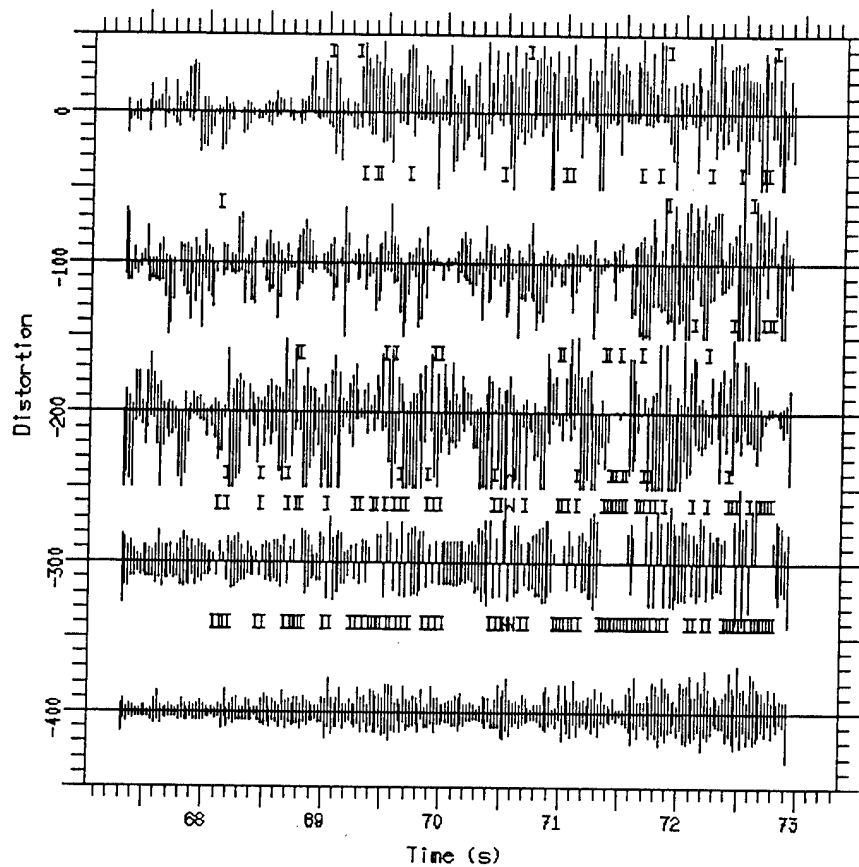
/bos/usr3/awr/dna/dna106a90ncv1rdd.pfx

15:27:27

Scatt 1.

Scatt 2.

Scatt 3.



25-Feb-02 15:27:24

Figure 21. Distortion Measurements for Doubled Imaging Duration.

0102

last action: Edit

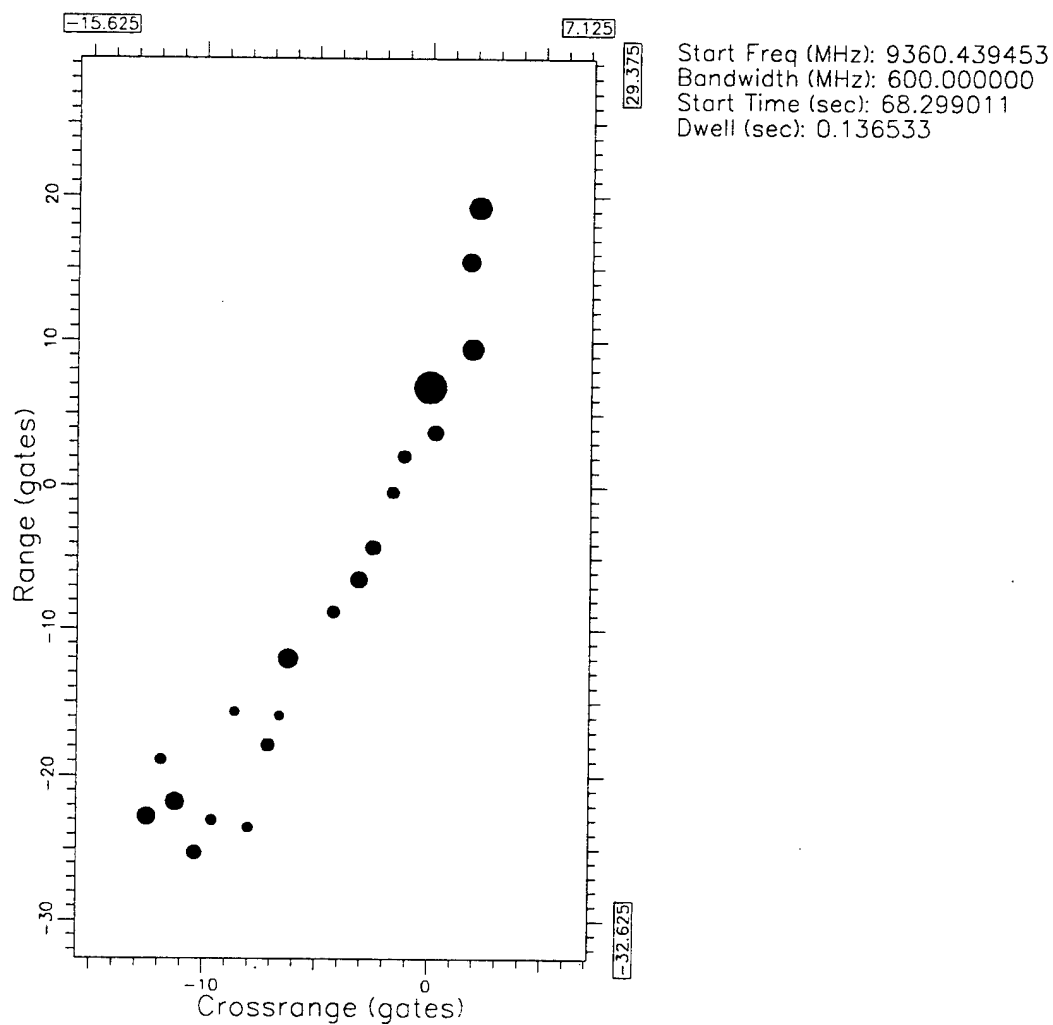
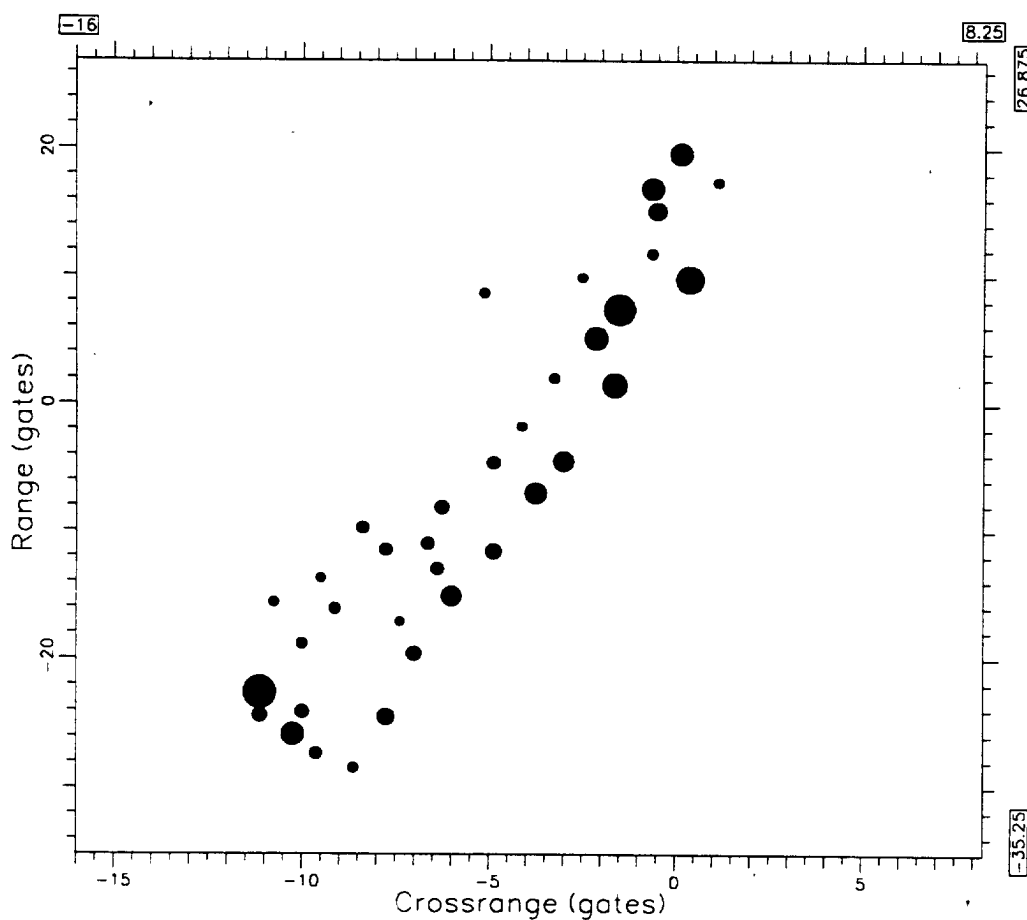


Figure 22. 0.137 s Image at 68.30 s.

0102

last action: Edit



Start Freq (MHz): 9360.439453  
Bandwidth (MHz): 600.000000  
Start Time (sec): 68.051544  
Dwell (sec): 0.136533

Figure 23. 0.137 s image at 68.05 s.

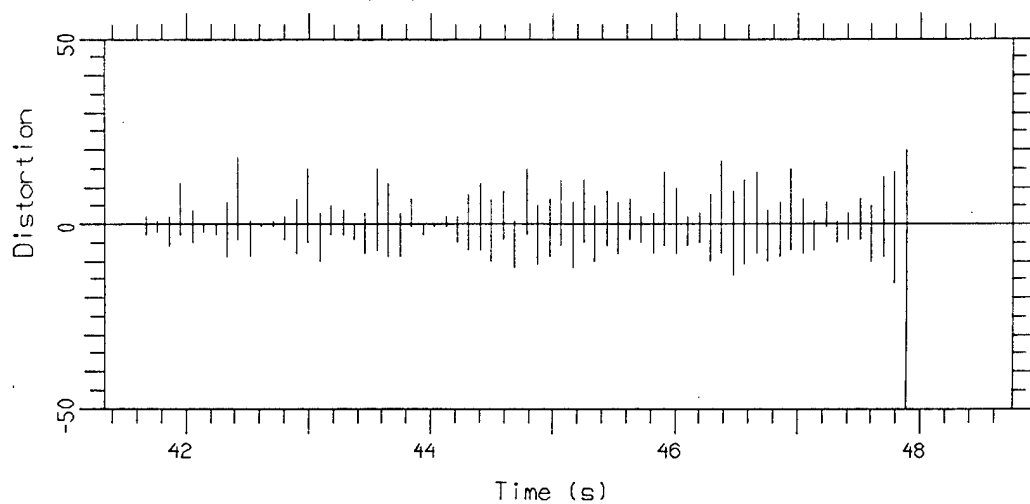
ImgDur 0.502

dra114a84cvbcompd.pfx

Scatt 1.

Scatt 2.

Scatt 3.



ImgDur 0.157

dra114a84cvbcompd.pfx

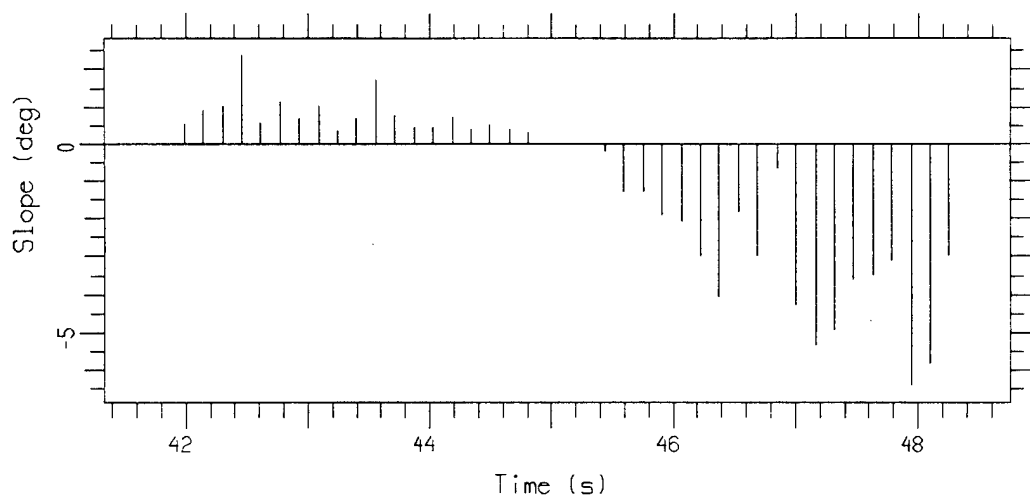


Figure 24. Distortion and Slope Measurements for Surrogate TEL on a Smooth Road.

0.02 last action: Edit

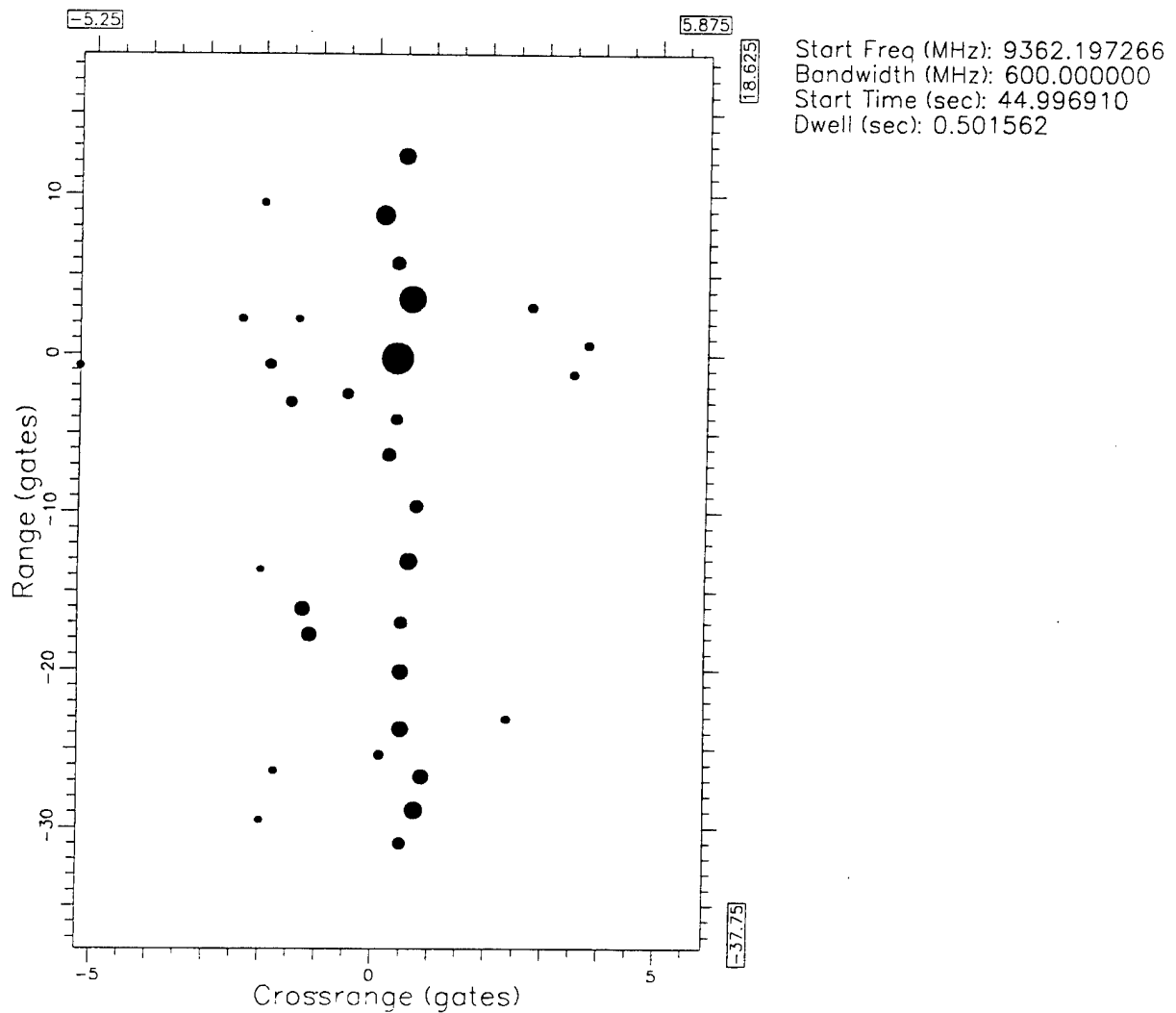
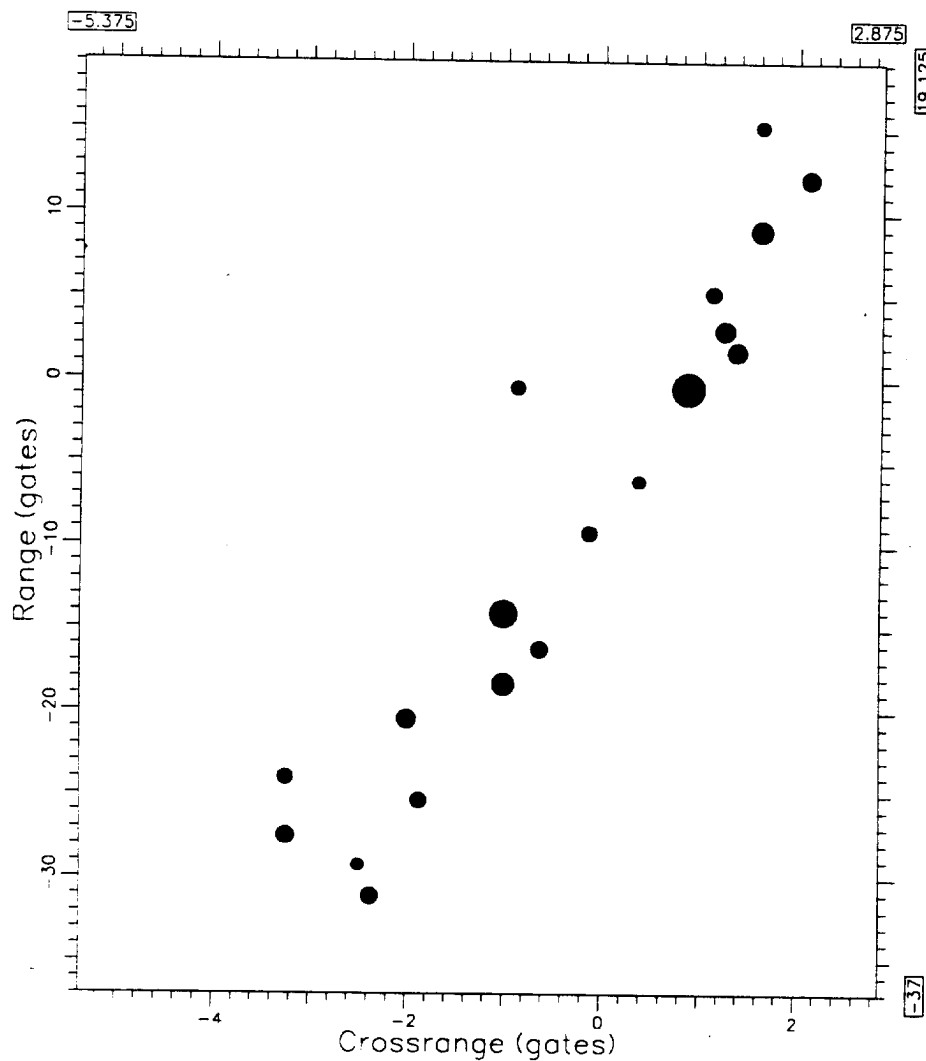


Figure 25. Image of Surrogate TEL Moving on Smooth Road at 45.0 s (0.5 s Imaging Interval).

0107

last action: Change Peak Scaling

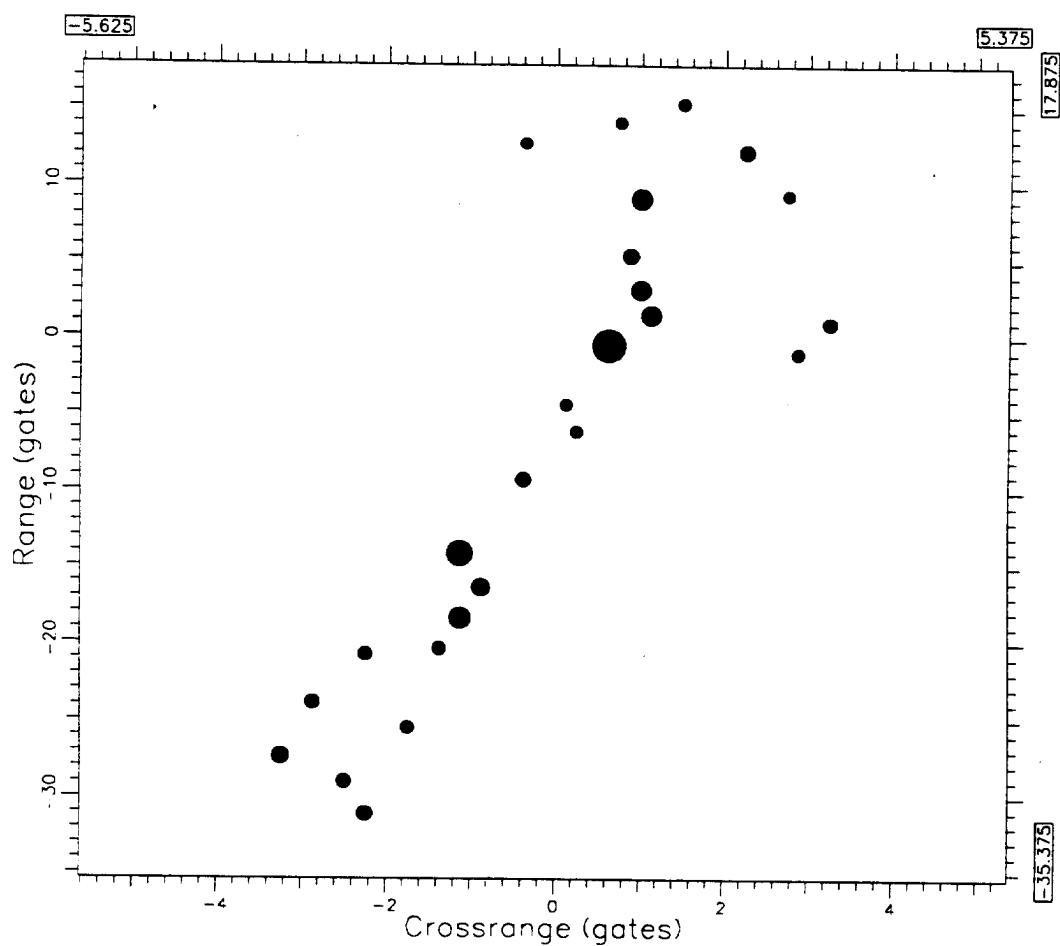


Start Freq (MHz): 9362.197266  
Bandwidth (MHz): 600.000000  
Start Time (sec): 42.238316  
Dwell (sec): 0.501562

Figure 26. Image of Surrogate TEL Moving on Smooth Road at 42.25 s (0.5 s Imaging Interval).

0105

last action: Edit

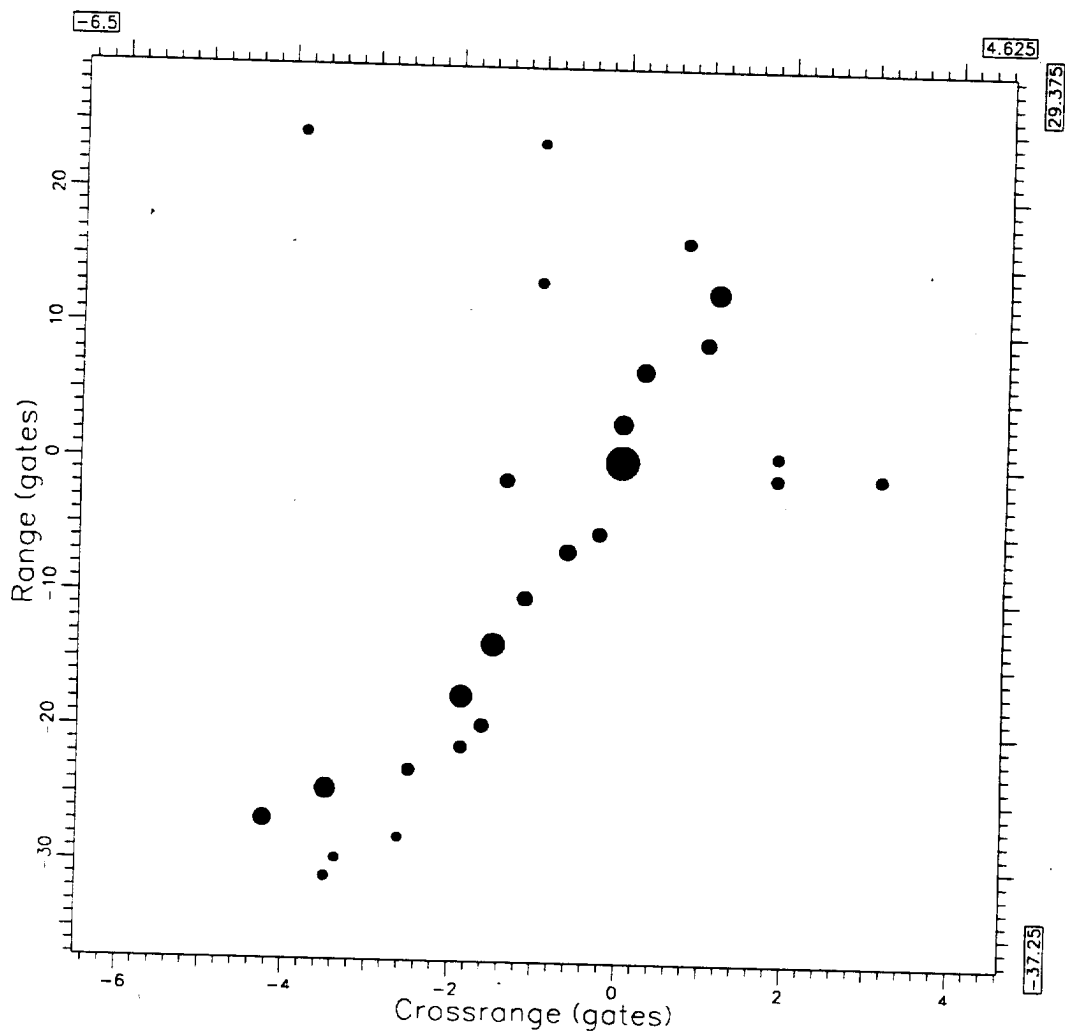


Start Freq (MHz): 9362.197266  
Bandwidth (MHz): 600.000000  
Start Time (sec): 42.144272  
Dwell (sec): 0.501562

Figure 27. Image of Surrogate TEL Moving on Smooth Road at 42.15 s (0.5 s Imaging Interval).

0105

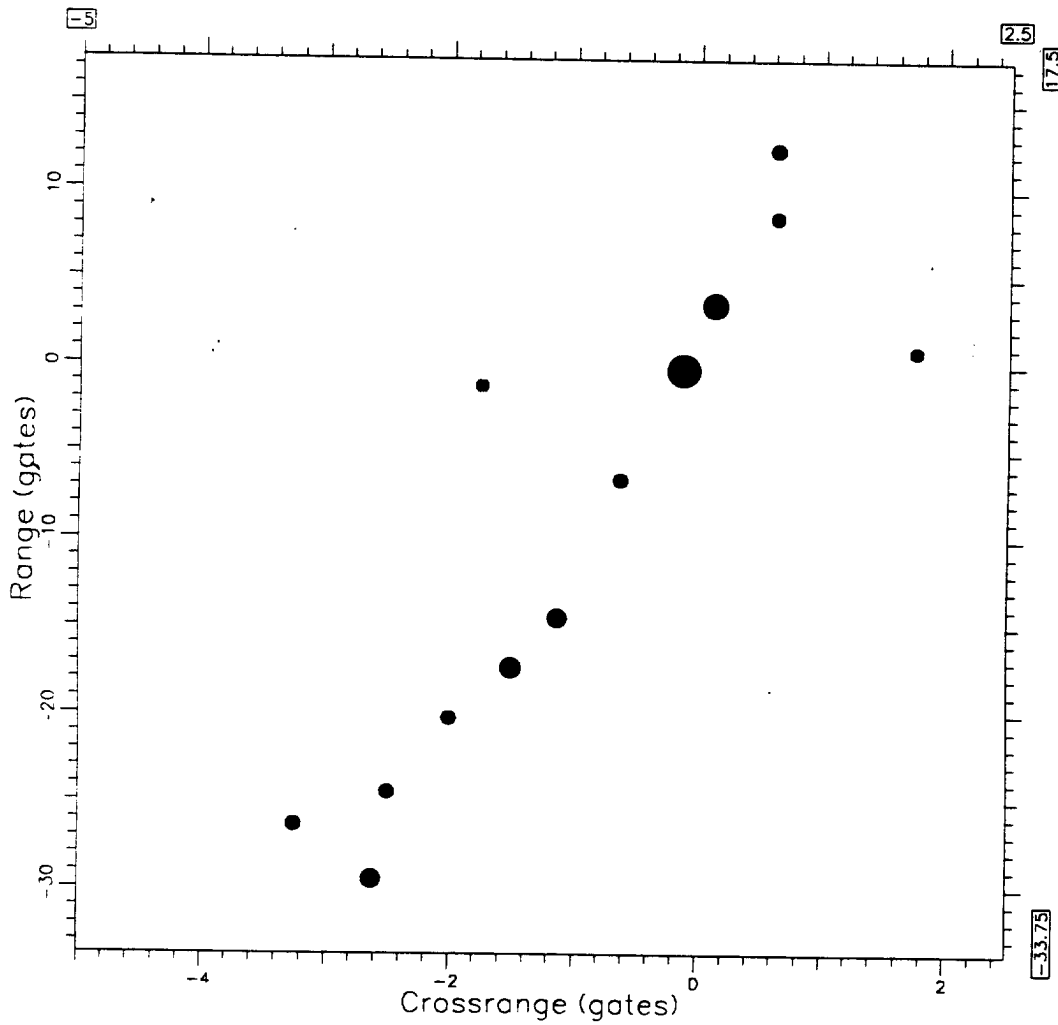
last action: Edit



Start Freq (MHz): 9362.197266  
Bandwidth (MHz): 600.000000  
Start Time (sec): 43.398178  
Dwell (sec): 0.501562

Figure 28. Image of Surrogate TEL Moving on Smooth Road at 43.4 s (0.5 s Imaging Interval).

0107 last action: Edit



Start Freq (MHz): 9362.197266  
Bandwidth (MHz): 600.000000  
Start Time (sec): 43.993782  
Dwell (sec): 0.501562

Figure 29. Image of Surrogate TEL Moving on Smooth Road at 44.0 s (0.5 s Imaging Interval).

01:04

last action: Edit

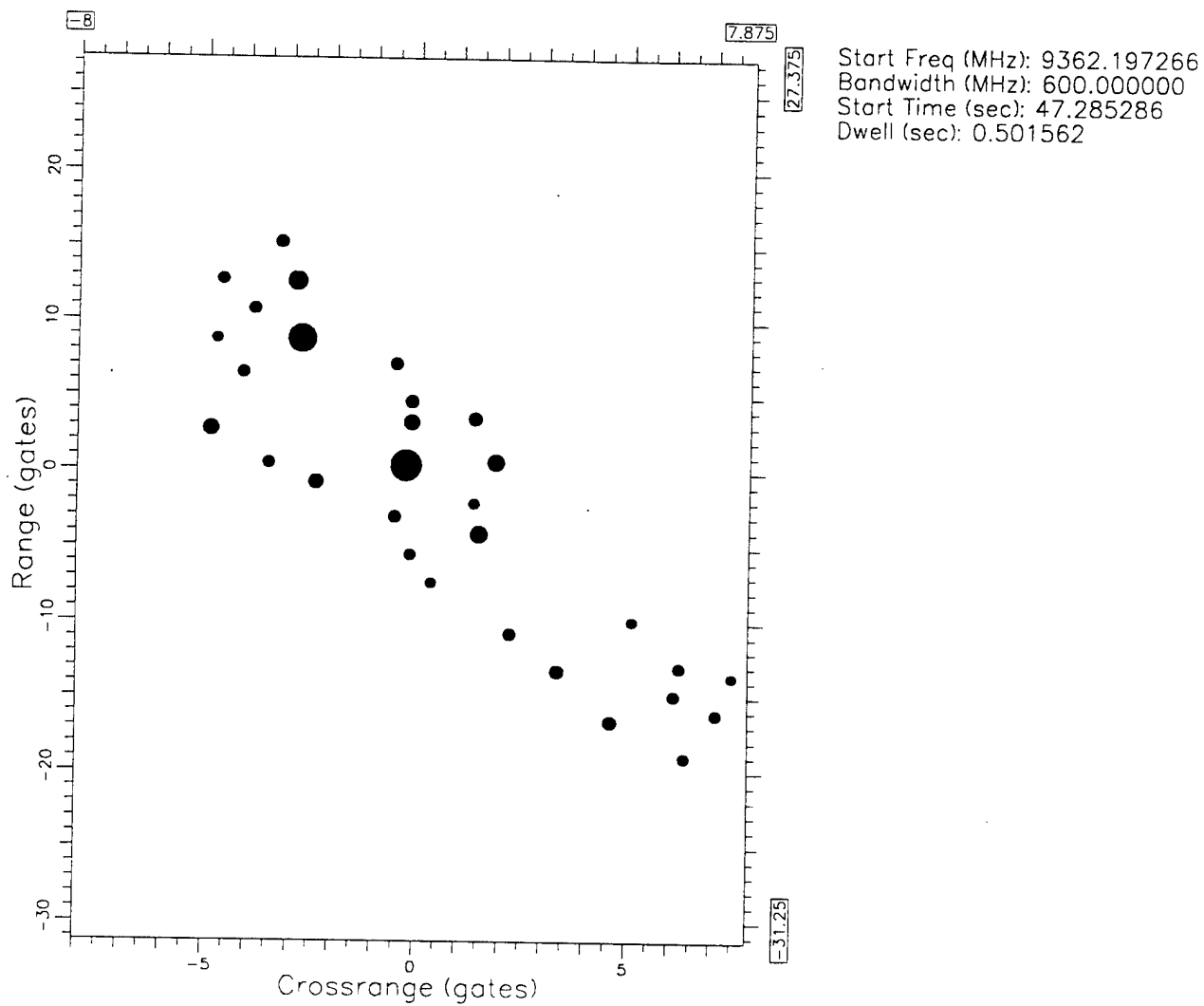
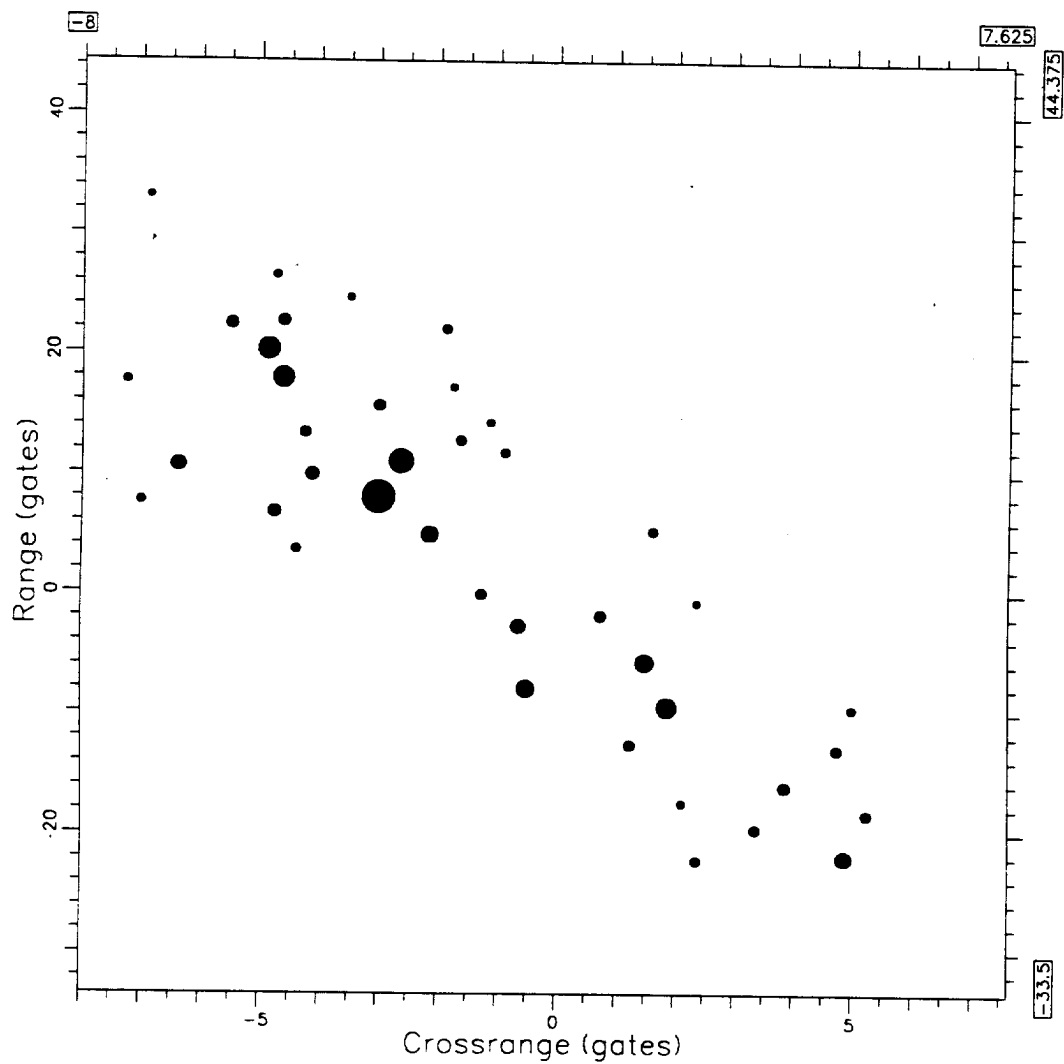


Figure 30. Image of Surrogate TEL Moving on Smooth Road at 47.3 s (0.5 s Imaging Interval).

0302

last action: Edit

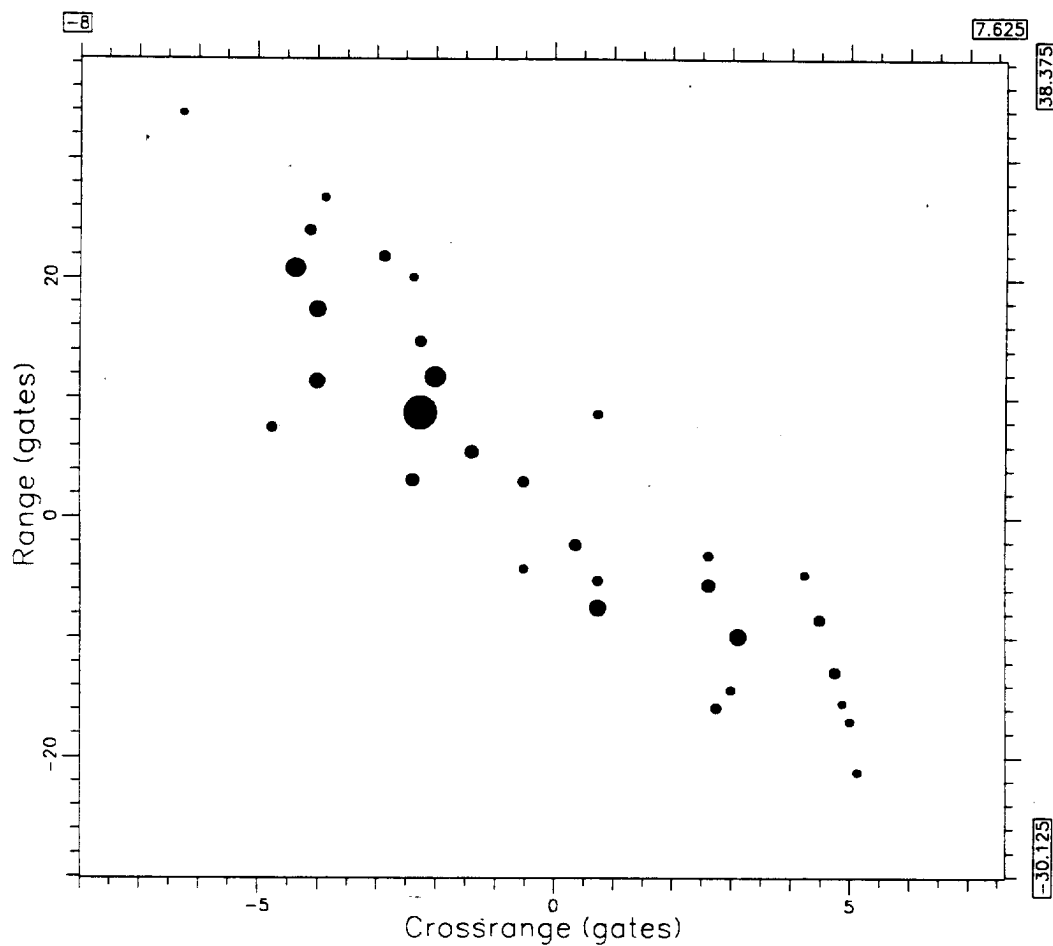


Start Freq (MHz): 9362.197266  
Bandwidth (MHz): 600.000000  
Start Time (sec): 46.094078  
Dwell (sec): 0.501562

Figure 31. Image of Surrogate TEL Moving on Smooth Road at 46.1 s (0.5 s Imaging Interval).

0302

last action: Edit

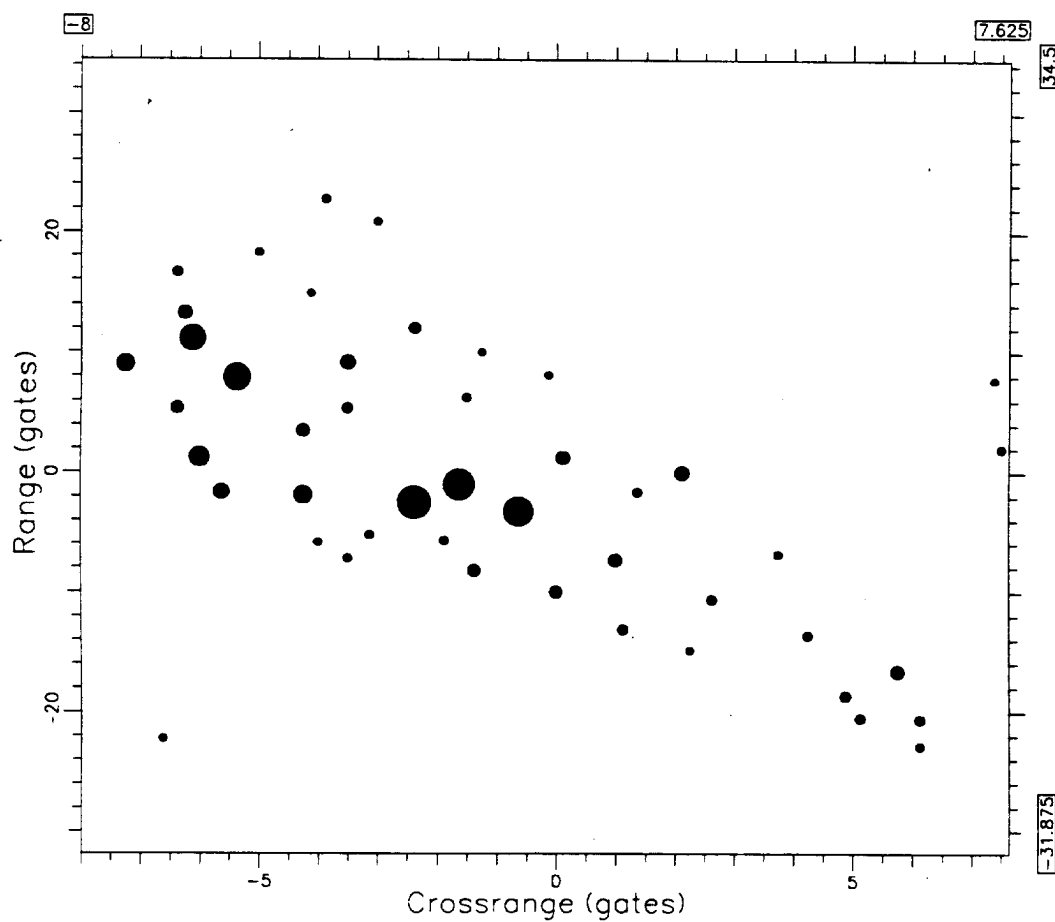


Start Freq (MHz): 9362.197266  
Bandwidth (MHz): 600.000000  
Start Time (sec): 46.344856  
Dwell (sec): 0.501562

Figure 32. Image of Surrogate TEL Moving on Smooth Road at 46.35 s (0.5 s Imaging Interval).

0302

last action: Edit



Start Freq (MHz): 9362.197266  
Bandwidth (MHz): 600.000000  
Start Time (sec): 47.786850  
Dwell (sec): 0.501562

Figure 33. Image of Surrogate TEL Moving on Smooth Road at 47.8 s (0.5 s Imaging Interval).

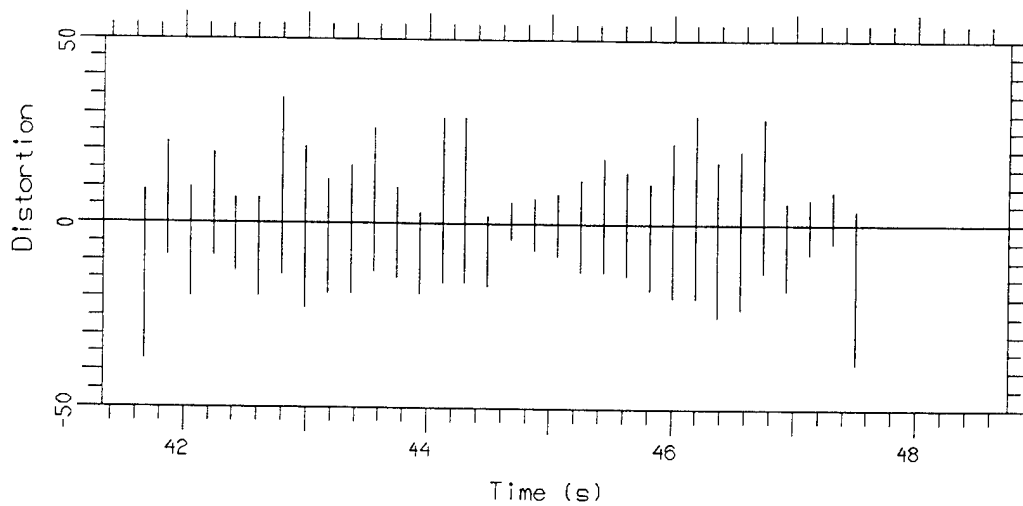
ImgDur 0.878

dra114a84cvbcompd.pfx

Scott 1.

Scott 2.

Scott 3.



ImgDur 0.157

dra114a84cvbcompd.pfx

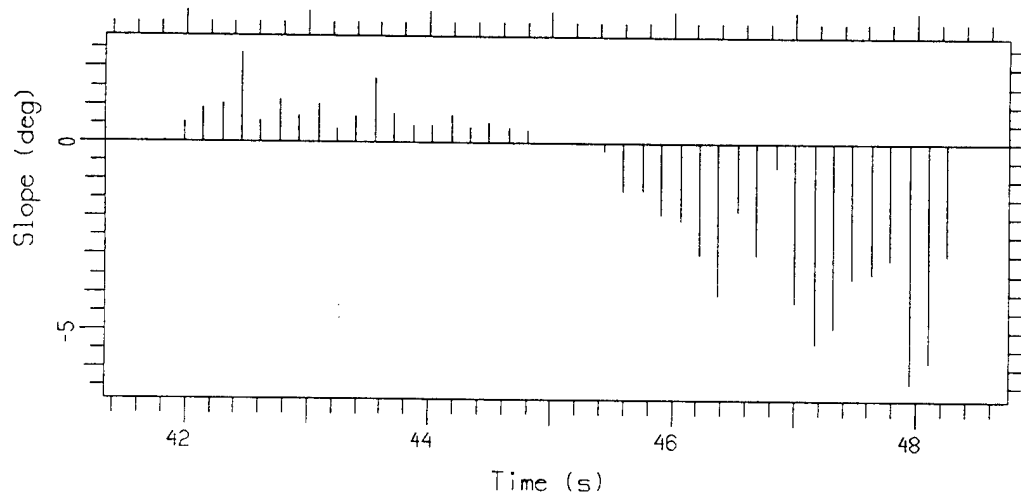
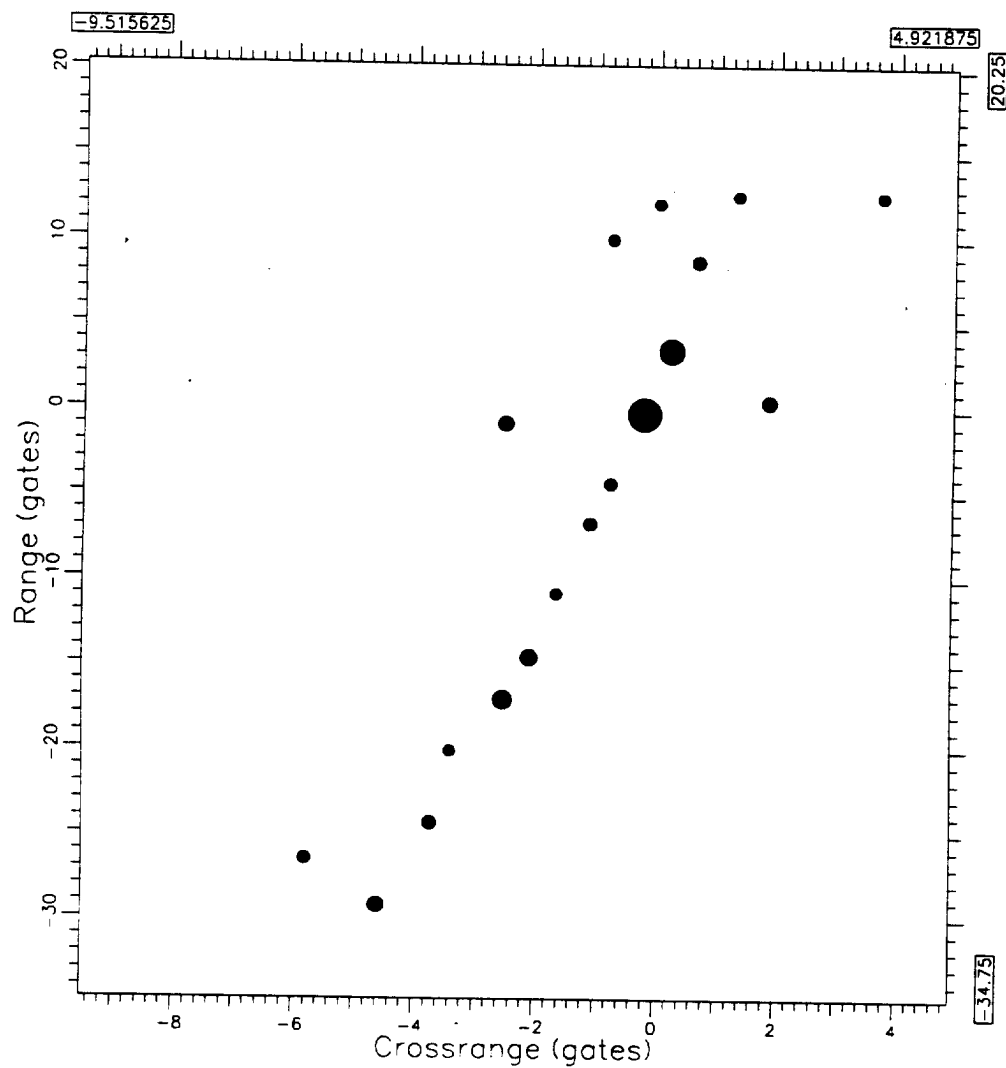


Figure 34. Distortion and Slope Measurements  
for Imaging Interval of 0.88 s.

0107

last action: Edit

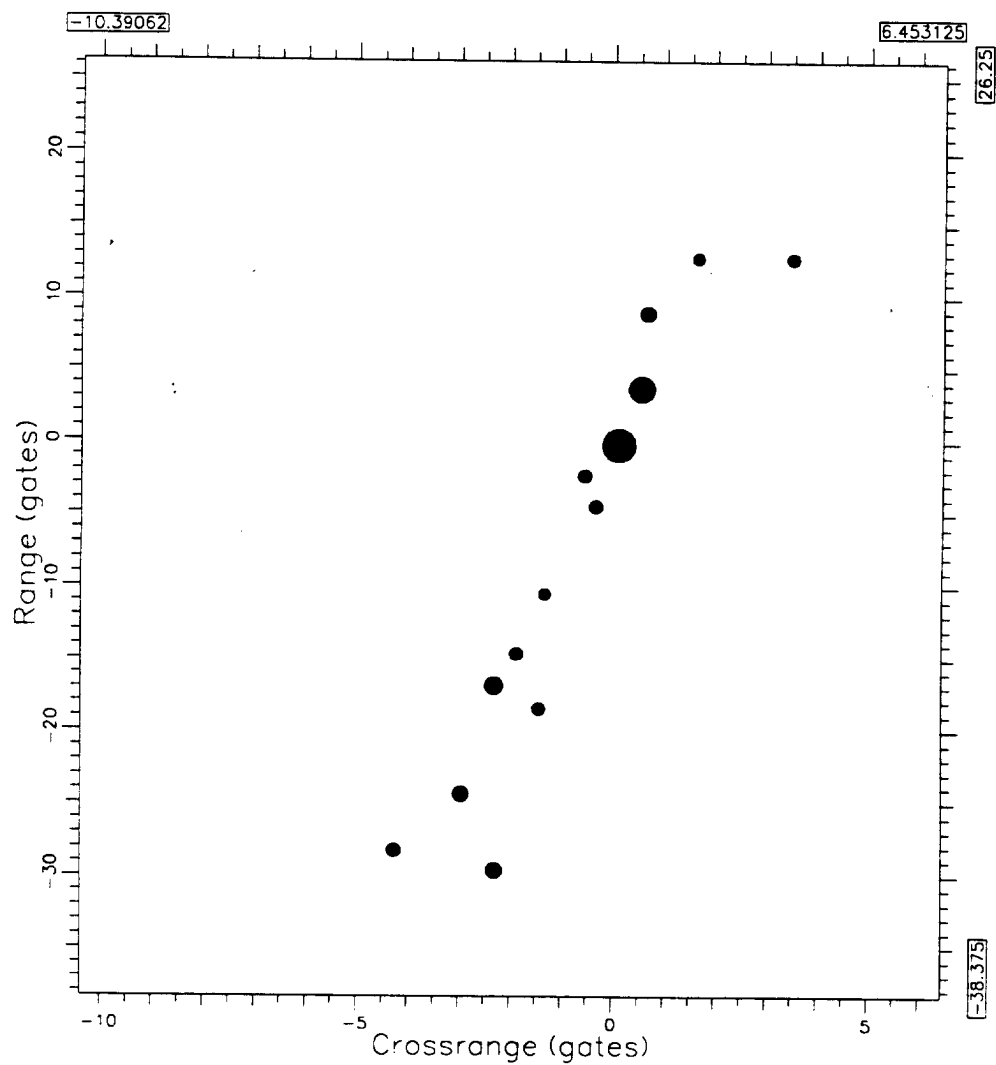


Start Freq (MHz): 9362.197266  
Bandwidth (MHz): 600.000000  
Start Time (sec): 43.899742  
Dwell (sec): 0.877734

Figure 35. Image of Surrogate TEL Moving on Smooth Road at 43.9 s (0.88 s Imaging interval).

0102

last action: Edit



Start Freq (MHz): 9362.197266  
Bandwidth (MHz): 600.000000  
Start Time (sec): 44.087826  
Dwell (sec): 0.877734

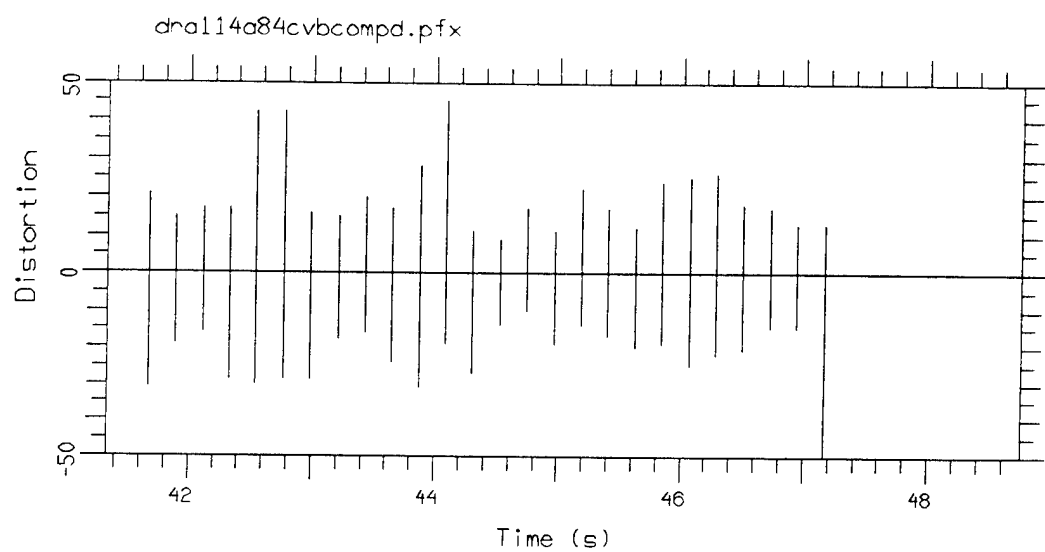
Figure 36. Image of Surrogate TEL Moving on Smooth Road at 44.1 s (0.88 s Imaging Interval).

ImgDur 1.160

Scott 1.

Scott 2.

Scott 3.



ImgDur 0.157

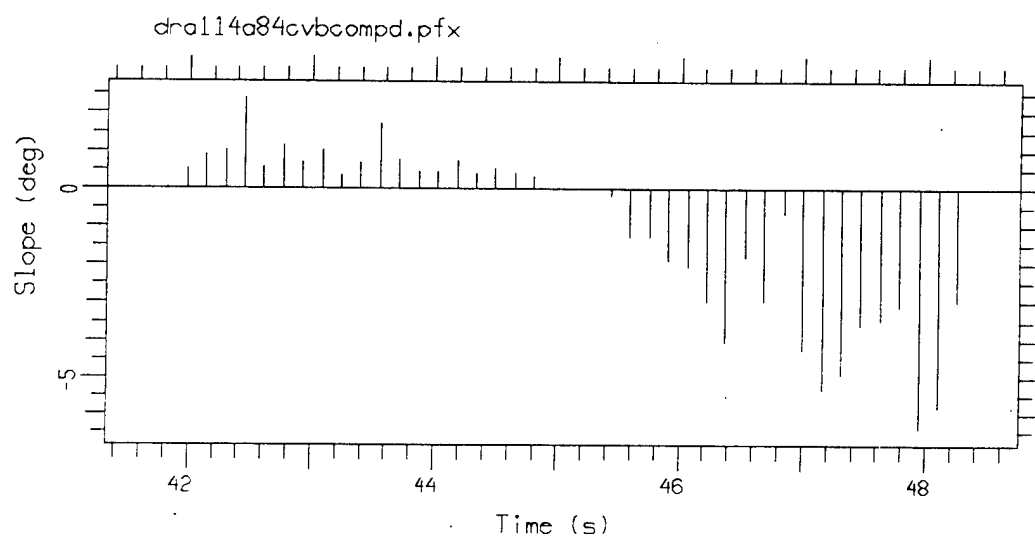


Figure 37. Distortion and Slope Measurements  
for Imaging Interval of 1.16 s.

01:02 last action: Edit

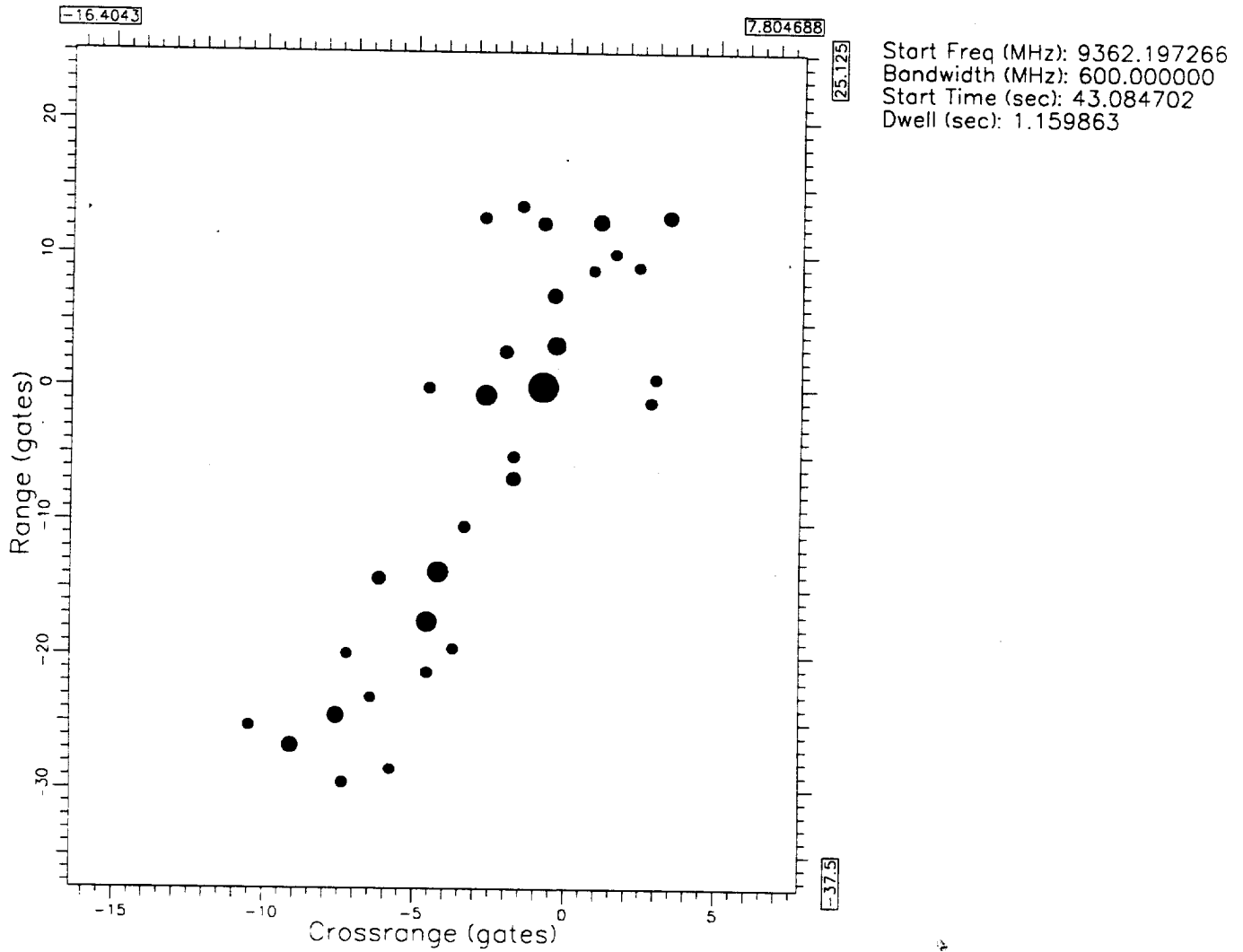


Figure 38. Image of Surrogate TEL Moving on Smooth Road at 43.1 s (1.16 s Imaging Interval).

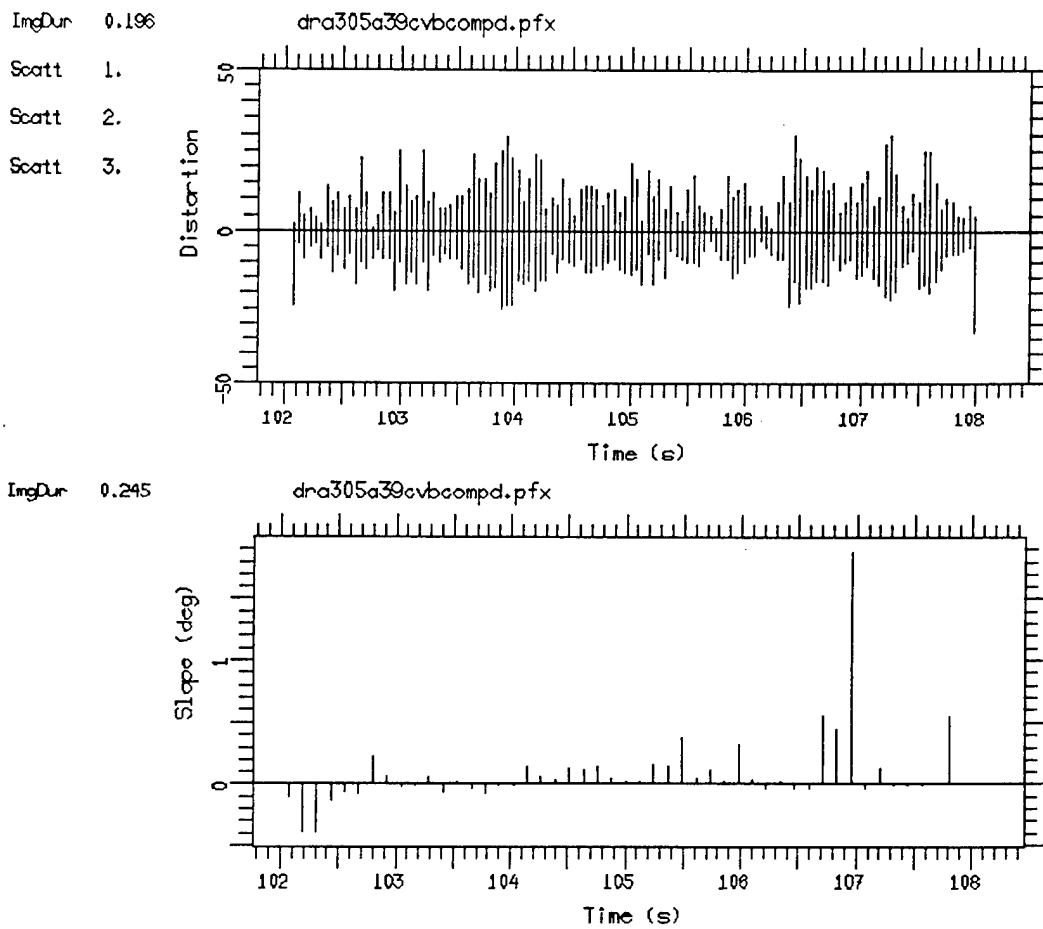
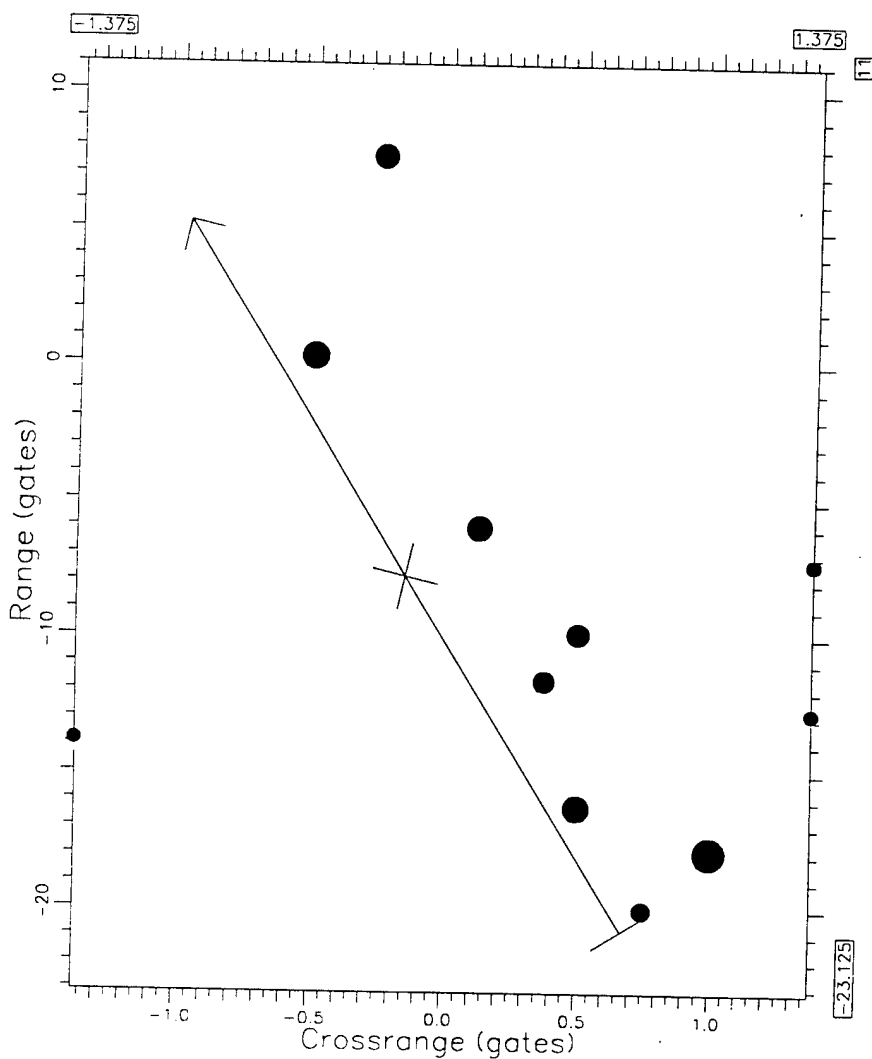


Figure 39. Distortion and Slope Measurements for Truck on a Bumpy Road.

0304

last action: Edit

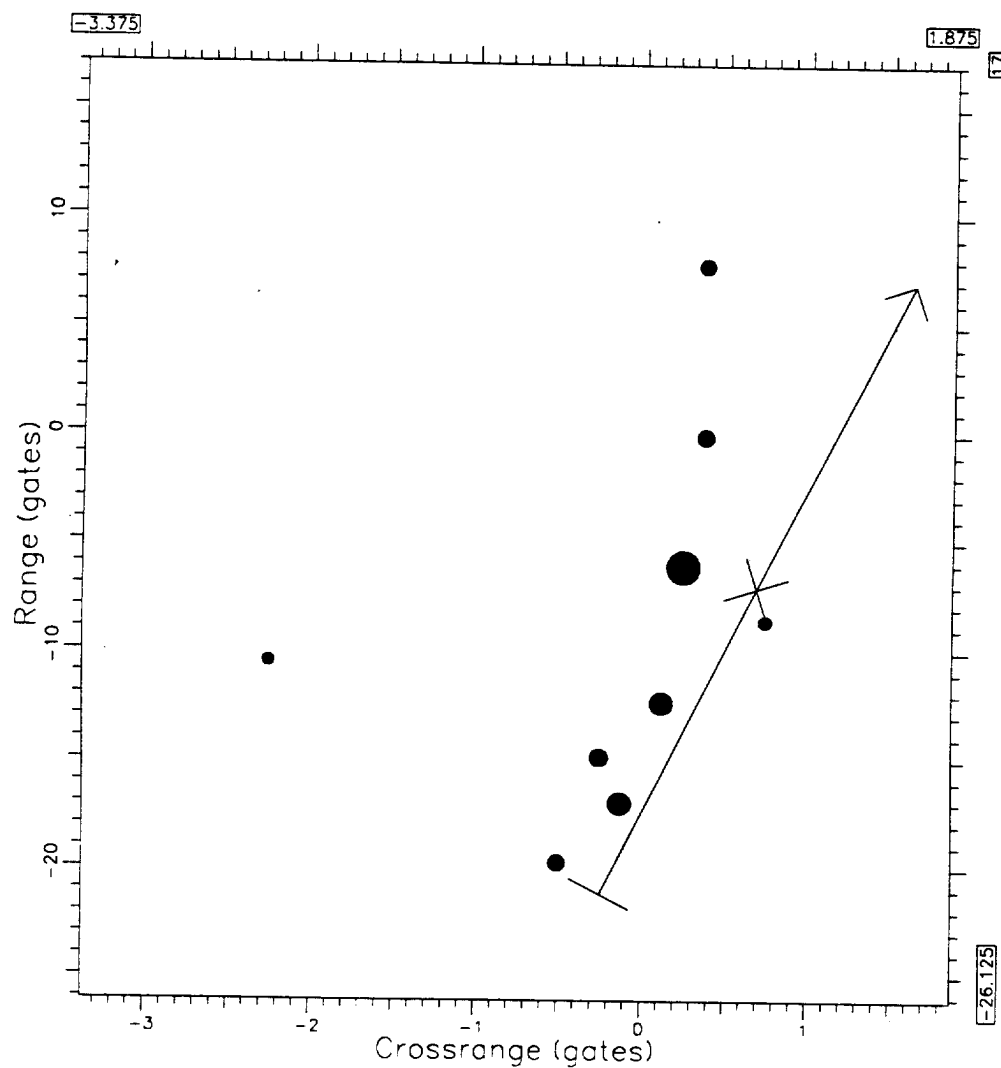


Start Freq (MHz): 9362.197266  
Bandwidth (MHz): 600.000000  
Start Time (sec): 102.311745  
Dwell (sec): 0.195625

Figure 40. Image of Truck on Bumpy Road at 102.3 s  
(0.2 s Imaging Interval).

0109

last action: Edit

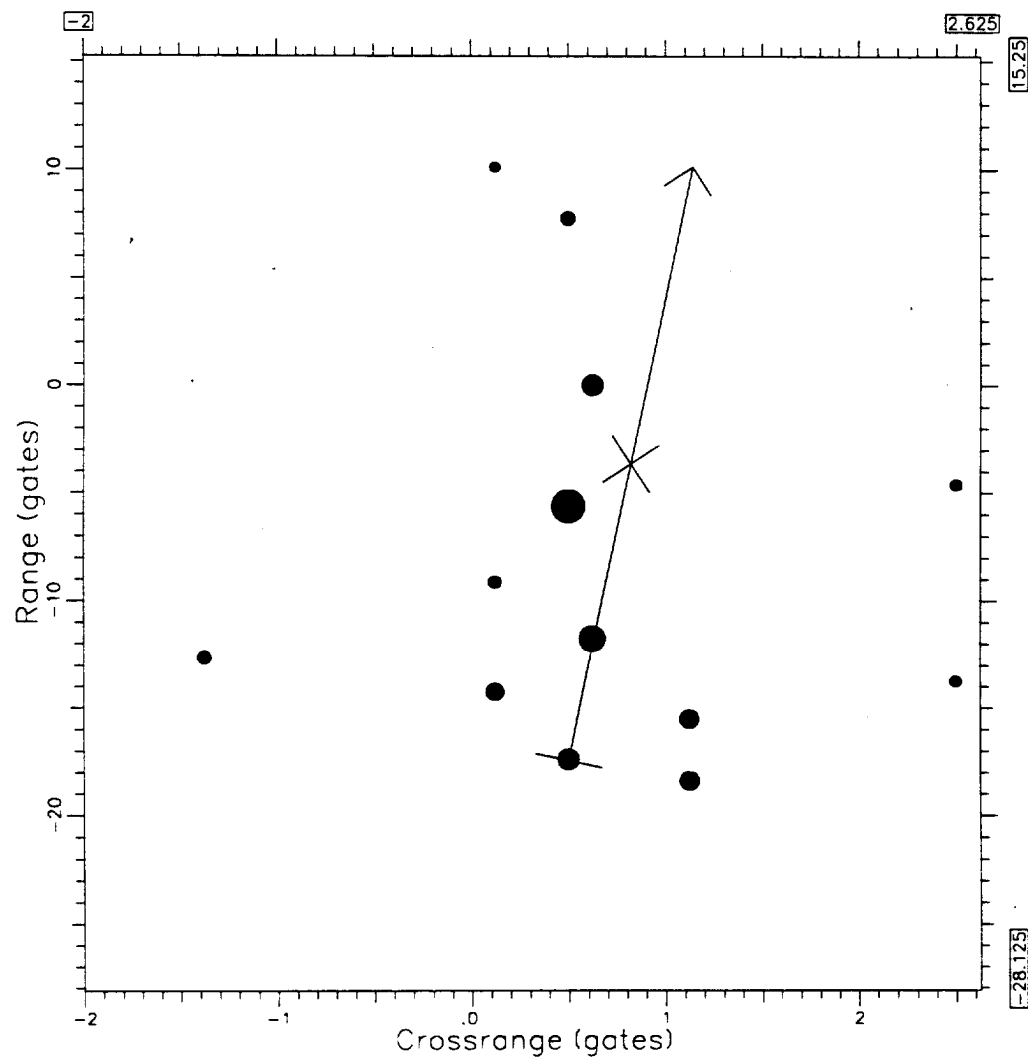


Start Freq (MHz): 9362.197266  
Bandwidth (MHz): 600.000000  
Start Time (sec): 105.735184  
Dwell (sec): 0.195625

Figure 41. Image of Truck on Bumpy Road at 105.75 s  
(0.2 s Imaging Interval).

0107

last action: Edit



Start Freq (MHz): 9362.197266  
Bandwidth (MHz): 600.000000  
Start Time (sec): 102.751900  
Dwell (sec): 0.195625

Figure 42. Image of Truck on Bumpy Road at 102.75 s  
(0.2 s Imaging Interval).

0302 last action: Edit

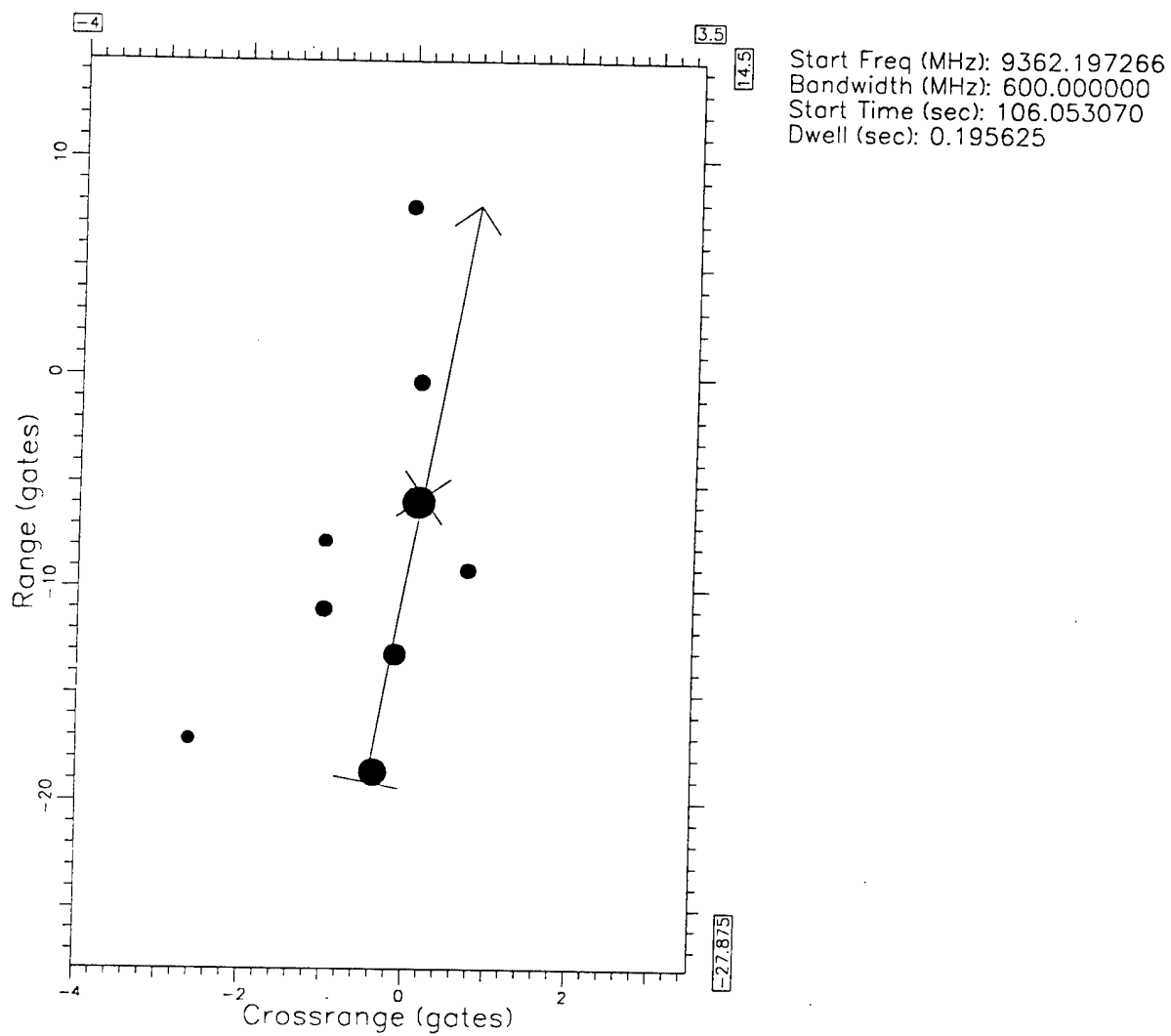


Figure 43. Image of Truck on Bumpy Road at 106.05 s  
(0.2 s Imaging Interval).

01:03

last action: Edit

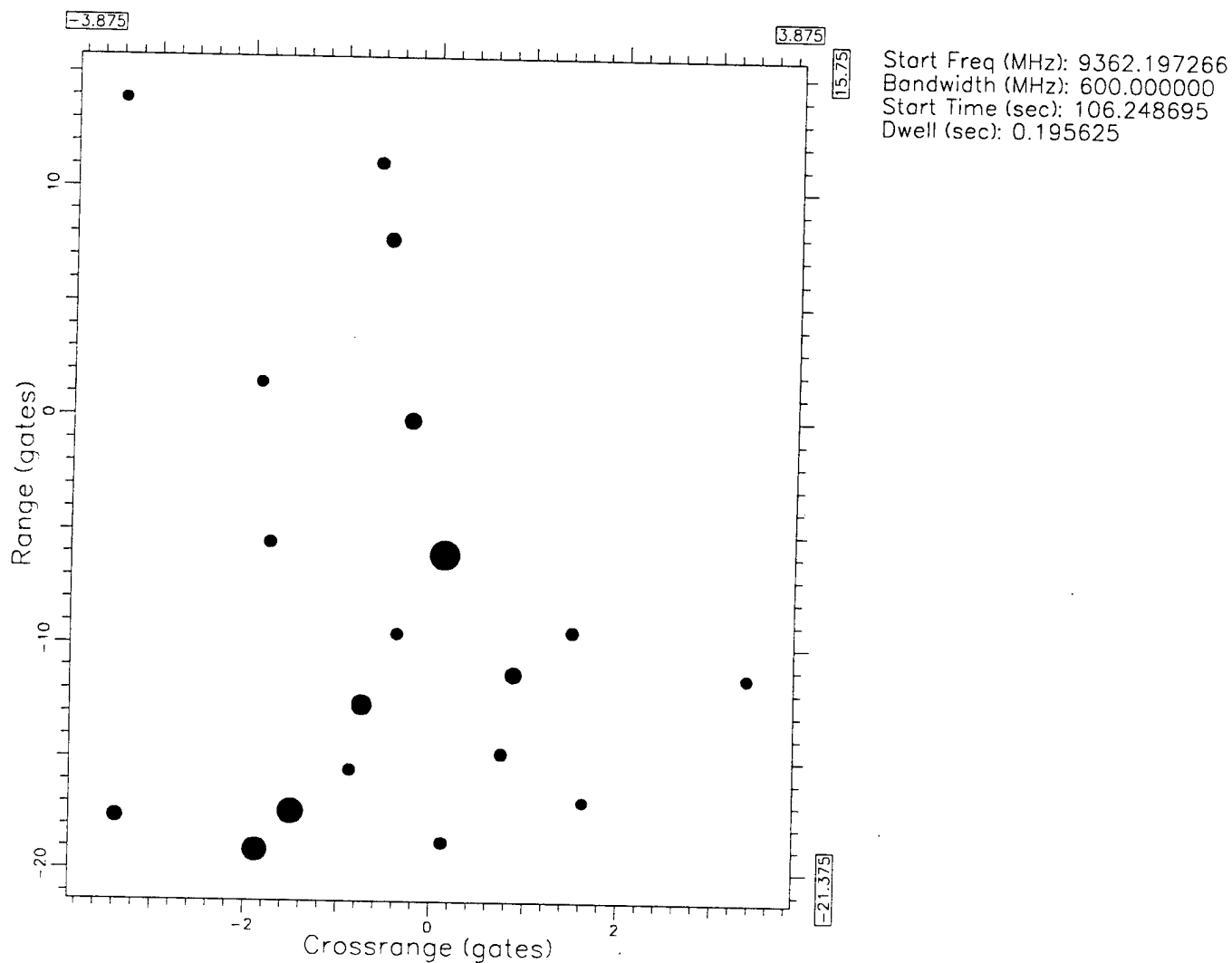


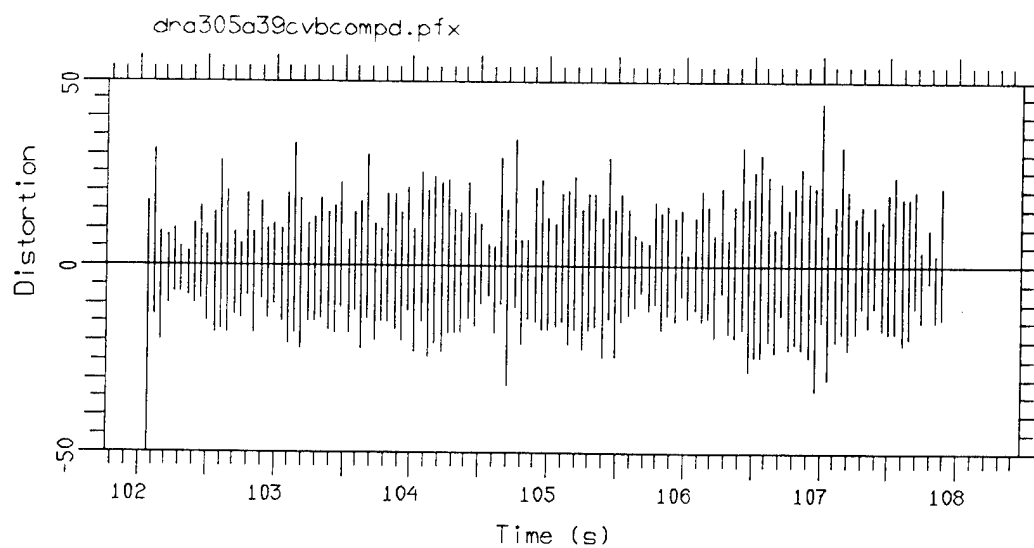
Figure 44. Image of Truck on Bumpy Road at 106.25 s  
(0.2 s Imaging Interval).

ImagDur 0.269

Scatt 1.

Scatt 2.

Scatt 3.



ImgDur 0.245

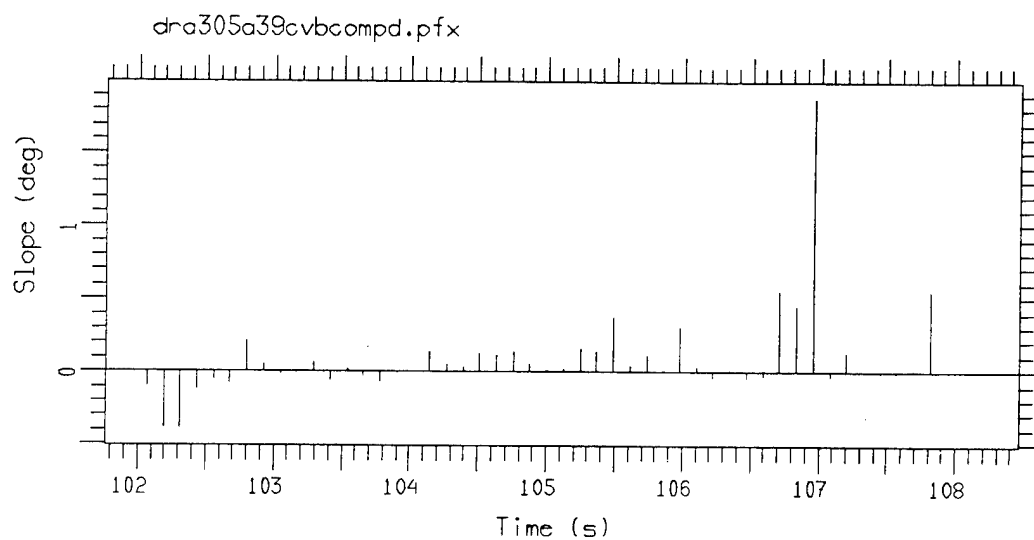
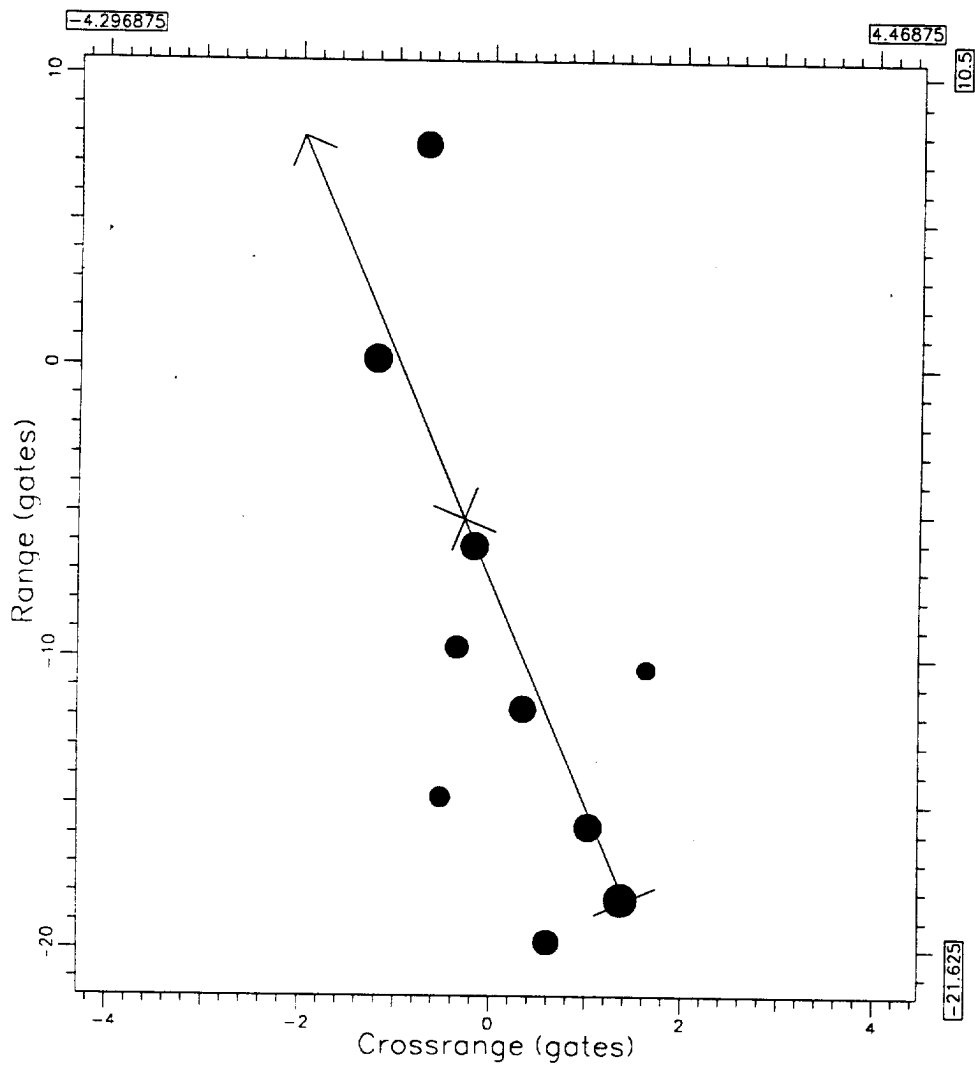


Figure 45. Distortion and Slope Measurements  
for 0.269 s Imaging Interval.

0106

last action: Compute Cut



Start Freq (MHz): 9362.197266  
Bandwidth (MHz): 600.000000  
Start Time (sec): 102.360649  
Dwell (sec): 0.268984

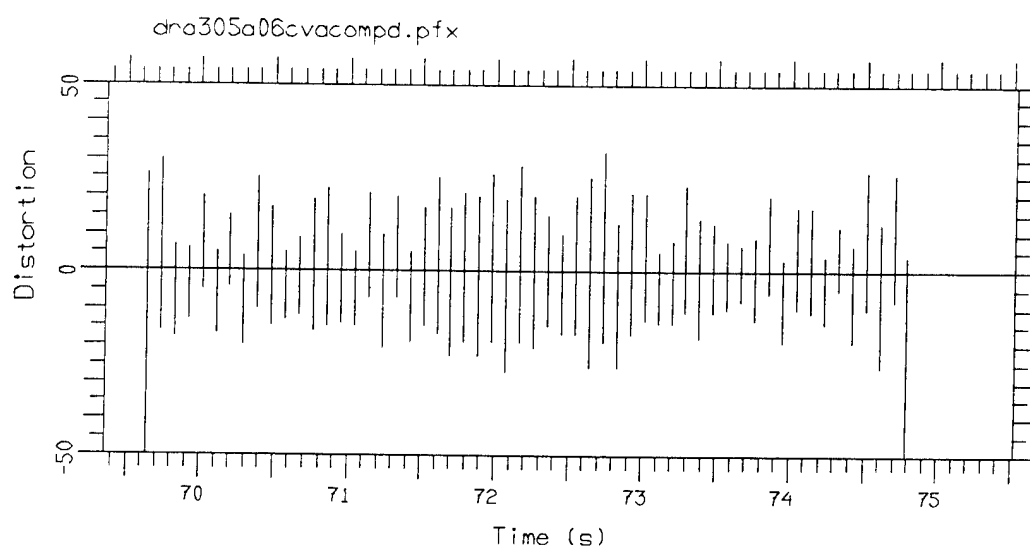
Figure 46. Image of Truck on Bumpy Road at 102.35 s  
(0.269 s Imaging Interval).

ImgDur 0.468

Scott 1.

Scott 2.

Scott 3.



ImgDur 0.234

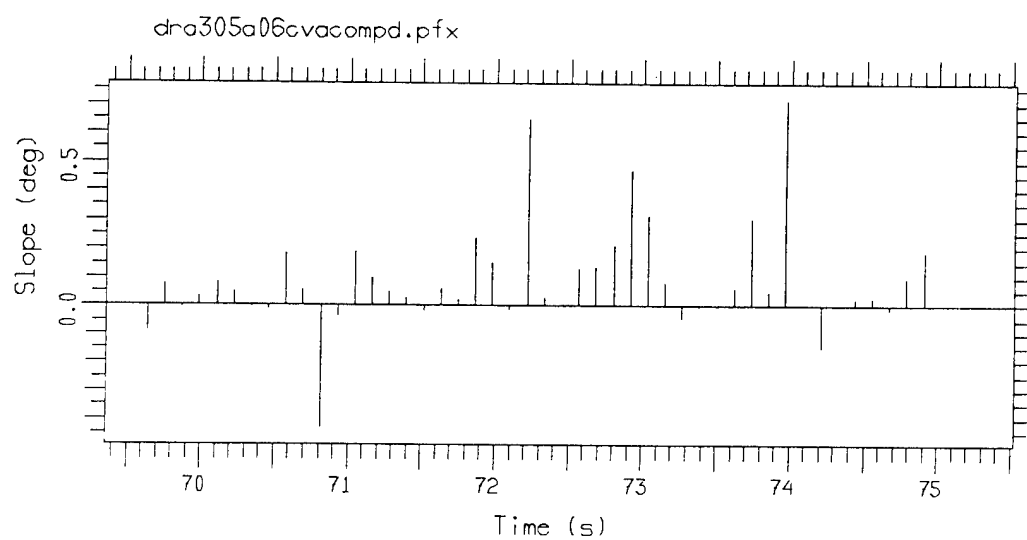


Figure 47. Distortion and Slope Measurements for Confuser on Bumpy Road.

0102 last action: Edit

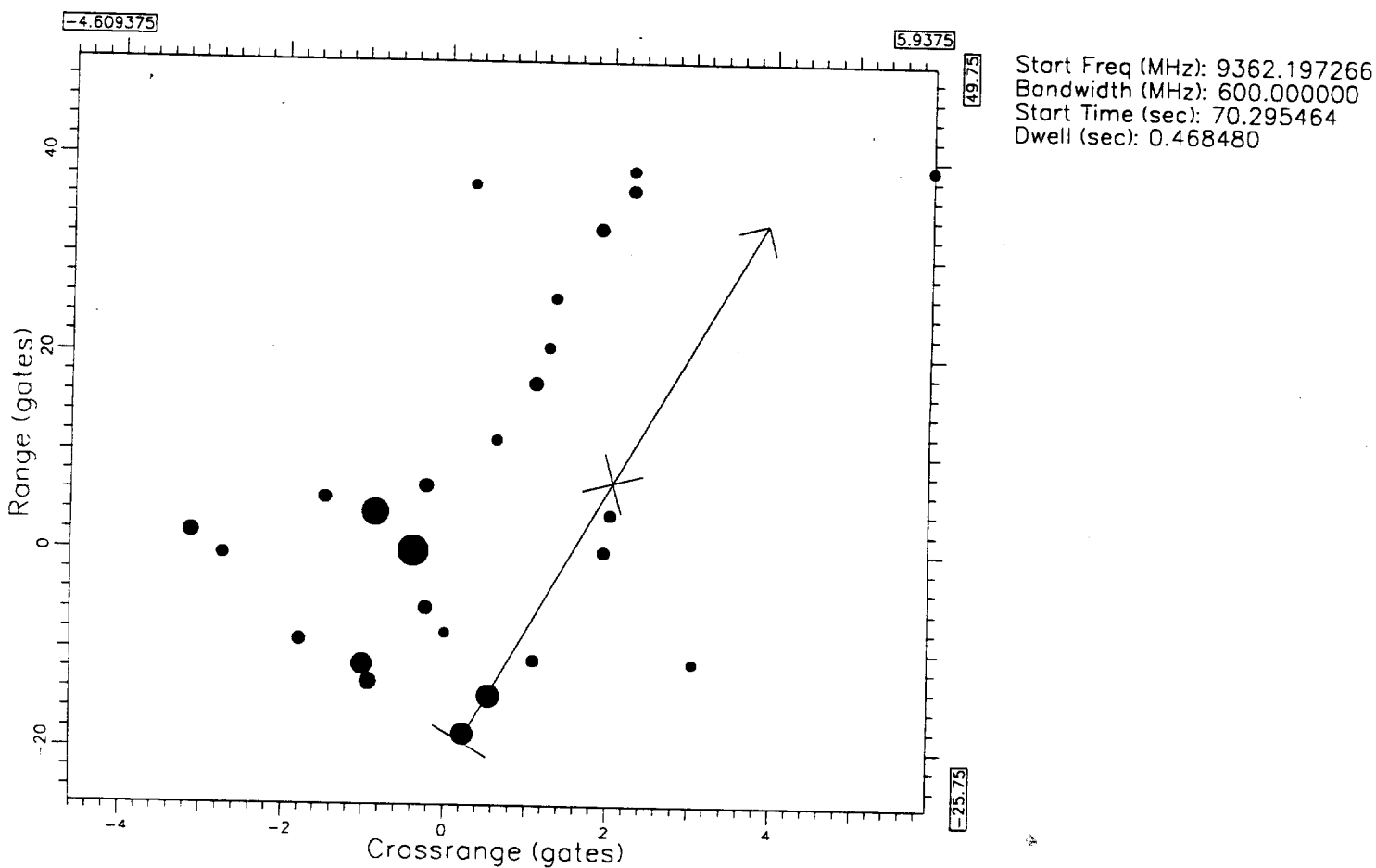
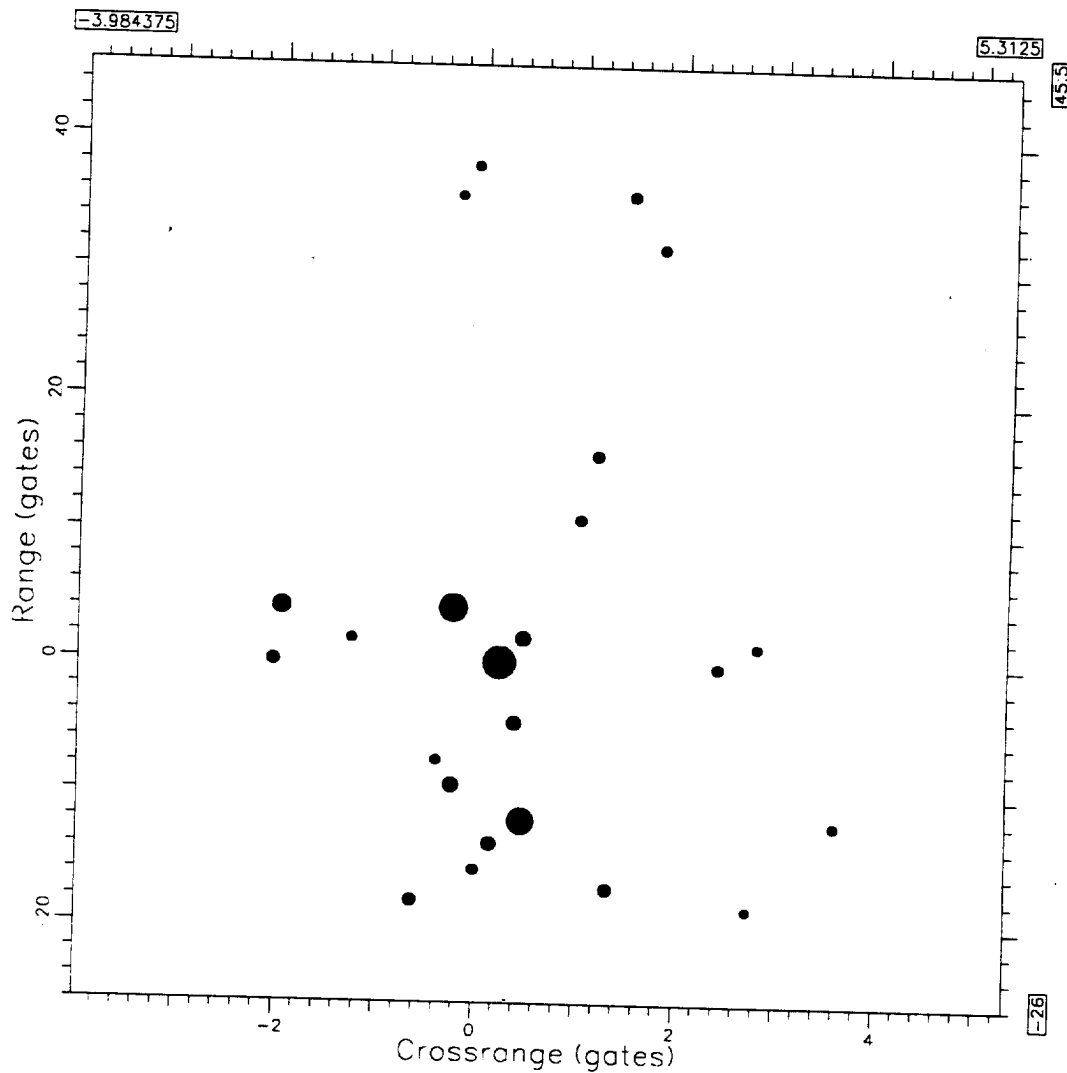


Figure 48. Best Image of Confuser on Bumpy Road.

0.02

last action: Edit

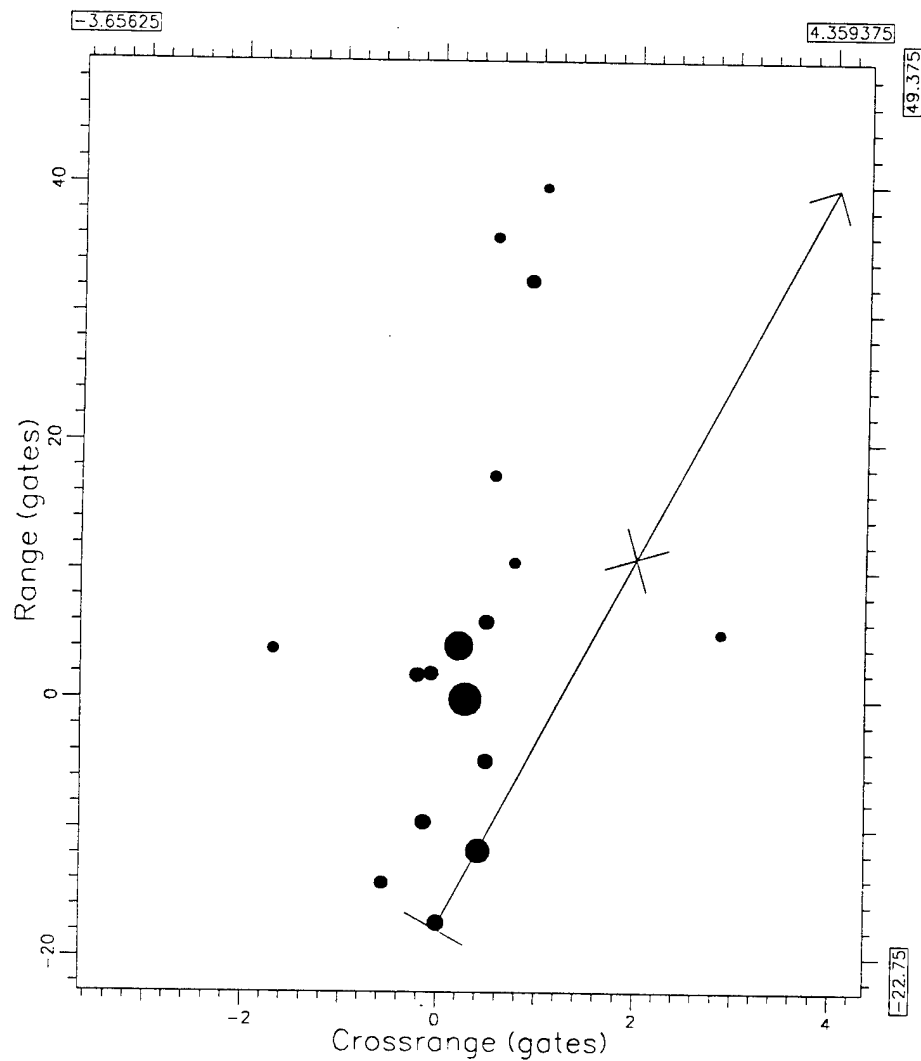


Start Freq (MHz): 9362.197266  
Bandwidth (MHz): 600.000000  
Start Time (sec): 73.949608  
Dwell (sec): 0.468480

Figure 49. Image of Confuser on Bumpy Road at 73.95 s  
(0.468 s Imaging Interval).

02

Last action: Edit

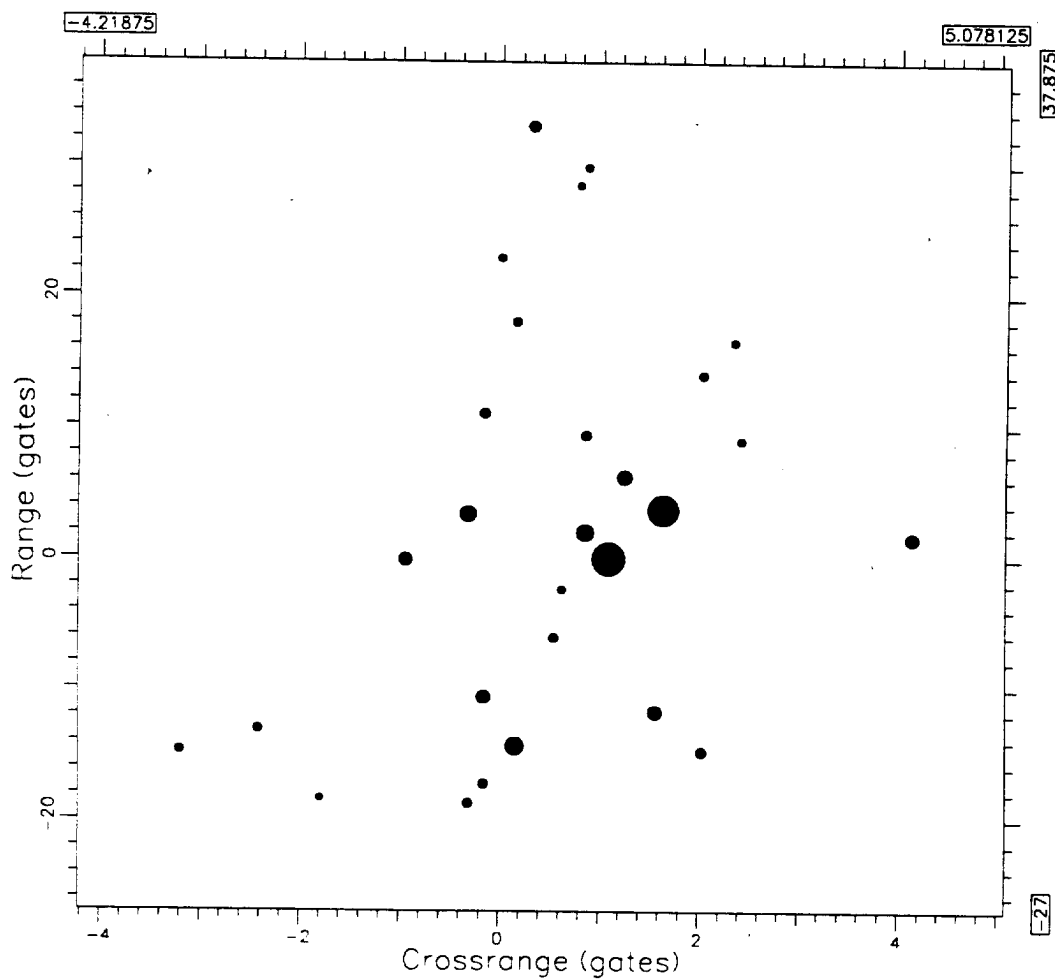


Start Freq (MHz): 9362.197266  
Bandwidth (MHz): 600.000000  
Start Time (sec): 73.902763  
Dwell (sec): 0.210816

Figure 50. Image of Confuser on Bumpy Road at 73.90 s  
(0.21 s Imaging Interval).

03

last action: Change Peak Scaling



Start Freq (MHz): 9362.197266  
Bandwidth (MHz): 600.000000  
Start Time (sec): 71.888298  
Dwell (sec): 0.468480

Figure 51. Image of Confuser on Bumpy Road at 71.9 s  
(0.468 s Imaging Interval).

Continue

Hard Copy

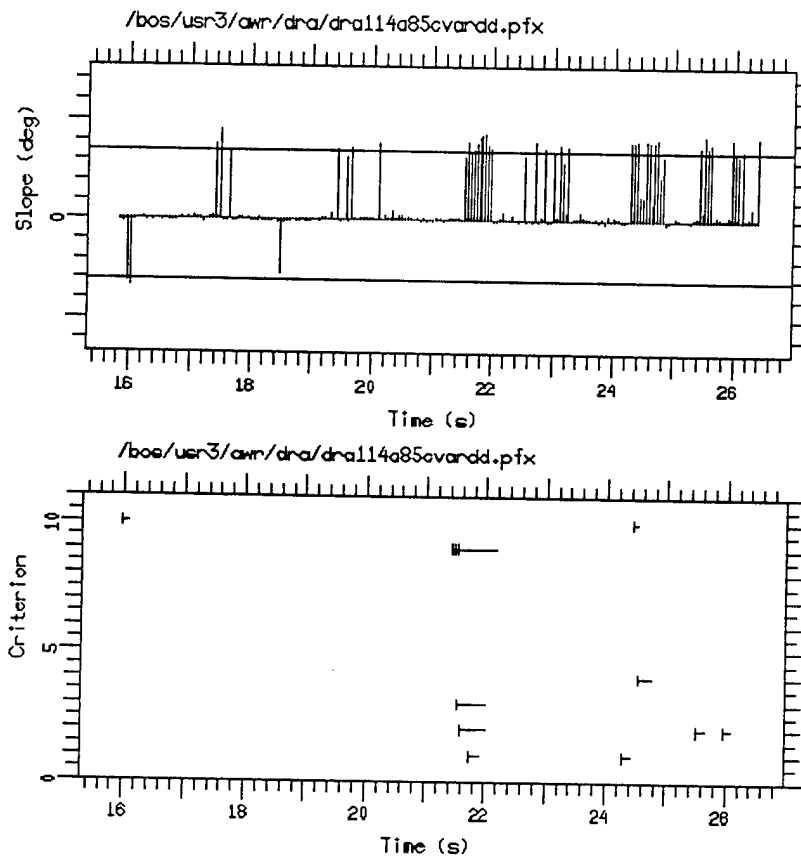
Switch XY

Zoom x2

IngDur 0.041

12:18:26

Slope (deg) -



28-Feb-02 12:18:24

Figure 52. Slope Measurements for the Surrogate TEL on the Smooth Road.

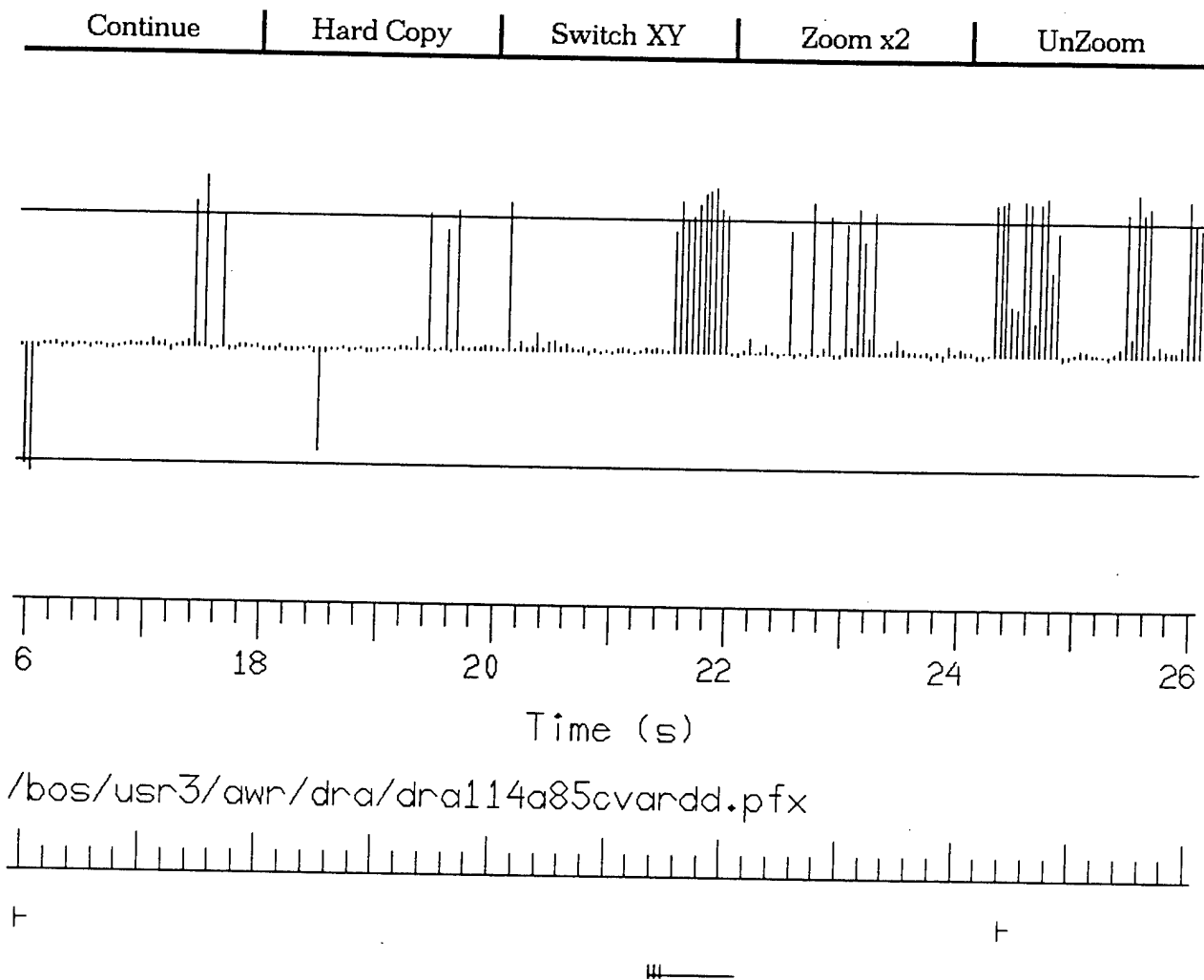


Figure 53. Expanded View of the Slope Bars.

0303 last action: Edit

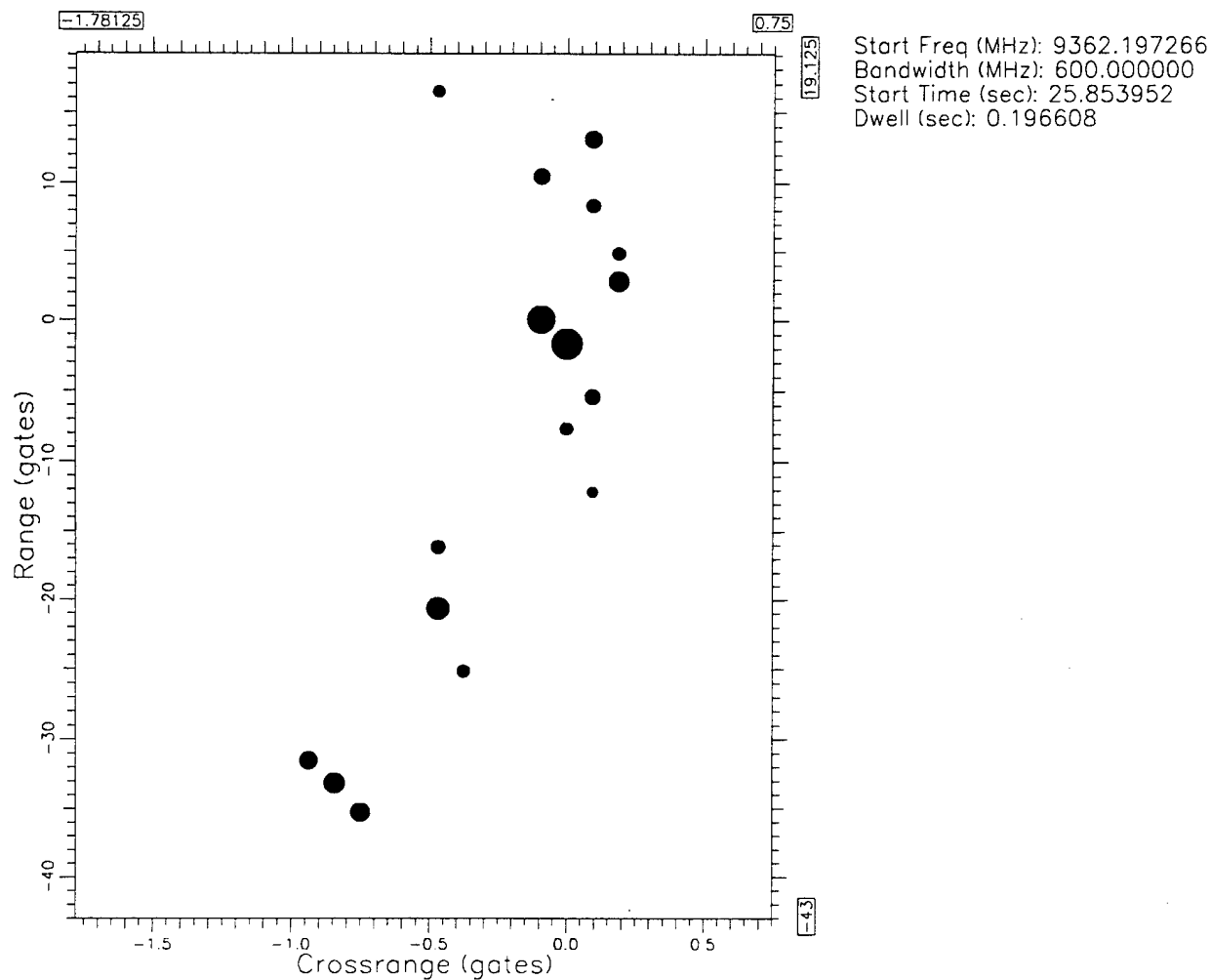
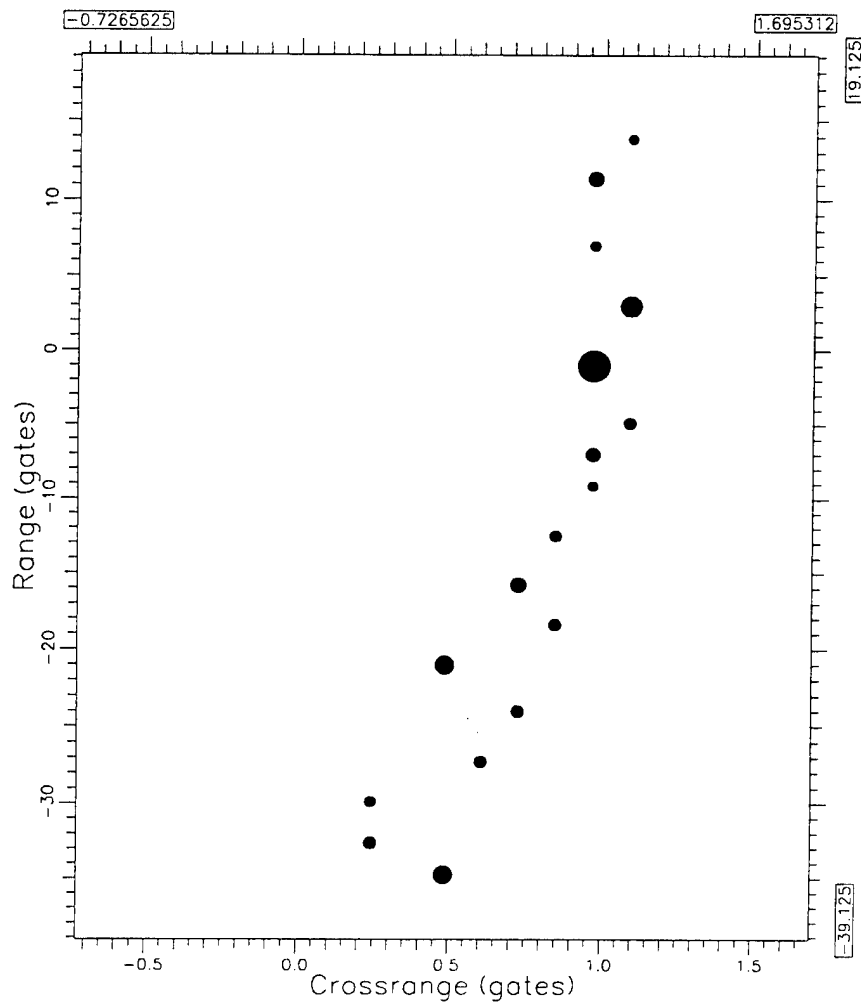


Figure 54. 0.2 s Image at 25.85 s.

0103 last action: Edit

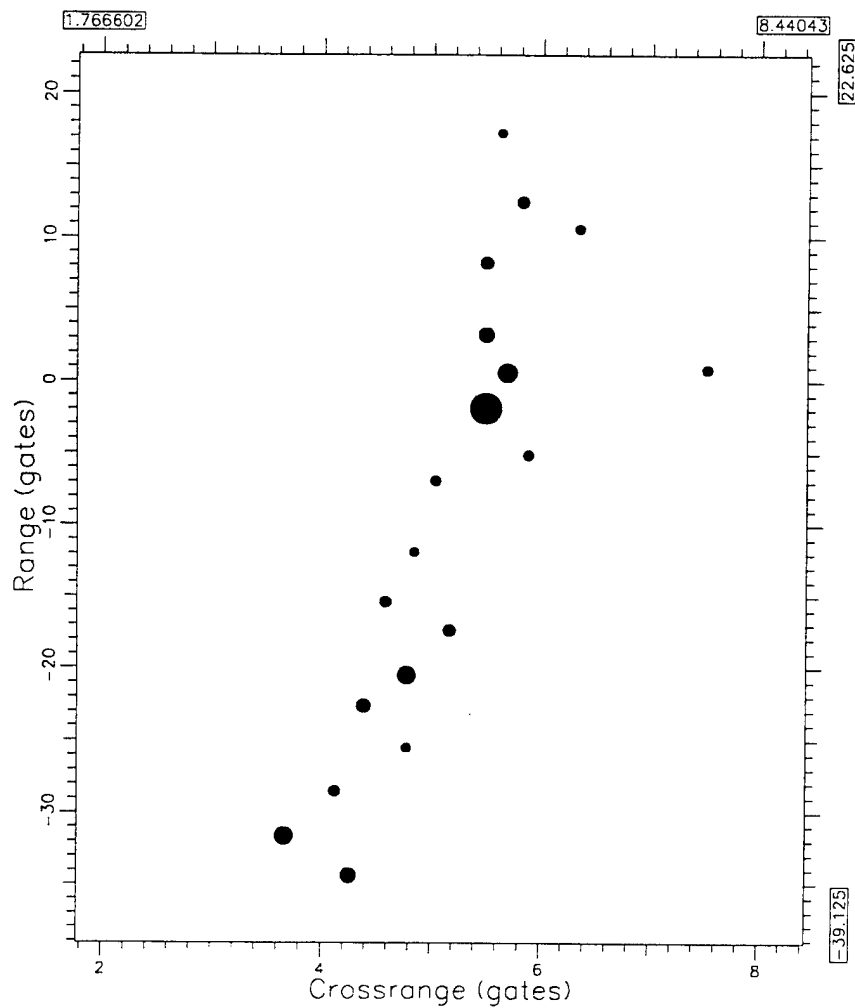


Start Freq (MHz): 9362.197266  
Bandwidth (MHz): 600.000000  
Start Time (sec): 25.403393  
Dwell (sec): 0.253952

Figure 55. 0.25 s Image at 25.40 s.

0303

last action: Edit

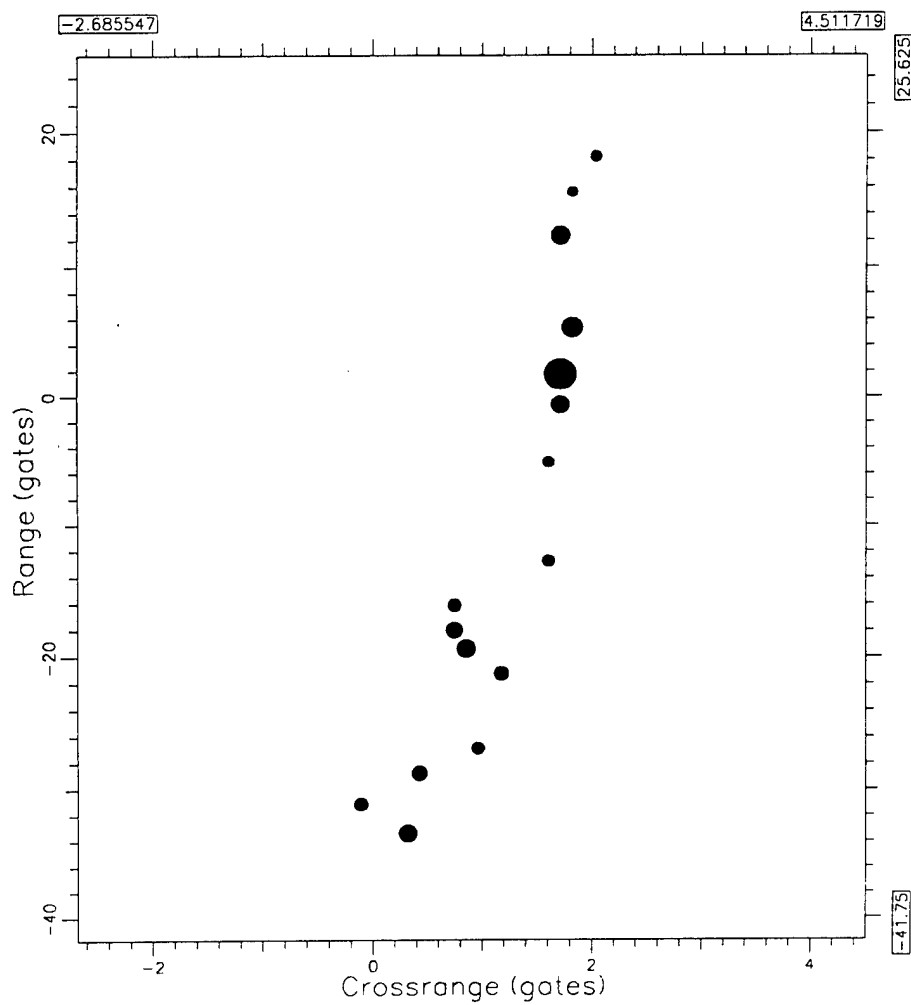


Start Freq (MHz): 9362.197266  
Bandwidth (MHz): 600.000000  
Start Time (sec): 24.297472  
Dwell (sec): 0.548864

Figure 56. 0.55 s Image at 24.3 s.

0103

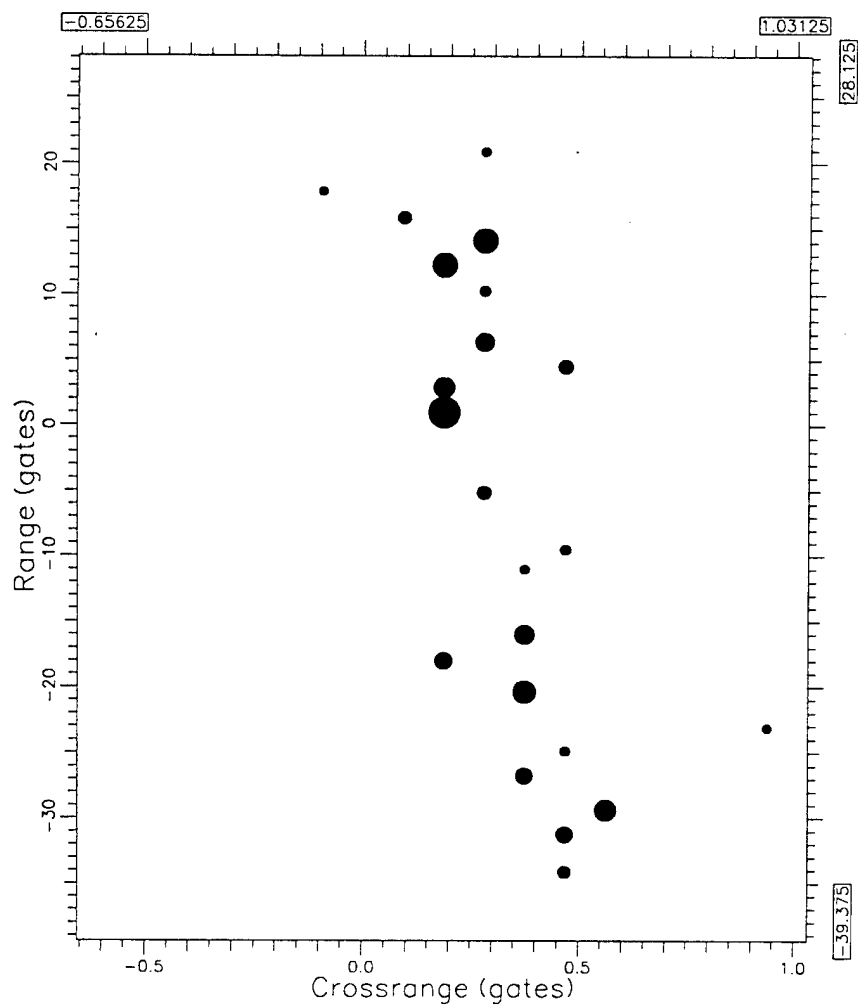
last action: Edit



Start Freq (MHz): 9362.197266  
Bandwidth (MHz): 600.000000  
Start Time (sec): 21.504000  
Dwell (sec): 0.450560

Figure 57. 0.45 s Image at 21.5 s.

0103 last action: Edit



Start Freq (MHz): 9362.197266  
Bandwidth (MHz): 600.000000  
Start Time (sec): 15.949824  
Dwell (sec): 0.098304

Figure 58. 0.1 s Image at 15.95 s.

0104 last action: Edit

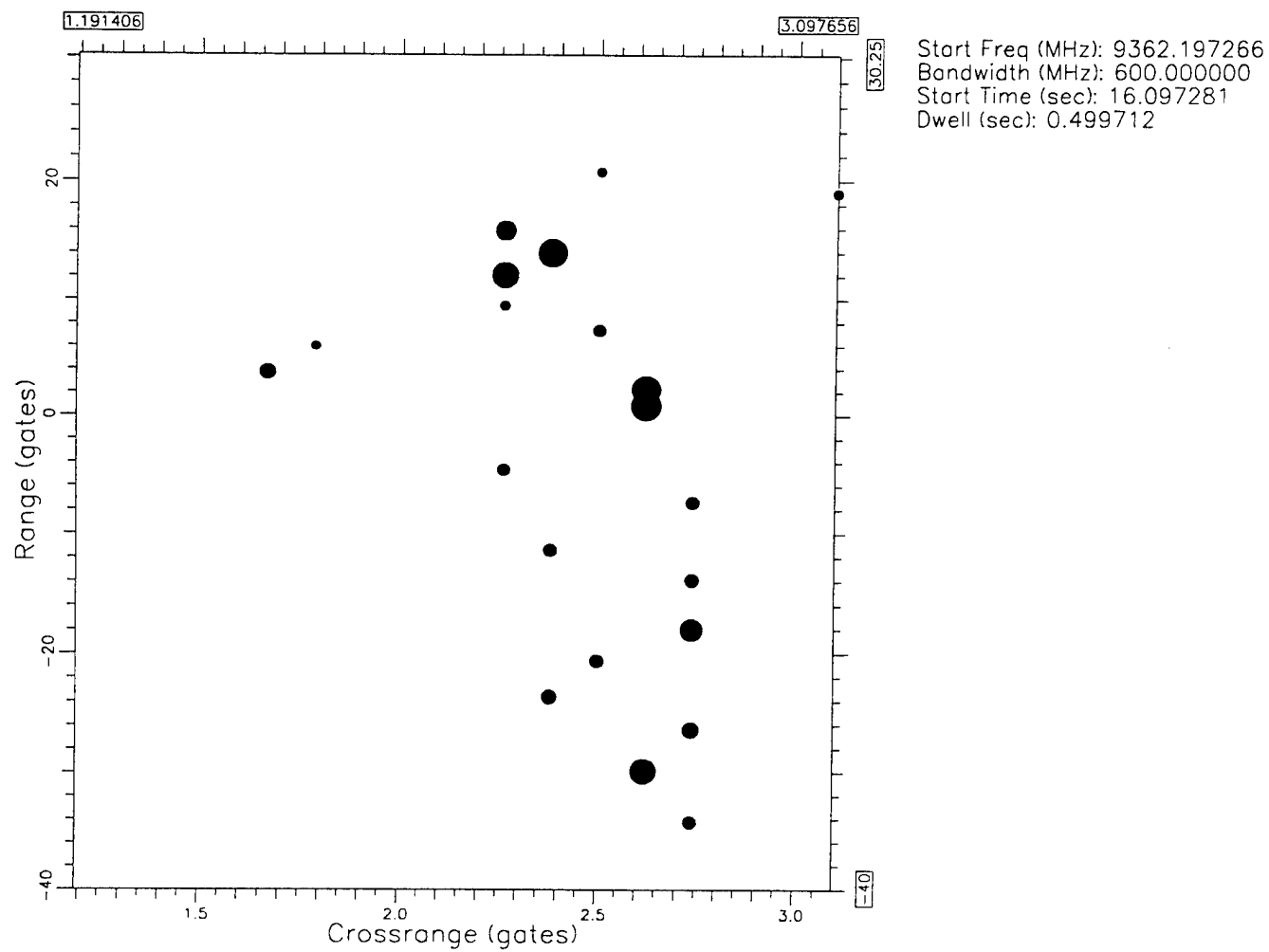
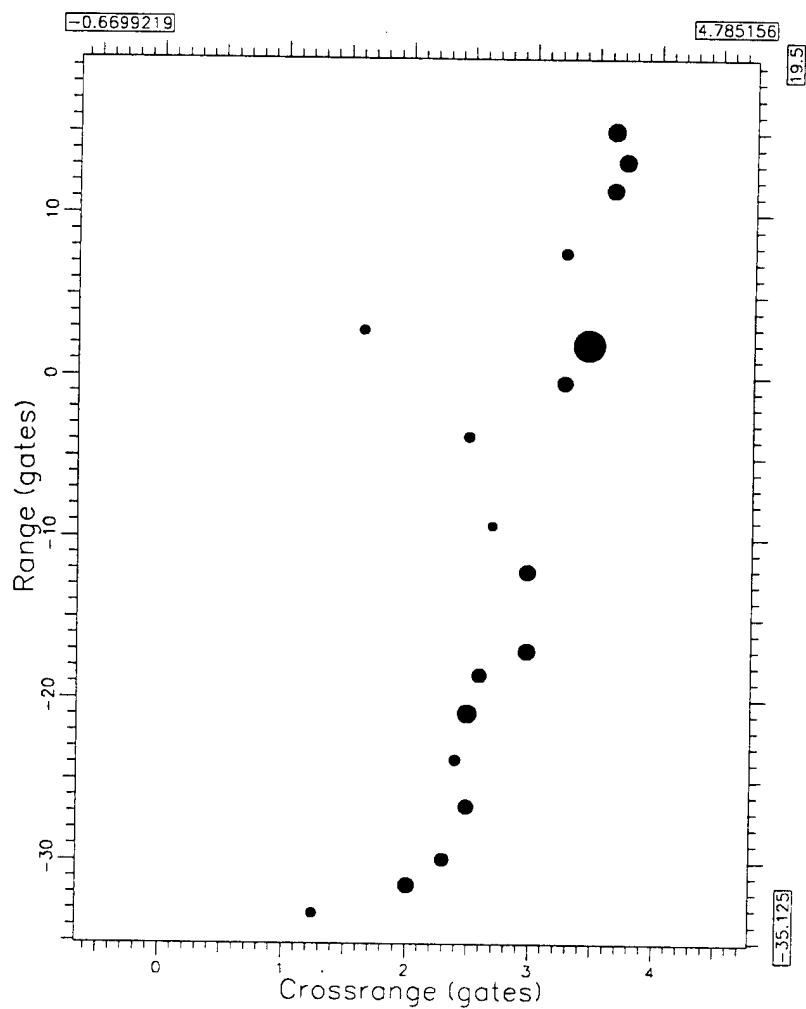


Figure 59. 0.5 s Image at 16.1 s.

0104

last action: Edit

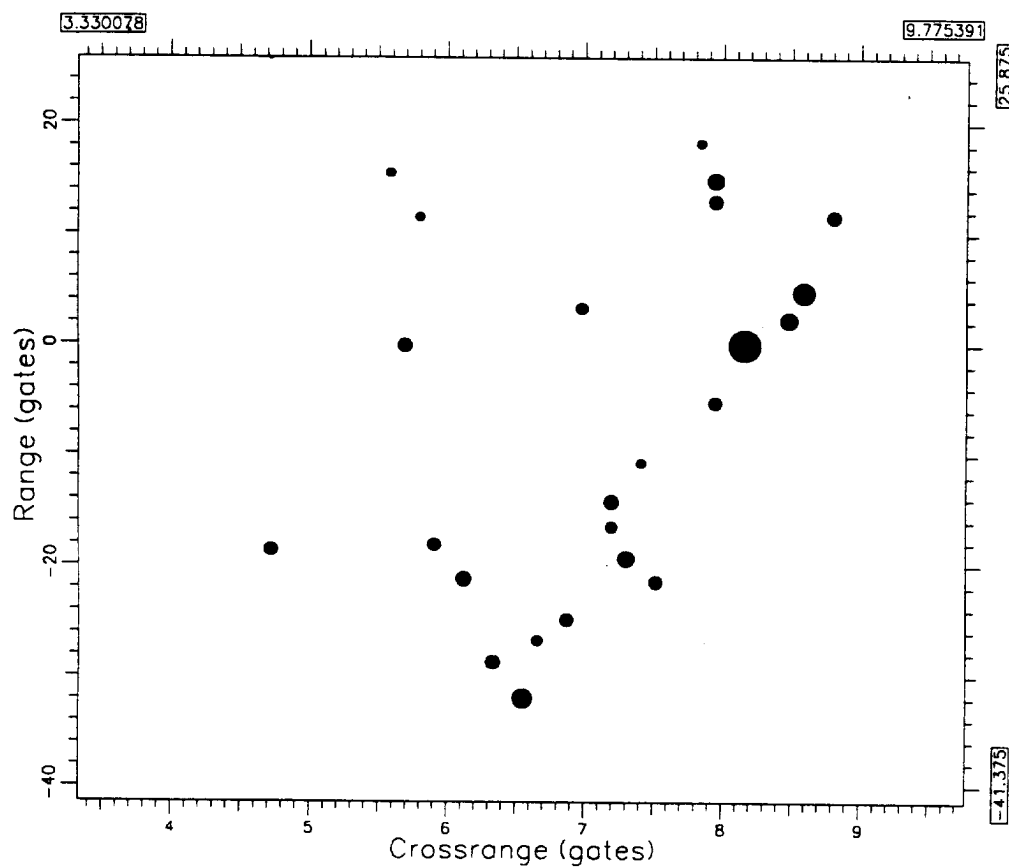


Start Freq (MHz): 9362.197266  
Bandwidth (MHz): 600.000000  
Start Time (sec): 17.301504  
Dwell (sec): 0.401408

Figure 60. 0.40 s Image at 17.3 s.

0303

last action: Edit



Start Freq (MHz): 9362.197266  
Bandwidth (MHz): 600.000000  
Start Time (sec): 22.396929  
Dwell (sec): 0.901120

Figure 61. 0.9 s Image at 22.4 s.